THE NERNST-PLANCK-POISSON REACTIVE TRANSPORT MODEL FOR CONCRETE CARBONATION AND CHLORIDE DIFFUSION IN CARBONATED AND NON-CARBONATED CONCRETE

THE NERNST-PLANCK-POISSON REACTIVE TRANSPORT MODEL FOR CONCRETE CARBONATION AND CHLORIDE DIFFUSION IN CARBONATED AND NON-CARBONATED CONCRETE

By

FERAS ALSHEET

BSc., MSc.

A Thesis Submitted to the School of Graduate Studies in Partial Fulfillment of the Requirements for the Degree Doctor of Philosophy

McMaster University

October 2020

Doctor of Philosophy (2020) McMaster University

(Civil Engineering) Hamilton, Ontario

TITLE: THE NERNST-PLANCK-POISSON REACTIVE TRANSPORT MODEL FOR CONCRETE CARBONATION AND CHLORIDE DIFFUSION IN CARBONATED AND NON-CARBONATED CONCRETE

AUTHOR: Feras Alsheet

BSc., MSc. (Eastern Mediterranean University)

SUPERVISOR: Dr. A. Ghani Razaqpur

NUMBER OF PAGES: xxi, 188

ABSTRACT

The intrusion of chlorides and carbon dioxide into a reinforced concrete (RC) structure can initiate corrosion of the reinforcing steel, which, due to its expansive nature, can damage the structure and adversely affects its serviceability and safety. Corrosion will initiate if at the steel surface the concrete free chloride concentration exceeds a defined limit, or its pH falls below a critical level. Hence, determination of the time to reaching these critical limits is key to the assessment of RC structures durability and service life. Due to the ionic nature of the chlorides and the bicarbonate anion (HCO_3^-) formed by the CO_2 in the multi-ionic pore solution, the transport of both species is driven by Fickian diffusion combined with electromigration and ionic activity, which can be mathematically expressed by the Nernst-Planck-Poisson (NPP) equations. For a complete representation of the phenomenon, however, the NPP equations must be supplemented by the relevant chemical equilibrium equations to ensure chemical balance among the various species within the concrete pore solution. The combination of NPP with the chemical equilibrium equations is often termed the NPP reactive transport model. In this study, such a model is developed, coded into the MATLAB platform, validated by available experimental data, and applied to analyze the time-dependent concrete carbonation and the movement of chlorides in carbonated and non-carbonated concrete. The results of these analyses can be used to predict the time to corrosion initiation. The transient one-dimensional governing equations of NPP are numerically solved using the Galerkin's finite element formulation in space and the backward (implicit) Euler scheme in the time domain. The associated system of chemical equilibrium equations accounts for the key homogeneous and heterogeneous chemical

reactions that take place in the concrete during carbonation and chlorides transport. At each stage of the analysis, the effects of these reactions on the changes in the pore solution chemical composition, pH, cement chloride binding capacity, concrete porosity, and the hydrated cement solids volumetric ratio are determined. The study demonstrates that given accurate input data, the presently developed NPP reactive transport model can accurately simulate the complex transport processes of chlorides and CO_2 in concrete as a reactive porous medium, and the ensuing physical and chemical changes that occur due to the reaction of these species with the pore solution and the other cement hydration products. This conclusion is supported by the good agreement between results of the current analyses with the corresponding available experimental data from physical tests involving carbonation, and chloride diffusion in non-carbonated and carbonated concrete.

DEDICATIONS

To Mohamed & Wafa,

Najla, Fawaz, & Faisal

Amal

ACKNOWLEDGMENTS

I would like to express my deep appreciation to my academic supervisor Dr. A. Ghani Razaqpur and administrative supervisor Dr. Lydell Wiebe. I was lucky to be supervised by such advisors who gave me encouragement, support, advice, and innovative ideas. I am especially grateful for our discussions that significantly impacted the quality of the dissertation. Special thanks are due to my supervisory committee members, Dr. Siva Sivakumaran and Dr. Younggy Kim for their valuable advice and suggestions. Their helpful comments and discussions during our meetings are greatly appreciated. Many thanks are due to Prof. Paul Ayers of the chemistry department at McMaster University for his advice with some chemistry applied un this research.

Many thanks to my former master's degree supervisor, Dr. Serhan Şensoy, in the Eastern Mediterranean University, who introduced me to the fundamentals of research and scientific investigation.

I am thankful for the financial support provided to me through my supervisor's Natural Sciences and Engineering Research Council (NSERC) of Canada Discovery Grant, the valuable Dean's Excellence Engineering Doctoral Award of McMaster University, and the Ahmed Ghobarah Scholarship. I am also grateful to SHARCNET (the shared hierarchical research computing network) in Ontario for giving me free access to its supercomputer facilities.

Last, but by no means least, I would like to say that no words can express my sincere gratitude to my parents, Mohamed and Wafa, my parents-in-law, Mohamed and Samar, to my sister, Najla, my brothers, Fawaz and Faisal, and my brother-in-law, Abdulrahman, for their patience, care, support and for everything they did, and are still doing for me. Without their continuous support, love, prayer and encouragement throughout my life, I would have never been the one I am now.

Special thanks are due to my wife, Amal, for her understanding, patience, and unwavering support and encouragement throughout both the tough and the good times in

this journey at McMaster University. She has happily supported me far beyond her fair share.

CO-AUTHORSHIP

This thesis has been prepared in accordance with the regulations for a sandwich thesis format or as a compilation of research papers stipulated by the faculty of graduate studies at McMaster University. This research presents the numerical and analytical work carried out solely by Feras Alsheet. Advice and guidance were provided during the entire research period by the academic supervisor Dr. A. Ghani Razaqpur, and he extensively edited the early drafts of the thesis. Information from outside sources which has been used in the present analyses or discussions has been cited where appropriate; all other materials are the sole work of the author. This thesis consists of the following manuscripts in the following chapters:

Chapter 2

Alsheet, F., and Razaqpur , A. G. (2020). " Quantification of electromigration and chemical activity effects on the reactive transport of chloride ions in the concrete pore solution. " ACI Materials Journal (Computational Materials). (in-press)

Chapter 3

Alsheet, F., and Razaqpur , A. G. (2020). " Modeling of concrete carbonation as a coupled Nernst-Planck-Poisson reactive transport process " Cement and Concrete Research. (under review)

Chapter 4

Alsheet, F., and Razaqpur , A. G. (2020). " A Reactive Transport Model for Chloride Movement in Pre-carbonated Concrete " Cement and Concrete Composites. . (Submitted for publications in October 2020.)

Appendix - A

Alsheet, Feras, and Razaqpur, A. G. (2018). " Effect of time-dependent chloride profile and temperature variation on chloride diffusion in concrete " Sixth International

Conference on the Durability of Concrete Structures, University of Leeds, Leeds, West Yorkshire, United Kingdom, (1), 788-794.

Table of Content

List of Figures

List of Tables

CHAPTER 1
INTRODUCTION

1.1 BACKGROUND AND MOTIVATION

Reinforced concrete (RC) is the most common material for constructing bridges, buildings, roads, dams, and other elements of modern infrastructures. Although concrete is generally a resilient and durable material in non-aggressive environments, the corrosion of the steel reinforcement in RC structures in aggressive environments damages and degrades RC structures (Papadakis et al. 1991), impairs their serviceability and endangers their safety. To avoid these problems, timely repair and rehabilitation works must be undertaken. Repairing the damage is costly, but lack of it can create greater economic losses and inconvenience for the infrastructure users. To undertake the necessary and timely repair/rehabilitation work, accurate prediction of the time to corrosion initiation is critical. Accordingly, the current research is aimed at the development of a theoretically robust method for estimating the time to corrosion initiation in RC structures exposed to chlorides (Cl^-) and carbon dioxide (CO_2) or their combination.

1.2 COMMON CAUSES OF REINFORCEMENT CORROSION

Normally, the passive rust layer formed on the steel rebars surface protects them from further corrosion, particularly in the high pH (>12) environment of concrete pore solution. However, corrosion can be initiated by either the drop in pH due to carbonation

or by sufficient accumulation of Cl^- at the surface of the rebars. The Cl^- in concrete originate from exposure to sea water or to deicing salts, with the latter being applied in cold regions to prevent ice formation on roads and bridges (Papadakis et al. 1991). Also, older structures may contain calcium chloride as a chemical additive. The CO_2 gas from the atmosphere enters concrete and dissolves in the concrete pore solution, forming carbonic acid. The acid reacts with the calcium hydroxide, $Ca(OH)_2$, termed Portlandite in cement chemistry, in the concrete pore solution to form calcite. Since concrete owes its high alkalinity to Portlandite, the consumption of the latter by carbonation causes a drop in the concrete pH and furnishes the conditions for steel depassivation and corrosion (Papadakis et al. 1991).

Chloride ions, on the other hand, diffuse in concrete through the pore solution and eventually accumulate at the steel reinforcement level. Once the concentration in the pore solution at the steel surface reaches a predefined critical level or threshold, the passive layer breaks down and corrosion commences (Hirao et al. 2005). Thus, to properly estimate the time to corrosion initiation in concrete, one needs to accurately model the CO_2 and chlorides transport processes and the changes that they instigate in the concrete physical and chemical properties. Additionally, there is experimental evidence (Suryavanshi and Narayan Swamy 1996; Goñi and Guerrero 2003; Geng et al. 2016; Zibara 2001) regarding the interaction between the two phenomena wherein carbonation can destabilize the bound chlorides and release them into the pore solution. It is important to mention that a part of the total chlorides that enter concrete is chemically bound or physical absorbed by the cement hydration products while the remaining part stays free in the pore solution. The two

are commonly termed bound and free chlorides, respectively, and it is the exceedance of the free chlorides concentration above the threshold that initiates corrosion. There is no general agreement about the precise magnitude of this threshold, but further discussion of it is beyond the scope of the current work. Note, carbonation changes the chemical and physical properties of concrete (Papadakis et al. 1991; Jeong et al. 2019), which adversely affect its chloride transport properties. Thus, modeling of this interaction is necessary for accurately predicting the time to corrosion initiation where both agents can enter concrete. However, it is important to mention that carbonation and chloride diffusion may not occur concurrently due to the difference in the rate of diffusion of CO_2 and Cl^-, and the inability of CO_2 to diffuse in fully saturated concrete, a condition that is more favourable for the Cl^- transport.

1.3 MODELLING OF CHLORIDES AND CARBON DIOXIDE CHEMICAL REACTIONS

The transport of Cl^- and CO_2 involves chemical interactions with the pore solution and with the solid phases of cement hydration products (Papadakis et al. 1991; Samson and Marchand 2007b). The chemical interactions can be modeled using either kinetics of the reactions (Papadakis et al. 1991), or via chemical equilibrium equations. (Thiery 2005; Samson and Marchand 2007b). The interactions affect the concentration of ions and solids in the pore structure and thus change the chemical and transport properties of the medium.

The ingress of Cl^- in concrete will slow down due to chloride binding. The binding can be attributed to physical and chemical mechanisms (Glass et al. 1997). Physical binding occurs when chloride ions are adsorbed on to the surface of the Calcium-Silicate-Hydrates (CSH) phase in hydrated cement (Hirao et al. 2005). This type of binding is believed to be weak (held by Van der Waal forces) and unstable, hence it can be ignored (Samson and Marchand 2006). Chemical binding is the result of the exchange between the sulfate ions in the Monosulfate (AFm) solid phase in hydrated cement and the chloride ions, leading to the production of Friedel's salt (FS). In the current study, the latter will be treated as the principal binding mechanism.

Two methods are used in the literature to quantify Cl^- binding: (i) applying empirical binding isotherms and (ii) using solidification/precipitation reactions. The most common types of isotherms are the Freundlich and Langmuir isotherms (Hirao et al. 2005), which relate the bound and free chloride by defined mathematical functions with unknown parameters . The functions must be fitted to experimental data to obtain values of these parameters. The second method follows the dissolution/precipitation reactions of FS in the concrete and quantifies binding based on the fundamental laws of chemistry. Thus, the latter method is adopted in the current work because it is more universal (Papadakis et al. 1991) and can cater to changes in the chemistry of pore solution due to changes in cement composition or the addition of supplementary cementitious materials.

1.4 MODELLING TRANSPORT OF CHEMICAL SPECIES IN CONCRETE AS A POROUS MEDIUM

Traditionally transport of CO_2 and Cl^- in concrete has been modelled as a Fickian diffusion process, which is represented by Eq. 1.1 in one-dimension and is known as Fick's second law of diffusion (Collepardi et al. 1970; Morinaga 1988; Takewaka and Mastumoto 1988; Saetta, et al. 1993; Uji et al.1990; Purvis and Babaei 1993; Gautefall and Vennesland 1994 ; Chatterji 1994a; Isgor and Razaqpur 2004)

$$\frac{\partial c}{\partial t} = \frac{\partial}{\partial x}\left(D\left(\frac{\partial c}{\partial x} \right) \right) \tag{1.1}$$

where D is the apparent diffusion coefficient (m^2/sec), c is the chloride or CO_2 concentration (mol/m^3), x is the distance measured from a reference surface (m) and t is time (sec).

The Fickian model lumps the chemical interactions of diffusing species with the concrete physical properties, such as its porosity and tortuosity, via the apparent diffusion coefficient, which is phenomenological and questionable in the case of multi-ionic solutions. It also makes no distinction between the transport of ionic and molecular species. Fick's model does not account for ionic movement by other modes of transport, e.g., electromigration, which can be significant in the case of the cement/concrete multi-ionic pore solution, depending on the nature and concentration of the ions involved.

On the other hand, a more advanced model considers the interaction between the ions in the pore solution and their chemical activity effect on the transport of the diffusing species.

The Nernst-Planck (NP) equation shown below includes the latter modes of transport (Samson and Marchand 2007)

$$\frac{\partial c_i}{\partial t} = \frac{\partial}{\partial x}\left[D_i \left(\underbrace{\frac{\partial c_i}{\partial x}}_{molecular} + \underbrace{\frac{z_i F}{RT} c_i \frac{d\psi}{dx}}_{electromigration} + \underbrace{c_i \frac{d \ln \gamma_i}{dx}}_{chemical\ activity} \right) + \underbrace{D_L c_i \frac{\partial w}{\partial x}}_{advection} \right] + r_i \qquad (1.2)$$

where c_i , z_i and γ_i, respectively, are the concentration, valence number and activity coefficient of species i , F is Faraday constant = 96,488.46 (C/mol), R is the ideal gas constant = 8.3143 (J/mol/K), T is temperature of the solution (K), ψ is the electric potential (V), r_i: source/sink term, accounting for the production/consumption of species i , and D_L is the water diffusivity coefficient (m/s^2). To solve for the electrical potential ψ in Eq. 1.2, it is supplemented by the Poisson's equation as follows

$$\frac{d}{dx}\left(\tau w \frac{d\psi}{dx} \right) + \frac{F}{\varepsilon} w \left(\sum_{i=1}^{n} z_i c_i \right) = 0 \qquad (1.3)$$

where ε (C/V/m) is the medium permittivity, *n* is the total number of species involved and τ is the tortuosity of concrete. The system of Eqs. 1.1 and 1.2 represents the Nernst-Planck-Poisson (NPP) transport model. When the NPP model is coupled with the system of equations governing chemical equilibrium in the concrete, the combined system is termed the NPP reactive transport model.

For correct modelling of carbonation, one must also model water movement in concrete because carbonation occurs in unsaturated concrete and the carbonation reactions result in the production of moisture (Papadakis et al.1991). Thus, the NPP equations must

be supplemented by Richard's equation (Taigbenu 1999) to track moisture distribution in unsaturated concrete. Other factors that can affect the ingress of Cl^- and CO_2 in concrete include the ambient temperature (Saetta and Vitaliani 2005; Samson and Marchand 2007a; Alsheet and Razaqpur 2018), surface concentration of chloride ions (Alsheet and Razaqpur 2018), and the chemical composition of the applied salt (Alsheet and Razaqpur 2020). In reality, the surface chloride concentration can vary seasonally as deicing salts are applied to the concrete surface in the winter only. Modeling heat transfer in concrete may be also important as the temperature varies daily and annually. Furthermore, the diffusion coefficient is function of temperature and their relationship is governed by the Arrhenius law (Martín-Pérez et al. 2000, Isgor and Razaqpur 2004). The temperature also affects the concrete chloride binding capacity. As stated by Isgor and Razaqpur (2004), neither the carbonation nor the chlorides reactions affect the concrete temperature, hence the temperature analysis can be independently performed, and its result can be used as input into the NPP reactive transport model. The governing mode of heat transfer in concrete is conduction, which is governed by Fourier's law of heat transfer in concrete, and it can be easily included in the analysis as its governing differential equation has the same form as the one governing Fick's second law of diffusion.

Detailed analysis of the temporal change of temperature and surface chloride concentration was performed as part of the current research (Alsheet and Razaqpur 2018) and is shown in Appendix-A. The chemical composition of the utilized deicing salt has significant effect on the transport of the chloride ion as it affects the physical and chemical properties of concrete (Alsheet and Razaqpur 2020; Suraneni et al. 2017). However, this

phenomenon can be accounted for by the reactive transport models through the inclusion of the relevant chemical equilibrium equations.

1.5 RESEARCH OBJECTIVES

The main objective of this dissertation is to develop a robust numerical procedure, based on the Nernst-Planck-Poisson reactive transport model, that can accurately predict the time to reinforcing steel corrosion initiation due to the ingress of carbon dioxide, chloride salts or their combination in Portland cement reinforced concrete.

More specifically, it is aimed to accomplish the following goals:

1) Modelling of chlorides ingress in concrete by the Nernst-Planck-Poisson reactive transport model and determining the spatial and temporal variation of the free chloride concentration in the concrete as well as the effects of the chloride ions on the concrete physical and chemical properties .

2) Modelling by the Nernst-Planck-Poisson reactive transport model the CO_2 ingress in Portland cement concrete and the ensuing carbonation process to determine their effects on the pore solution chemistry, including its pH, the hydrated cement solid phases volume fraction, and the concrete porosity,

3) Modelling by the Nernst-Planck-Poisson reactive transport model chloride ingress in pre-carbonated concrete, the ensuing chemical interactions and determining their effects on the concrete physical and chemical properties, including its pore solution pH, solid phases volumetric ratio, porosity and chloride binding capacity.

This research will include writing of computer programs within the MATLAB platform and the numerical solution of the governing differential equations by finite element, formulated on the basis of the Galerkin's weighted residual method. The research will not involve any other analytical work or physical tests.

1.6 ORGANIZATION OF THE DISSERTATION

This dissertation comprises five chapters:

- Chapter 1 presents the motivation and objectives of the dissertation as well as background information pertaining to the research program.
- Chapter 2 contains modeling the chloride ions reactive transport in the concrete. It quantifies the contribution of molecular diffusion, electromigration, and chemical activity to the transport of the chloride ions and the changes in the volumetric ratios of the different phases in the hydrated cement. Moreover, it shows the effect of different types of deicing salts on the concentration of the hydrated cement solid phases, the pore solution and its pH, and porosity of concrete.
- Chapter 3 deals with modeling of the concrete carbonation process as a reactive transport phenomenon. The detailed chemical equilibrium equations of carbonation are considered to accurately capture the effect of carbonation on the concrete pH, pore solution chemical composition, hydrated cement solid phases volumetric ratio, and the transport properties of concrete. To the writer's knowledge, concrete

carbonation has not been previously modelled by the NPP reactive transport model as done here.

- Chapter 4 presents the reactive transport model for chloride movement in pre-carbonated concrete and the physical and chemical interactions that occur during this process. To the writer's knowledge, this type of modelling the combined effects of carbonation and chloride ingress on the concrete physical and chemical properties has not been previously reported in the open literature.
- Chapter 5 presents the dissertation summary, major conclusions, and recommendations for future research.
- Appendix - A presents modeling the effect of temporal change in temperature and surface chloride concentration on the chloride binding capacity and chloride transport in concrete. In this analysis, chloride diffusion is modelled by Fick's second law of diffusion.
- Appendix - B provides a walkthrough of the core computer program used in the research. It explains its objectives, input, and output. This appendix also includes sample input and output for the chloride transport problem.

It should be noted that although each chapter presents a standalone journal manuscript, Chapters 2, 3, and 4 collectively describe a cohesive research program as outlined in Chapter 1 of the dissertation. Nonetheless, for completeness of the standalone chapters/manuscripts, some overlap exists, including the finite element formulation of Nernst-Planck-Poisson's equation and some of the chemical equilibrium equations.

1.7 MAJOR CONTRIBUTIONS

- Chapter 2: In the past, most researchers have applied Fick's 2nd law to model chloride and carbon dioxide ingress in concrete. This law accounts for transport due to the difference in the concentration of the diffusing between two points in the medium. However, it is well known that other modes of transport also exist. The Nernst-Planck (NP) model accounts for these additional modes, including electromigration, chemical activity, and advection. When applying the NP model, in most studies it has been implemented under the assumption of electroneutrality and/or null current, which is a special case of Poisson equation, which relates the electric potential to charge density. Only a few researchers in the field of concrete have solved the fully coupled the NP- Poisson (NPP) equations. In this work the fully coupled NPP equations are solved. Using the NPP model, the contribution of each mode transport to the total chloride transport in concrete was quantified. To the writer's knowledge, this type of quantification, based on NPP, has not been reported in the past.
- Chapter 3: Review of literature reveals that most researchers have assumed CO_2 transport in concrete as a Fickian process. Only one researcher has modelled the process by applying the NP equation under the assumption of electroneutrality. A novelty of the present work is the coupling of the NP equation with the Poisson equation without the a priori imposition of the electroneutrality assumption. Also, in previous studies, either the chemical interactions among the different species in concrete were ignored or partially included. In the current work, the detailed interactions between the chemical species are modelled. Moreover, the operator

splitting approach is applied to separate the transport processes from the chemical interactions, which allows for the inclusion of complex chemical reactions in the model without affecting the numerical stability of the overall solution.

- Chapter 4: Available literature shows some numerical models that deal with combined chloride diffusion and carbonation. Some researchers used the traditional Fickian diffusion model while others applied the Nernst-Planck (NP) transport model under the assumption of electroneutrality. Irrespective of the type of transport model, they applied semi-empirical isotherms to model the chloride binding. In some cases, the binding isotherm parameters were also empirically adjusted to account for the effects of carbonation. In the current study, chloride binding is modeled following chemical equilibrium by the formation of Friedel's salt by ion-exchange mechanism. The effect of carbonation on chloride ions diffusion is considered by modifying their diffusion coefficient as function of the reduction in concrete porosity and/or degree of moisture saturation induced by carbonation. The chemical equilibrium among the various species within the concrete pore solution is satisfied and the change in the species concentration caused by chloride diffusion or carbonation is quantified. Moreover, the change in concrete porosity is evaluated by tracking the changes in the solid phases volume due to the chemical reactions within the concrete pore structure. The writer believes that the fundamental approach developed in the current work is new, it minimizes empiricism, and it can be extended to the chemical interaction among other species during their transport in concrete, such as combined chloride and sulfate attack.

1.8 REFERENCES

Alsheet, F., and Razaqpur, A. G. 2018. “Effect of Time-Dependent Chloride Profile and Temperature Variation on Chloride Diffusion in Concrete.” In *Sixth International Conference on the Durability of Concrete Structures (ICDCS 2018)*, 788–94. Leeds, West Yorkshire, United Kingdom: Purdue e-Pubs. https://docs.lib.purdue.edu/icdcs/2018/dsm/3/.

Alsheet, F., and Razaqpur, A. G. 2020. “Quantification of Electromigration and Chemical Activity Effects on the Reactive Transport of Chloride Ions in the Concrete Pore Solution.” *ACI Material Journal* (in press).

Chatterji, S. 1994(a). "Transportation of ions through cement based materials. Part 2. Adaptation of the fundamental equations and relevant comments." *Cement and Concrete Research*. 24 (6): 1010-1014. https://doi.org/http://dx.doi.org/10.1016/0008-8846(94)90023-X.

Collepardi, M., Marciallis, A., and Turriziani, R.. 1970. "The Kinetics of Chloride Ions Penetration In Concrete" (in Italian). Il Cemento, 4: p. 157-164.

Galindez, J.M. and Molinero, J. On the Relevance Of Electrochemical Diffusion For The Modeling Of Degradation Of Cementitious Materials. Cement & Concrete Composites, 2010. 32(5): p. 351-359. https://doi.org/10.1016/j.cemconcomp.2010.02.006.

Gautefall, O. and Vennesland. 1994. "Methods for Determination of Chloride Diffusivity in Concrete". REPCON-report A16, Statens Vegvesen, Vegdirektoratet, Oslo, Norway.

Geng, J., Easterbrook, D., Liu, Q.-F., and Li, L.-Y.. 2016. “Effect of Carbonation on Release of Bound Chlorides in Chloride-Contaminated Concrete.” *Magazine of Concrete Research* 68 (7): 353–63. https://doi.org/10.1680/jmacr.15.00234.

Glass, G. K., Hassanein, N. M., and Buenfeld, N. R.. 1997. “Neural Network Modelling of Chloride Binding.” *Magazine of Concrete Research* 49 (181): 323–35. https://doi.org/10.1680/macr.1997.49.181.323.

Goñi, S., and Guerrero, A.. 2003. “Accelerated Carbonation of Friedel’s Salt in Calcium Aluminate Cement Paste.” *Cement and Concrete Research* 33 (1): 21–26. https://doi.org/https://doi.org/10.1016/S0008-8846(02)00910-9.

Hirao, H., Yamada, K., Takahashi, H., and Zibara, H.. 2005. “Chloride Binding of Cement Estimated by Binding Isotherms of Hydrates.” *Journal of Advanced Concrete Technology* 3 (1): 77–84. https://doi.org/10.3151/jact.3.77.

Isgor, O.B. and Razaqpur, A.G. 2004 "Finite Element Modeling of Coupled Heat Transfer, Moisture Transport And Carbonation Processes In Concrete Structures". Cement & Concrete Composites. 26(1): p. 57-73. https://doi.org/10.1016/s0958-9465(02)00125-7

Jeong, J, Ramezani, H., and Chuta, E.. 2019. “Reactive Transport Numerical Modeling of Mortar Carbonation: Atmospheric and Accelerated Carbonation.” *Journal of Building Engineering* 23: 351–68. https://doi.org/10.1016/j.jobe.2019.01.038.

Martín-Pérez, B, Zibara, H., Hooton, R. D., and Thomas, M. D. A.. 2000. “A Study of the Effect of Chloride Binding on Service Life Predictions.” *Cement and Concrete Research* 30 (8): 1215–23. https://doi.org/https://doi.org/10.1016/S0008-

8846(00)00339-2.

Morinaga, S. 1988. "Prediction of Service Lives Of Reinforced Concrete Buildings Based On Rate Of Corrosion Of Reinforcing Steel". Shimizu Corp: Japan. p. 82–89.

Papadakis, V. G., Vayenas, C. G., and Fardis, M. N.. 1991. “Fundamental Modeling and Experimental Investigation of Concrete Carbonation.” *ACI Materials Journal* 88 (4): 363–73.

Saetta, A.V., Scotta, R.V., and Vitaliani, R.V.. 1993. Analysis of Chloride Diffusion Into Partially Saturated Concrete. ACI Materials Journal. 90(5): p. 441-451.

Saetta, A.V., and Vitaliani, R.V.. 2005. “Experimental Investigation and Numerical Modeling of Carbonation Process in Reinforced Concrete Structures: Part II. Practical Applications.” *Cement and Concrete Research* 35 (5): 958–67. https://doi.org/10.1016/j.cemconres.2004.06.023.

Samson, E., and Marchand, J.. 2007a. “Modeling the Effect of Temperature on Ionic Transport in Cementitious Materials.” *Cement and Concrete Research* 37 (3): 455–68. https://doi.org/https://doi.org/10.1016/j.cemconres.2006.11.008.

Samson, E., and Marchand, J.. 2007b. “Modeling the Transport of Ions in Unsaturated Cement-Based Materials.” *Computers & Structures* 85 (23–24): 1740–56. https://doi.org/10.1016/j.compstruc.2007.04.008.

Samson, E., and Marchand, J.. 2006. “Multiionic Approaches to Model Chloride Binding in Cementitious Metrials.” In *2nd International RILEM Symposium on Advances in Concrete through Science and Engineering*, edited by M. Jolin and F. Paradis J. Marchand, B. Bissonnette, R. Gagné, 101–122. Quebec City, Canada: RILEM

Publication SARL. https://doi.org/10.1617/2351580028.008.

Suraneni, R., Monical, J., Unal, E., Farnam, Y., and Weiss, J.. 2017. “Calcium Oxychloride Formation Potential in Cementitious Pastes Exposed to Blends of Deicing Salt.” *ACI Materials Journal* 114 (4): 631–41. https://doi.org/10.14359/51689607.

Suryavanshi, A. K., and Swamy, R. N.. 1996. “Stability of Friedel’s Salt in Carbonated Concrete Structural Elements.” *Cement and Concrete Research* 26 (5): 729–41. https://doi.org/10.1016/S0008-8846(96)85010-1.

Taigbenu, A. E.. 1999. “Unsaturated Flow (Richards Equation).” In *The Green Element Method*, edited by Akpofure E Taigbenu, 217–30. Boston, MA: Springer US. https://doi.org/10.1007/978-1-4757-6738-4_8.

Takewaka, K. and Mastumot, S.. 1988. "Quality and Cover Thickness Of Concrete Based On The Estimation Of Chloride Penetration In Marine Environments". Concrete in Marine Environment: Proceedings. 109: p. 381-400.

Thiery, M.. 2005. “Modélisation de La Carbonatation Atmosphérique Des Matériaux Cimentaires : Prise En Compte Des Effets Cinétiques et Des Modifications Microstructurales et Hydriques.” Ecole Nationale Des Ponts et Chaussees.

Uji, K., Matsuoka Y., and Maruya T. 1990. Formulation of An Equation For Surface Chloride Content Of Concrete Due To Permeation Of Chloride. Corrosion of Reinforcement in Concrete. p. 258-267.

Zibara, H.. 2001. “Binding of External Chlorides by Cement Pastes.” University of Toronto. http://hdl.handle.net/1807/15366.

CHAPTER 2

QUANTIFICATION OF ELECTROMIGRATION AND CHEMICAL ACTIVITY EFFECTS ON THE REACTIVE TRANSPORT OF CHLORIDE IONS IN THE CONCRETE PORE SOLUTION

2.1 ABSTRACT

The Nernst-Planck-Poisson (NPP) and a modified Fick's diffusion models, including the reactions among the chemical species within the concrete pore solution, are implemented in a one-dimensional finite element program. The program results are validated by comparison with available experimental data in the literature. The effect of the modelling method on chloride concentration, concrete pH and changes in the concrete pore solution composition are investigated. It is demonstrated that among the three diffusion modes captured by the NPP model, molecular diffusion dominates chloride diffusion in concrete followed by electromigration while the chemical activity gradient has negligible effect. Based on the model results, it is determined that for accurate and efficient prediction of concrete salt concentration, pH and changes in its chemical composition engendered by the diffusion of salts, the full NPP model must be used rather than the Fick's model even though the former is theoretically more complex and computationally more resource intensive than the latter.

2.2 INTRODUCTION

Deicing salts are used in cold regions to lower the freezing temperature of water and prevent ice formation on roads for improved driving conditions and higher safety. One of the main constituents of these salts is the chloride ion which induces significant damage in reinforced concrete structures by de-passivating the steel reinforcement and accelerating its corrosion. Similarly, chlorides from sea water entering concrete accelerate reinforcement corrosion in seaside and offshore concrete structures.

Chlorides permeate concrete primarily by diffusion via the concrete pore solution, a phenomenon that is commonly modelled using Fick's second law, expressed for one-dimensional diffusion as Eq. 2.1 (Collepardi et al. 1970; Morinaga 1988; Takewaka and Mastumoto 1988; Saetta et al.1993; Uji et al. 1990; Purvis and Babaei 1993; Gautefall and Vennesland 1994 ; Chatterji 1994a; Isgor and Razaqpur 2004)

$$\frac{\partial c}{\partial t} = \frac{\partial}{\partial x}\left(D\left(\frac{\partial c}{\partial x} \right) \right) \tag{2.1}$$

where D is the apparent diffusion coefficient (m^2/sec), c is the chloride concentration (mol/m^3), x is the distance measured from a reference surface (m) and t is time (sec).

This law makes no distinction between the diffusion of charged ions and uncharged molecules and is theoretically suitable for modelling molecular diffusion only because it ignores the effect of the electrostatic field created by the ions on their transport in an electrolyte such as the concrete pore solution. The movement of ions in a solution under the influence of an electric field is termed electromigration. Since the concrete pore solution and seawater contain several ionic species, including chlorides, theoretically their

electrochemical interactions are expected to affect the chloride concentration and penetration depth in concrete members. Note, electromigration is not only affected by the magnitude of the charge of the ions but also by size of their hydrated radius, a phenomenon represented by the concept of ionic mobility (Moore 1972).

The exceedance of the free chloride concentration above a predefined threshold in the concrete adjacent to the reinforcing steel is commonly used as the criterion for corrosion initiation and the end of service life (Monteiro et al. 1985). There is no general agreement about the magnitude of this threshold, but further discussion of it is beyond the scope of the current work. Note, the end of service life means without extensive repair/rehabilitation the structure may not be able to function at the end of this period.. To determine analytically/numerically the free and chemically bound chloride proportions in concrete, the common practice is to apply an empirical chloride binding isotherm (Tang and Nilsson 1993) in conjunction with Fick's diffusion law. The accuracy of the results of this approach depends on the accuracy of the values of the empirically obtained diffusion coefficient and the relevant parameters of the adopted isotherm. Besides the free chloride content, another key factor that governs corrosion of reinforcing steel is the concrete pH (Bertolini et al. 2004), which cannot be determined using models based on the traditional Fick's law. Consequently, the accuracy of Fick's law in its classical form for predicting corrosion initiation needs more rigorous assessment.

To model the effects of the foregoing phenomena on concrete free chloride concentration and pH and on corrosion initiation, one can apply the multi-ionic Nernst-Planck-Poisson's (NPP) model as it can tackle the aforementioned phenomena in a systematic and

comprehensive manner (Chatterji 1994b; Samson and Marchand 1999) and without resorting to too much empiricism. For gaining greater insight into the chemical interactions among the various species in the concrete pore solution and to get a more accurate estimate of the chloride binding, the NPP transport model can be supplemented by the laws of conservation of mass and charge governing the various species involved in the chemical reactions and mass transport within the concrete pore solution. Clearly, using such NPP chemical reactive transport model is much more difficult to apply on a routine basis due to the need for more detailed input data and the numerical difficulties associated with the solution of the governing equations, but ultimately the question that needs to be answered is whether the application of the latter model is justified in all situations or is only necessary in special cases. The answer to this question is part of the focus of the current investigation. Research on the NPP model with application to chloride diffusion in concrete has been conducted by many researchers in the past and a summary of the more recent works is presented in Table 2.1. It can be observed that all the researchers referred to in Table 2.1 (Li and Page 2000; Wang et al. 2005; Szyszkiewicz-Warzecha et al. 2016; Johannesson et al. 2007; Damrongwiriyanupap et al. 2013; Truc et al. 2000; Yu et al. 2015; Samson and Marchand 2007; Pivonka et al. 2007; Krabbenhoft and Krabbenhoft 2008; Xia and Li 2013) have considered molecular diffusion and electromigration in their numerical models, but they have either ignored electroneutrality and chemical equilibrium in the pore solution or have used different approaches to account for them. To determine the electrostatic field generated by the ions in the pore solution, the Nernst-Planck (NP) equation need to be coupled with the Poisson's equation. Some researchers have solved the coupled NP-

Poisson's equations (Samson and Marchand 2007; Yu et al. 2015; Szyszkiewicz-Warzecha et al. 2016), others have introduced the requirements of the Poisson's equation via the imposition of the electroneutrality condition (Li and Page 2000; Damrongwiriyanupap et al. 2013; Johannesson et al. 2007; Truc et al. 2000; Pivonka et al. 2007; Krabbenhoft and Krabbenhoft 2008; Xia and Li 2013; Wang et al. 2005) or by the imposition of null current constraint (Truc et al. 2000). In the current investigation, the Poisson's equation will be directly incorporated into the system of governing equations of the problem without resorting to simplifying assumptions.

Due to the differences among the diffusion coefficients of the various ionic and molecular species within the concrete and the presence of numerous chemicals within the cementitious paste, chemical reactions occur among the species, resulting in the formation of new phases. Some researchers (Truc et al. 2000; Li and Page 2000; Wang et al. 2005; Damrongwiriyanupap et al. 2013) have modeled these reactions by the artful device of binding isotherms, which is an empirical method and is based on the a priori presence of certain ions within the concrete. Others (Johannesson et al. 2007; Samson and Marchand 2007; Yu et al. 2015) have relied on rigorous chemical equilibrium equations to represent reaction and the interaction between the ions in the pore solution and the solid phases in the concrete. In the present study, a rigorous chemical reactions module is included in the model and its utility will be demonstrated by analyzing the effects of different salts on chloride diffusion and binding.

2.2.1 Governing Equations of the Problem

Samson and Marchand (Samson and Marchand 1999, Samson and Marchand 2007; Samson and Marchand 2006; Samson et al. 2003), among others, have presented the governing equation of non-advective chloride transport in concrete as

$$\frac{\partial c_i}{\partial t} = \frac{\partial}{\partial x}\left[D_i \left(\underbrace{\frac{\partial c_i}{\partial x}}_{molecular} + \underbrace{\frac{z_i F}{RT} c_i \frac{d\psi}{dx}}_{electromigration} + \underbrace{c_i \frac{d \ln \gamma_i}{dx}}_{chemical\ activity} \right) \right] + r_i \qquad (2.2)$$

where c_i , z_i and γ_i, respectively, are the concentration, valence number and activity coefficient of species i, F is Faraday constant = 96,488.46 (C/mol), R is the ideal gas constant = 8.3143 (J/mol/K), T is temperature of the solution (K), ψ is the electric potential (V), r_i : source/sink term, accounting for the production/consumption of species i .

The electromigration term in Eq. 2.2 accounts for the interaction between the various ions diffusing through the concrete pore solution and the effect of their electric fields on each other's diffusion. The electric potential satisfies the thermodynamic equilibrium of the system by regulating the movement of the charged species. Furthermore, as indicated by the chemical activity term in Eq. 2.2, the diffusion rate also depends on the diffusing ions chemical activity, which is a measure of the effective concentration of an ion in the solution. Hence, the NP model accounts more accurately than the Fick's model for the phenomena which govern the transport of multi-ionic species in concrete. However, unlike the Fick's model which lends itself to relatively simple closed-form solution, the NP model requires significantly more effort to obtain a solution. Theoretically the NP model seems more

accurate, but practically the extent of this accuracy is not evident. Consequently, in this study the extent of the deviation of a somewhat improved Fick's model results from those given by the NP model will be investigated.

For a solution containing i ($i = 1, n$) ionic species, Eq. 2.2 can be applied to each species at a time, thus generating *n* equations, but due to the presence of the electric potential term, there will be ($n+1$) unknowns. Therefore, to obtain a unique solution another relation is necessary among the unknowns of the problem. The required extra relation can be obtained by utilizing the Poisson's equation (i.e. Gauss's law or Maxwell's first equation for the electric field, in the current context) which relates the electric potential to the charge distribution as (Christopher and Shipman 1968)

$$\frac{d^2\psi}{dx^2} + \frac{F}{\varepsilon}\left(\sum_i z_i c_i\right) = 0 \tag{2.3}$$

where ε is the permittivity of the medium, given by the multiplication of the dielectric constant of the medium by the permittivity of the vacuum ($C^2/N/m^2$).

The set of Eqs. 2.2 and 2.3 provides a system of nonlinear equations, referred to as Nernst-Planck-Poisson's (NPP or PNP) model or equation, that can capture the effects of key parameters on the diffusion of one or several types of molecules and ions in concrete (Samson and Marchand 1999; Johannesson et al. 2007; Sergi et al. 1992; Chatterji 1994b). In ionic solutions, the charge concentration is not uniform throughout the solution; therefore, the solution in the electrode vicinity is distinguished from the bulk solution (Newman and Thomas-Alyea 2004). Given the assumption of non/low reactive solution, the bulk solution is approximated as electrically neutral and the electroneutrality is enforced

via Eq. 2.4 below. Moreover, the current density due to movement of charged species, ic, is expressed by Eq. 2.5.

$$\sum_i z_i c_i = 0 \tag{2.4}$$

$$ic = F \sum_i z_i J_i \tag{2.5}$$

These assumptions are a simplification of the original intent of the Poisson's equation. The application of Poisson's equation is mandatory in the electrode vicinity where electroneutrality is violated. However, due to the stiff nature of the Poisson's differential equation, and to avoid numerical stability problems, researchers (Truc et al. 2000; Damrongwiriyanupap et al. 2013; Krabbenhoft and Krabbenhoft 2008; Li and Page 2000; Johannesson et al. 2007) in the area of chloride diffusion have adopted Eqs. 2.4 and/or 2.5 without loss of accuracy because diffusion occurs in the bulk solution and there are no electrodes involved. In addition, many researchers (Trucet al. 2000; Krabbenhoft and Krabbenhoft 2008; Chatterji 1994a; Lorente et al. 2007; Damrongwiriyanupap et al. 2013; Li and Page 2000; Wang et al. 2005; Johannesson et al. 2007; Szyszkiewicz-Warzecha et al. 2016) have ignored the chemical activity gradient term in Eq. 2.2 to simplify the problem. The validity of the latter simplification will be examined in the current investigation.

The chemical activity coefficient can be evaluated using various chemical models, varying in complexity from simple (e.g. Debye-Hückel, and Davies (Moore 1972)), to complex (e.g. Pitzer (Pitzer 1991)). The Modified Davies relationship in Eq. 2.6 is reported to yield good results for a wide range of ionic strengths (Samson et al. 1999), thus it is adopted in the current research.

$$\ln \gamma_i = Az_i^2 \left(\frac{\sqrt{I}}{1 + a_i B\sqrt{I}} - \frac{\left(0.2 - 4.17x10^{-5} I\right) I}{\sqrt{1000}} \right) \tag{2.6}$$

where *I* is the ionic strength (mM) given by Eq. (2.6a), A and B are temperature dependent parameters given by equations Eqs. (2.6b) and (2.6c), and a_i is a fitting parameter (m) whose value for common ions in concrete is shown in Table 2.2.

$$I = 0.5 \sum_i z_i^2 C_i \tag{2.6a}$$

$$A = \frac{\sqrt{2} F^2 e_0}{8\pi \left(\varepsilon RT\right)^{3/2}} \tag{2.6b}$$

$$B = \sqrt{\frac{2F^2}{\varepsilon RT}} \tag{2.6c}$$

where e_0 is the electric charge of one electron 1.602x10^{-19} C.

Previous researchers (Galindez and Molinero 2010; Marchand and Samson 2009) have compared results of Fick's and NPP models, but a detailed examination of the literature review reveals that the contribution of each term in Eq. 2.2 to the concentration profiles of ions and solid phases has not been adequately assessed. In the current study, a finite element model is developed and implemented following Samson et al. (Samson and Marchand 2007), but they used the closed-form solution of Fick's equation in conjunction with an empirical coefficient for the diffusion component of chloride transport in the cement paste (Marchand and Samson 2009). On the contrary, as shown later, in the current study, the diffusion coefficient of each species is selected/assigned individually based on their diffusion properties in a solution. This enables one to model the diffusion of each species

separately without being influenced by the presence of the concomitant species. Based on this procedure, the traditional Fick's modelled is modified to find the concurrent diffusion of several species in the concrete pore solution. Although Samson et al. also investigated the companion ions effect on the ions transport, they did not study this effect in the specific case of chloride diffusion. Hence, in this study the effects of different chlorides salts on the pH, solid phases, and chloride concentration profile are investigated. It should be mentioned that (Galindez and Molinero 2010) also used an average diffusion coefficient for all the species when applying the Fick's model.

Accurate evaluation of the free chloride concentration in the concrete at its interface with the steel reinforcement is necessary to predict the corrosion initiation period. The concentration is commonly determined using Fick's second law with an empirical diffusion coefficient. Although this is simple and convenient, it does not reflect the effects of other phenomena on diffusion of chlorides in concrete. A more accurate but complex model for non-advective chloride transport in saturated concrete is represented by the Nernst-Planck-Poisson's (NPP) equation. Here, a modified Fick's model is applied to chemically reacting multi-species diffusion and its results are compared with those of the NPP model. Furthermore, the relative contribution of diffusion, electromigration and chemical activity gradient on diffusion of three types of salt is investigated. It is discovered that Fick's model may lead to inaccurate the estimation of the concrete free chloride content.

2.3 THEORETICAL BASIS OF THE ADOPTED MODEL

The system of Eqs. 2.2 and 2.3 is strictly applicable to diffusion in chemical solutions. However, concrete is considered as a reactive porous medium; consequently, the latter

equations need to be modified to account for the characteristics of concrete. Accordingly, following (Samson and Marchand 2007), the modified equations based on mass balance can be written as

$$\frac{\partial\left(w_s c_i^s\right)}{\partial t}+\frac{\partial\left(wc_i\right)}{\partial t}-\frac{\partial}{\partial x}\left(wD_i\left(\underbrace{\frac{dc_i}{dx}}_{molecular}+\underbrace{\frac{z_i F}{RT}c_i\frac{d\psi}{dx}}_{electro-migration}+\underbrace{c_i\frac{d\ln\gamma_i}{dx}}_{chemical\ activity}\right)\right)+wr_i=0 \tag{2.7a}$$

$$\frac{d}{dx}\left(\tau w\frac{d\psi}{dx}\right)+\frac{F}{\varepsilon}w\left(\sum_{i=1}^{n}z_i c_i\right)=0 \tag{2.7b}$$

where c_i^s is the concentration of the solid phase (mol/m^3), w_s is the volumetric solid phase content (m^3/m^3), w is the volumetric water content (m^3/m^3), τ is apparent tortuosity of the concrete pore structure, which includes the effect of tortuosity and constrictiveness of the porous medium, n is the number of species, and r_i is the source/sink term to account for chemical production/consumption of species i.

The diffusion coefficient for the porous medium can be written as (Shackelford and Daniel 1991; Samson and Marchand 2007)

$$D_i=\tau D_i^0 P\left(D\right) \tag{2.8}$$

where, D_i^0 is the diffusion coefficient of species i in free-water (m^2/sec). Value of D_i^0 for OH, Na, K, SO_4, Ca, Cl, and $Al(OH)_4$ used in the current investigation are 10^{-9} times 5.27, 1.33, 1.96, 1.07, 0.792, 2.03, 0.54 m^2/s, respectively (Rumble et al, 2019), $P\left(D\right)$ is a

coefficient that reflects the effect of the medium porosity change (due to dissolution/precipitation of solids) on diffusion, given as (Samson and Marchand 2007)

$$P(D) = \frac{e^{4.3\phi/V_p}}{e^{4.3\phi_o/V_p}} \tag{2.9}$$

where ϕ_o is the initial porosity of concrete , ϕ is the porosity of concrete at a given age, per Eq. 2.10, and v_p is the volumetric paste content (m^3/m^3) of concrete

$$\phi = \phi_o + \sum_{m=1}^{M} \left(V_m^{ini} - V_m \right) \tag{2.10}$$

In Eq. 2.10, V_m^{ini} and V_m, respectively, are the initial and instantaneous volumetric content of a given solid phase (m^3/m^3), and M is the total number of solid phases. The above procedure is used to find the diffusion coefficients for both the Fick's and NPP model.

Local chemical equilibrium can be assumed at each point in the medium for the majority of ionic transport problems (Barbarulo et al. 2000). This allows one to separate the physical transport of the ions from the chemical equilibrium. This yields the conservation of mass as Eq. 2.11:

$$\frac{\partial(wc_i)}{\partial t} - \frac{\partial}{\partial x}\left(wD_i \left(\underbrace{\frac{dc_i}{dx}}_{molecular} + \underbrace{\frac{z_i F}{RT} c_i \frac{d\psi}{dx}}_{electric\ coupling} + \underbrace{c_i \frac{d\ln\gamma_i}{dx}}_{chemical\ activity} \right) \right) = -wr_i - \frac{\partial\left(w_s c_i^s\right)}{\partial t} \tag{2.11}$$

in which the right-hand terms can be evaluated in a separate chemical module and solved after solving the physical transport problem represented by the left-hand side of Eq. 2.11.

This is known as the operator-splitting approach and was applied due to its computational and modeling efficiencies (Yeh and Tripathi 1989). The validity of the local equilibrium assumption in concrete was established by Samson et al. (Samson and Marchand 2007), which justifies its implementation in the present formulation. Moreover, this assumption allows the use of a set of algebraic equations to enforce the chemical equilibrium rather than using the kinetics of reactions.

The implementation involves two computational modules which can be applied sequentially with (SIA) or without iteration (SNIA) between the transport and chemical modules. The SNIA was selected here due to its computational advantages and yielding good results for judiciously selected time steps.

2.3.1 Chloride Binding

Once chlorides enter concrete, they are partly bound by the other chemical species present in the concrete. Many researchers (Truc et al. 2000; Nilson 2008; Saetta et al. 1993) have used empirical chloride binding isotherms (e.g. Freundlich and Longmire isotherms) to model this phenomenon, but in the current study, based on ion-exchange theory, chloride binding is modeled as a chemical reaction producing Friedel's salt (Appelo 1996; Jones et al. 2003; Johannesson et al. 2007).

$$\left[\underbrace{AFm^{+}-SO_4^{2-}}_{monosulfate}\right]+2Cl^{-}\rightleftarrows\left[\underbrace{AFm^{+}-2Cl^{-}}_{Friedel's\ salt}\right]+SO_4^{2-} \qquad (2.12)$$

This basically relates the binding of chloride to the exchange between the sulfate and chloride ions in the monosulfate solid phase. Other forms of binding (i.e. physical binding)

is neglected in this research as it is reported to contribute negligibly to bind chlorides (Samson and Marchand 2006).

2.3.2 Chemical Reactions Modeling

Chemical reactions are modeled using the law of mass action which has the conservation of charges embedded in it (Moore 1972) and is represented by

$$K_m = \prod_{i=1}^{N} c_i^{\nu_{mi}} \gamma_j^{\nu_{mi}} \quad ; m = 1,...,M \tag{2.13}$$

where c_i is the molar concentration of ionic species (M), ν_{mi} is the stoichiometric coefficient of species i in the m^{th} solid, and K_m is the solubility constant of the m^{th} solid. Values for the common solid phases in concrete are given in Table 2.3 (Samson and Marchand 2006).

The different solid phases in concrete have common ions. Hence, one should solve the mass action equations for the solids simultaneously. This produces a nonlinear system of algebraic equations whose solution requires an iterative procedure.

2.4 FINITE ELEMENT FORMULATION

2.4.1 Transport Model Formulation

Equations (2.7a) and (2.7b) are solved by applying the Galerkin's weighted residual method (Zienkiewicz 1977). For convenience, without loss of generality, the details of the

formulation are presented for two ionic species, but in the computer program that is developed any number of species can be specified as demonstrated later.

For two species, the unknowns of the problem are the species concentrations, c_1, c_2, and the electrostatic potential, ψ. As Eqs. 2.7 (a) and (b) are second order partial differential equations, a two-node linear finite element would suffice to obtain a solution. The element nodal degrees of freedom (DOF) are the foregoing unknowns.

Let *u(x)* represent a typical field variable c_i or ψ, then

$$u_i(x) = a_1 + a_2 x = N_1 u_{i1} + N_2 u_{i2} \tag{2.14}$$

where a_1, a_2 are coefficients, which can be solved for in terms of the nodal values u_{i1}, u_{i2}, of the variable, and N_1, N_2 are shape functions

$$\begin{bmatrix} N_1 & N_2 \end{bmatrix} = \begin{bmatrix} 1 - \frac{x}{l} & \frac{x}{l} \end{bmatrix} \tag{2.15}$$

with l being the element length and x being a local coordinate. Hence, substituting for c_1, c_2 and ψ per Eq. 2.14 into the governing Eqs. (2.7a) and (2.7b), leads to the following residuals

$$R_1 = \frac{\partial (w c_1)}{\partial t} - \frac{\partial}{\partial x}\left(w D_1 \left(\frac{\partial c_1}{dx} + \frac{z_1 F}{RT} c_1 \frac{d\psi}{dx} + c_1 \frac{d \ln \gamma_1}{dx} \right) \right) \tag{2.16}$$

$$R_2 = \frac{\partial (w c_2)}{\partial t} - \frac{\partial}{\partial x}\left(w D_2 \left(\frac{\partial c_2}{dx} + \frac{z_2 F}{RT} c_2 \frac{d\psi}{dx} + c_2 \frac{d \ln \gamma_2}{dx} \right) \right) \tag{2.17}$$

$$R_3 = \frac{d}{dx}\left(\tau w \frac{d\psi}{dx} \right) + \frac{F}{\varepsilon} w \left(\sum_{i=1}^{N} z_i c_i \right) \tag{2.18}$$

Using the standard Galerkin's method (Logan 2001; Segerlind 1984), the following integral equation can be written by integrating over the volume, V, of the element

$$I = \int_V [N] R_i(x) dV = 0 \qquad ;(\text{i} = 1,2,3) \tag{2.19}$$

In expanded for, Eq. 2.19 is written as

$$I = A\int_l \begin{bmatrix} \zeta_1 & \zeta_2 & \zeta_3 \end{bmatrix} \begin{bmatrix} w & 0 & 0 \\ 0 & w & 0 \\ 0 & 0 & 0 \end{bmatrix} \begin{bmatrix} \dot{c}_1 \\ \dot{c}_2 \\ \dot{\psi} \end{bmatrix} dx +$$

$$+A\int_l \begin{bmatrix} \frac{d\zeta_1}{dx} & \frac{d\zeta_2}{dx} & \frac{d\zeta_3}{dx} \end{bmatrix} \begin{bmatrix} wD_1 & 0 & \frac{D_1 z_1 F}{RT} wc_1 \\ 0 & wD_2 & \frac{D_2 z_2 F}{RT} wc_2 \\ 0 & 0 & \tau w \end{bmatrix} \begin{bmatrix} c_{1,x} \\ c_{2,x} \\ \psi_{,x} \end{bmatrix} dx +$$

$$+A\int_l \begin{bmatrix} \frac{d\zeta_1}{dx} & \frac{d\zeta_2}{dx} & \frac{d\zeta_3}{dx} \end{bmatrix} \begin{bmatrix} wD_1 \frac{d\ln\gamma_1}{dx} & 0 & 0 \\ 0 & wD_2 \frac{d\ln\gamma_2}{dx} & 0 \\ 0 & 0 & 0 \end{bmatrix} \begin{bmatrix} c_1 \\ c_2 \\ \psi \end{bmatrix} dx + \tag{2.20}$$

$$+A\int_l \begin{bmatrix} \zeta_1 & \zeta_2 & \zeta_3 \end{bmatrix} \begin{bmatrix} 0 & 0 & 0 \\ 0 & 0 & 0 \\ -\frac{F}{\varepsilon} wz_1 & -\frac{F}{\varepsilon} wz_2 & 0 \end{bmatrix} \begin{bmatrix} c_1 \\ c_2 \\ \psi \end{bmatrix} dx + B.I. = 0$$

where ζ_i is the weighing function for variable i, l is the length of element, and $B.I.$ are the boundary terms which are omitted as only Dirichlet-type boundary conditions are specified.

For a two-node linear element,

$$\begin{bmatrix} c_1 \\ c_2 \\ \psi \end{bmatrix} = [N][U_n] \tag{2.21}$$

$$[N] = \begin{bmatrix} N_1 & 0 & 0 & N_2 & 0 & 0 \\ 0 & N_1 & 0 & 0 & N_2 & 0 \\ 0 & 0 & N_1 & 0 & 0 & N_2 \end{bmatrix} \tag{2.22}$$

$$[U_n] = [c_{11} \quad c_{21} \quad \psi_1 \quad c_{12} \quad c_{22} \quad \psi_2]' \tag{2.23}$$

where c_{ij} is the concentration of species i at node j of the element. By applying integration by parts, after the minimization, one can write

$$[M]^e = A\int_l [N]^T [C][N]dx \tag{2.24}$$

$$[K]^e = A\int_l [B]^T [k_I][B]dx + A\int_l [N]^T [k_{II}][N]dx + A\int_l [B]^T [k_{III}][N]dx \tag{2.25}$$

where

$$[C] = \begin{bmatrix} w & 0 & 0 \\ 0 & w & 0 \\ 0 & 0 & 0 \end{bmatrix} \tag{2.26}$$

$$[B]=\begin{bmatrix} N_{1,x} & 0 & 0 & N_{2,x} & 0 & 0 \\ 0 & N_{1,x} & 0 & 0 & N_{2,x} & 0 \\ 0 & 0 & N_{1,x} & 0 & 0 & N_{2,x} \end{bmatrix} \tag{2.27}$$

$$[k_I]=\begin{bmatrix} wD_1 & 0 & \frac{D_1 z_1 F}{RT} wc_1 \\ 0 & wD_2 & \frac{D_2 z_2 F}{RT} wc_2 \\ 0 & 0 & \tau w \end{bmatrix} \tag{2.28}$$

$$[k_{II}]=\begin{bmatrix} wD_1 \frac{d\ln\gamma_1}{dx} & 0 & 0 \\ 0 & wD_2 \frac{d\ln\gamma_2}{dx} & 0 \\ 0 & 0 & 0 \end{bmatrix} \tag{2.29}$$

$$[k_{III}]=\begin{bmatrix} 0 & 0 & 0 \\ 0 & 0 & 0 \\ -\frac{F}{\varepsilon} wz_1 & -\frac{F}{\varepsilon} wz_2 & 0 \end{bmatrix} \tag{2.30}$$

By applying direct assembly of $[M]^e$ and $[K]^e$ matrices, the following system of equation can be obtained:

$$[M]\left[\dot{U}\right]+[K][U]=0 \tag{2.31}$$

The equations are semi-discretized in space. Thus, time-discretization of the quasi-harmonic Nernst-Plank equation was done following first-order single time-step algorithm with implicit Euler scheme as follows:

$$[M_t]\left[\frac{U_t - U_{t-\Delta t}}{\Delta t}\right] + [K_t][U_t] = 0 \tag{2.32}$$

$$\left(M_t + \Delta t\, K_t\right)U_t = \left[M_t\, U_{t-\Delta t}\right] \tag{2.33}$$

$$\left[\widehat{K}\right][U_t] = \left[\widehat{F}\right] \tag{2.34}$$

where U_t are the unknowns values at current time step, $U_{t-\Delta t}$ are the values from previous time step, Δt is the time-step, and $[M]$ is a lumped matrix by summation of rows method. This improves the convergence of selected time-discretization scheme.

Thus, Eq. 2.31 provides a system of nonlinear algebraic equations which need to be solved at each time-step. Several methods can be used to solve this system (Heath 2002); here the Newton-Raphson's method was applied. The nonlinear terms in the tangent matrix make small contribution to convergence rate, thus, the tangent matrix without the nonlinear terms is shown in Eq. 2.35.

$$\left[K_T^e\right] = \left[M^e\right] + \Delta t\left[K^e\right] \tag{2.35}$$

All the variables appearing in Eqs. 2.28, 2.29, and 2.30 are evaluated at the integration points based on Gauss quadrature.

2.4.2 Chemical module

Applying the mass action equation to the different solid phases yields a system of nonlinear algebraic equations which need to be solved simultaneously.

The unknowns of the problem are the concentrations of solids required to restore the chemical equilibrium to the system of phases X_{CH}, X_{AFt}, X_{AFm} and X_{FS}, with the latter symbols denoting the quantities of portlandite, ettringite, monosulfates and Friedel's salt, respectively.

The Newton-Raphson method is applied to solve this system of equations. The chemical balance equations included in this study are as follows:

$$R_{CH} = \{Ca\}\{OH\}^2 - K_{CH} \tag{2.36}$$

$$R_{AFt} = \{Ca\}^6\{OH\}^4\{SO_4\}^3\{Al(OH)_4\}^2 - K_{AFt} \tag{2.37}$$

$$R_{AFm} = \{Ca\}^4\{OH\}^4\{SO_4\}\{Al(OH)_4\}^2 - K_{AFm} \tag{2.38}$$

$$R_{FS} = \{Cl\}^2[AFm]/\{SO_4\}[FS] - K_{FS} \tag{2.39}$$

and values of the relevant equilibrium constants are shown in Table 2.3.

Thus, the concentration of the ions can be represented in terms of the amount of the solids dissolution/precipitation necessary to restore equilibrium of $X_m s$.

$$[Ca] = [Ca]^0 + X_{CH} + 6X_{AFt} + 4X_{AFm} \tag{2.40}$$

$$[OH] = [OH]^0 + 2X_{CH} + 4X_{AFt} + 4X_{AFm} \tag{2.41}$$

$$[SO_4] = [SO_4]^0 + 3X_{AFt} + X_{AFm} - X_{FS} \tag{2.42}$$

$$\left[Al(OH)_4\right] = \left[Al(OH)_4\right]^0 + 2X_{AFt} + 2X_{AFm} \tag{2.43}$$

$$[Cl] = [Cl]^0 + 2X_{FS} \tag{2.44}$$

where the magnitude of the quantities inside the $[\ ]^0$ brackets is provided by the transport module, but they do not satisfy equilibrium and need to be corrected to satisfy equilibrium. The chemical activity is evaluated at each iteration following Eq. 2.6.

The Jacobian matrix used in the Newton-Raphson method is given by Eq. 2.45 and is derived by considering chemical activity as constant in each iteration. For more details the reader can refer to Samson et al. (Samson and Marchand 2006).

$$[K_T] = \begin{bmatrix} \frac{\partial R_{CH}}{\partial X_{CH}} & \frac{\partial R_{CH}}{\partial X_{AFt}} & \frac{\partial R_{CH}}{\partial X_{AFm}} & \frac{\partial R_{CH}}{\partial X_{FS}} \\ \frac{\partial R_{AFt}}{\partial X_{CH}} & \frac{\partial R_{AFt}}{\partial X_{AFt}} & \frac{\partial R_{AFt}}{\partial X_{AFm}} & \frac{\partial R_{AFt}}{\partial X_{FS}} \\ \frac{\partial R_{AFm}}{\partial X_{CH}} & \frac{\partial R_{AFm}}{\partial X_{AFt}} & \frac{\partial R_{AFm}}{\partial X_{AFm}} & \frac{\partial R_{AFm}}{\partial X_{FS}} \\ \frac{\partial R_{FS}}{\partial X_{CH}} & \frac{\partial R_{FS}}{\partial X_{AFt}} & \frac{\partial R_{FS}}{\partial X_{AFm}} & \frac{\partial R_{FS}}{\partial X_{FS}} \end{bmatrix} \tag{2.45}$$

Finally, the solid phases content is updated using the following relation:

$$S_m^t = S_m^{t-1} - wX_m\Gamma_m / \rho \tag{2.46}$$

where S_m is the content of solid phase m [g/kg of concrete], Γ_m is the molar mass of the solid m [g/mol], ρ is the density of saturated concrete [kg/m^3], and superscript t indicates the time-step. It should be mentioned that the change in the solid content is accompanied

by change in volumetric water content, but in the current model the later change is assumed to be negligible. The validity of this assumption may need further investigation.

2.4.3 Computer Implementation

The above procedures are implemented in a computer program following the flowchart in Fig. 2.1.

2.5 MODEL VERIFICATION

2.5.1 Model Description

The finite element model was developed within the MATLAB platform (The MathWorks Inc. 2018) and was verified by comparing its results with Samson et al. test results (Samson and Marchand 2006). The test samples were 50-60 mm concrete disks subjected to sodium chloride solution on one face and sealed by wax on the other face and the sides. They were moist cured from 28 days to more than a year. The experiments were conducted in a temperature-controlled environment, thus temperature effect is neglected in this study. The concrete mixture proportions, porosity and the cement and concrete pore solution initial compositions are given in Table 2.4. The table also gives the diffusion coefficients of the ions present in the pore solution and the initial concentration of the four solid phases, viz. Portlandite, Ettringite, Monosulfate, and Friedel's salt.

The samples were subjected to 0.5 M sodium chloride solution which was maintained constant throughout the test. Measurement of total chloride content was performed

following ASTM C1556 layer-by-layer acid dissolution procedure (ASTM 2016) in 3-4 mm depth increments. Companion samples were prepared to evaluate the transport properties of the medium (Samson et al. 2003).

The finite element mesh used for modelling diffusion through the concrete discs comprised a non-uniform mesh of 100 elements. The element length was chosen as 0.1 mm for the first 5 mm from the exposed surface, 0.5 mm for the region located from 5 to 10 mm from the exposed surface, and 1 mm for the remining depth. The time step was selected as 1800 sec.

2.5.2 Comparison of Finite Element Results with Experimental Data

In Fig. 2.2 the computed total chloride profiles are compared with corresponding experimental profiles obtained after one month (1M) and eight months (8M) of exposure. The model results are based on the comprehensive implementation of the NPP model, accounting for the three modes of transport mentioned earlier. It can be seen that the computed profiles are in reasonable agreement with their experimental counterparts.

2.6 FURTHER ANALYSIS OF THE MODEL RESULTS

2.6.1 Effect of the Three Modes of Transport in NPP on Concentration of chemical Species and Concrete pH

In order to examine possible simplification of Eq. 2.2, three simulations were performed, considering: (1) only molecular diffusion, (2) molecular diffusion and electromigration,

and (3) the full NPP, including chemical activity. The properties of the concrete used in these simulations are those given in Table 2.4. The results of the simulations are presented in Figs. 2.3-2.7.

In Fig. 2.3 it can be observed that molecular diffusion dominates the transport of chlorides with significant, albeit much smaller, contribution by electromigration. As expected, due to the relatively dilute nature of the pore solution, the contribution of chemical activity seems to be practically negligible and this agrees with the prevailing practice when modelling chloride diffusion in concrete. It should be mentioned that this simulation is conducted assuming fully saturated condition. However, in the case of concrete under wet/dry cycles, which is out of the scope of this work, transport by advection is expected to be significant at depths close to the exposed surface.

Figure 2.4 shows the variation of concrete pH through the test specimen thickness after one and eight months of exposure to a sodium chloride solution. Again, the effect of chemical activity on pH variation is negligible but that of electromigration is noticeable. After one month of exposure, electromigration tends to lower the pH within the first 17.5 mm from the exposed surface while it increases it below that depth. So, the effect is not uniform and depends on the chloride concentration within the concrete. Comparing the one month and eight months pH profiles, the pH seems to be decreasing with time in the region closer to the exposed surface (first 12.5 mm from the exposed surface) and increasing beyond that. Practically, this would make the reinforcement located closer to the exposed surface more vulnerable to corrosion. Clearly, the traditional Fick's law models are not able to provide information about pH and its variation through the concrete.

The effect of the chloride diffusion mode on ettringite formation after one month of exposure is shown in Fig. 2.5. It can be seen that neither electromigration nor chemical activity has significant effect on the formation of this phase. Further study may be required to determine their effects in concretes made with cements of different composition and after much longer exposure periods.

The FEM results also show that electromigration and chemical activity make negligible contribution to the production/consumption of all four solid phases considered in this study. Consequently, the Fick's model, in the manner formulated in this investigation, i.e. uncouple diffusion of chemically interacting species, would predict the change in solid phases concentration satisfactorily.

2.6.2 Effect of the deicing Salt composition on Concentration of Chemical Species and Concrete pH

Finally, the effect of the diffusion of different types of salts on chloride and Friedel's salt concentrations predicted by the NPP model are shown in Fig. 2.6 while their effect on concrete pH is shown in Fig. 2.7. Notice that the salts of monovalent sodium and potassium behave similarly while that of calcium has significantly different behavior. After one month of diffusion under identical conditions, NaCl and KCl lead to much higher concentration of chloride in the concrete compared $CaCl_2$. Similarly, the former two salts generate the same amount of Friedel's salt while the latter produces noticeably higher amount. With reference to Fig. 2.7, NaCl and KCl have similar effect on concrete pH while $CaCl_2$ causes

higher reduction in pH. Thus, the NPP provides more comprehensive information about the chemical state of the concrete after exposure to different types of salts or other chemicals than the Fick's model.

2.6.3 Effect of Modelling on Computer Resources Requirements

Figure 2.8 shows the computer memory and CPU time requirements for the one-month chloride diffusion simulation by the different models. There is significant saving in the CPU time required, about 50% in the case of Fick's model compared to the full NPP model. However, the memory demand for the Fick's model is only 1% less than that of the full NPP, which is clearly negligible. There is, however, significant difference between both the CPU time and the memory requirements of the models with and without the inclusion of chemical activity. This difference can be attributed to more computation time required to achieve convergence of the numerical solution. Thus, including chemical activity in the model tends to accelerate convergence. Therefore, although the chemical activity has negligible effect on the chloride concentration and pH profiles of concrete, it seems to have beneficial effect on achieving rapid convergence of the numerical solution.

Based on the above observations, it is clear that the full NPP model is practically more accurate and efficient than applying the modified Fick's model or than a model that includes diffusion and electromigration only.

2.7 CONCLUSIONS

The Nernst-Planck Poisson's (NPP) and the modified Fick's diffusion models are implemented in the Galerkin's finite element formulation. The NPP includes molecular diffusion, electromigration and diffusion due to chemical activity. Both models are formulated to account for chemical reactions between the diffusing salt ions and the chemicals in the concrete pore solution, but in the Fick's model no interaction is considered among the chemicals at the transport stage. The NPP model results are validated with available experimental data in the literature. Subsequently, the modelling effects on chloride diffusion, concrete pH, solid phases formation and salt type diffusion on chloride concentration and concrete pH are investigated. The results of the study support the following conclusions:

1. Electromigration, a mode of chemical transport activated by the electrostatic field created by ions in a solution and included in the NPP model, has significant effect on the transport of chlorides in concrete.
2. Transport due to chemical activity gradient has negligible effect on chloride concentration or pH of concrete, but speeds up the convergence of the numerical process if included in the model.
3. Fick's law neglects the electrical interaction among concurrently diffusing ions in the concrete pore solution and thus does not accurately predict the effects of salt type and other chemicals in the pore solution on concrete pH and its chloride concentration.

4. The presence and diffusion of companion ions during chloride diffusion in concrete affect chloride binding, concrete pH and chloride concentration.
5. Although models based on Fick's law require less CPU time, their results are less accurate than those of the NPP model.
6. Diffusion of calcium chloride leads to higher production of Friedel's salt, lower chloride concentration and lower pH compared to diffusion of sodium chloride and potassium chloride, with the latter two salts giving similar results.

To obtain more theoretically accurate and comprehensive information about the changes to the concrete chemical composition due to diffusion of salts, the application of NPP model is recommended. However, the extent of this accuracy cannot be generalized because it will depend on the magnitude of the governing parameters of the problem. Nevertheless, in the specific case of the current example, the difference in Cl- concentration predicted by the current model versus the Fickean model is 24 to 85 percent. When referring to the accuracy of a model or simulation, this is relative, but in the context of the present work, ±10% difference between the experimental and corresponding computed values is deemed to be acceptable and any smaller difference implies high accuracy. Given the microscopically heterogeneous nature of concrete, it is important to base the accuracy on an overall criterion or norm such as the Euclidean norm.

2.8 ACKNOWLEDGMENTS

The first author gratefully acknowledges the financial support of McMaster University and the Natural Sciences and Engineering Research Council Canada (NSERC) in support of this research. The second author wishes to thank NSERC for its financial support of the investigation through its Discovery Grant program. The second author is also grateful for the generous financial support given by the Tianjin government, the Government of China and Nankai University to complete this research and get it ready for publication.

2.9 REFERENCES

Appelo, C.A.J., Multicomponent Ion Exchange and Chromatography in Natural Systems. Reactive Transport In Porous Media, 1996. 34: p. 193-227.

ASTM, ASTM C1556 - 11a: Standard Test Method for Determining The Apparent Chloride Diffusion Coefficient of Cementitious Mixtures By Bulk Diffusion. 2016, ASTM International: West Conshohocken, PA

Barbarulo, R., Marchand, J., Snyder, K.A., Prené, S. Dimensional Analysis of Ionic Transport Problems in Hydrated Cement Systems - Part 1. Theoretical Considerations. Cement and Concrete Research, 2000. 30(12): p. 1955-1960. https://doi.org/10.1016/s0008-8846(00)00383-5.

Bertolini, L., Elsener, B., Pedeferri, P., and Polder, R. Corrosion of steel in concrete : Prevention, Diagnosis, Repair. 2004: Wiley.

Chatterji, S. (b), Transportation of Ions Through Cement Based Materials. Part 2. Adaptation of The Fundamental Equations and Relevant Comments. Cement and Concrete Research, 1994. 24(6): p. 1010-1014. https://doi.org/http://dx.doi.org/10.1016/0008-8846(94)90010-8.

Chatterji, S. (a). "Transportation of Ions Through Cement Based Materials. Part 2. Adaptation of The Fundamental Equations and Relevant Comments." *Cement and Concrete Research*, 1994. 24 (6): 1010-1014. https://doi.org/http://dx.doi.org/10.1016/0008-8846(94)90023-X.

Christopher, H.A. and Shipman, C.W. Poisson's Equation as A Condition of Equilibrium in Electrochemical Systems. Journal of The Electrochemical Society, 1968. 115(5): p. 501-506. https://doi.org/10.1149/1.2411292.

Collepardi, M., Marciallis, A., and Turriziani, R. The Kinetics of Chloride Ions Penetration in Concrete (in Italian). Il Cemento, 1970. 4: p. 157-164.

Damrongwiriyanupap, N., Li, L.Y. and Xi, Y.P. Coupled Diffusion of Multi-Component Chemicals in Nonsaturated Concrete. Computers and Concrete, 2013. 11(3): p. 201-222.

Galindez, J.M. and Molinero, J. On the Relevance of Electrochemical Diffusion for The Modeling of Degradation of Cementitious Materials. Cement & Concrete Composites, 2010. 32(5): p. 351-359. https://doi.org/10.1016/j.cemconcomp.2010.02.006.

Gautefall, O. and Vennesland, Methods for Determination of Chloride Diffusivity in Concrete. 1994 REPCON: Statens Vegvesen, Vegdirektoratet, Oslo, Norway.

Heath, M. T.. Scientific Computing: An Introductory Survey. SIAM. Philadelphia: 2018: McGraw-Hill.

Isgor, O.B. and Razaqpur, A.G. Finite Element Modeling of Coupled Heat Transfer, Moisture Transport and Carbonation Processes in Concrete Structures. Cement & Concrete Composites, 2004. 26(1): p. 57-73. https://doi.org/10.1016/s0958-9465(02)00125-7

Johannesson, B., Yamada, K., Nilsson, L.O. and Hosokawa, Y. Multi-Species Ionic Diffusion in Concrete With Account to Interaction Between Ions in The Pore Solution And The Cement Hydrates. Materials and Structures, 2007. 40(7): p. 651-665. https://doi.org/10.1617/s11527-006-9176-y.

Jones, M.R., Macphee, D.E., Chudek, J.A., Hunter, G., Lannegrand, R., Talero, R., Scrimgeour, S.N. Studies Using 27Al MAS NMR Of AFm And AFt Phases And The Formation Of Friedel's Salt. Cement and Concrete Research, 2003. 33(2): p. 177-182. http://dx.doi.org/10.1016/S0008-8846(02)00901-8.

Krabbenhoft, K. and Krabbenhoft, J. Application of the Poisson-Nernst-Planck Equations to The Migration Test. Cement and Concrete Research, 2008. 38(1): p. 77-88. https://doi.org/10.1016/j.cemconres.2007.08.006.

Li, L.Y. and Page, C.L. Finite Element Modelling of Chloride Removal From Concrete By An Electrochemical Method. Corrosion Science, 2000. 42(12): p. 2145-2165. https://doi.org/10.1016/s0010-938x(00)00044-5.

Logan, D. L. A First Course in the Finite Element Method. Fifth Edit. Stamford, CT: 2012: Cengage Learning.

Lorente, S., Voinitchi, D., and Bégué-Escaffit, P. The Single-Valued Diffusion Coefficient for Ionic Diffusion Through Porous Media. Journal of Applied Physics, 2007. 101(2). https://doi.org/10.1063/1.2426375.

Marchand, J. and Samson, E., Predicting the Service-Life Of Concrete Structures - Limitations Of Simplified Models. Cement & Concrete Composites, 2009. 31(8): p. 515-521. https://doi.org/10.1016/j.cemconcomp.2009.01.007.

Monteiro, P.J.M., Gjorv, O.E., and Mehta, P.K. Microstructure of The Steel-Cement Paste Interface in The Presence Of Chloride. Cement and Concrete Research, 1985. 15(5): p. 781-784. https://doi.org/10.1016/0008-8846(85)90143-7.

Moore, W.J., Physical Chemistry [by] Walter J. Moore. 1972: Longman

Morinaga, S., Prediction of Service Lives of Reinforced Concrete Buildings Based on Rate of Corrosion of Reinforcing Steel. 1988, Shimizu Corp: Japan. p. 82–89.

Newman, J. and Thomas-Alyea, K.E. Electrochemical Systems, 3rd Edition. 2004: Wiley

Nilson, L.O., Models For Chloride Ingress Into Concrete - From Collepardi To Today. Advances in Concrete Structural Durability, Proceedings of Icdcs2008, Vols 1 and 2, 2008: p. 36-42..

Pitzer, K.S., Activity Coefficients in Electrolyte Solutions. 1991: CRC Press. 75–153.

Pivonka, P., Smith, D., and Gardiner, B. Investigation of Donnan equilibrium in charged porous materials—a scale transition analysis. Transport in Porous Media, 2007. 69(2): p. 215-237. https://doi.org/10.1007/s11242-006-9071-6.

Purvis, R.L. and Babaei, K. Methodology for The Protection and Rehabilitation of Reinforced Concrete Bridge Components With Chloride-Induced Corrosion. 10th Annual International Bridge Conference, Official Proceedings, 1993: p. 209-218.

Rumble, J.R., Lide, D.R.and Bruno, T.J. CRC Handbook of Chemistry and Physics : a Ready-Reference Book of Chemical and Physical Data. 2019: CRC Press/ Taylor & Francis.

Saetta, A.V., Scotta, R.V., and Vitaliani, R.V. Analysis of Chloride Diffusion Into Partially Saturated Concrete. ACI Materials Journal, 1993. 90(5): p. 441-451.

Samson, E., Lemaire, G., Marchanda, J., Beaudoinc, J.J. Modeling Chemical Activity Effects in Strong Ionic Solutions. Computational Materials Science, 1999. 15(3): p. 285-294. https://doi.org/10.1016/s0927-0256(99)00017-8.

Samson, E. and Marchand, J. Numerical Solution of The Extended Nernst-Planck Model. Journal of Colloid and Interface Science, 1999. 215(1): p. 1-8. https://doi.org/10.1006/jcis.1999.6145.

Samson, E. and Marchand, J. Modeling the Transport of Ions in Unsaturated Cement-Based Materials. Computers & Structures, 2007. 85(23-24): p. 1740-1756. https://doi.org/10.1016/j.compstruc.2007.04.008.

Samson, E., Marchand, J. and Snyder, K.A. Calculation of Ionic Diffusion Coefficients on The Basis of Migration Test Results. Materials and Structures, 2003. 36(257): p. 156-165. https://doi.org/10.1617/14002.

Samson, E. and Marchand, J. Multiionic Approaches to Model Chloride Binding in Cementitious Materials. 2006, RILEM Publication SARL.

Segerlind, L. J. 1984. Applied Finite Element Analysis. Second Ed. United States of America: John Wiley and Sons.

Sergi, G., Yu, S.W., and. Page, C.L. Diffusion of Chloride And Hydroxyl Ions in Cementitious Materials Exposed to A Saline Environment. Magazine of Concrete Research, 1992. 44(158): p. 63-69.

Shackelford, C.D. and Daniel, D.E. Diffusion in Saturated Soil .1. Background. Journal of Geotechnical Engineering-ASCE, 1991. 117(3): p. 467-484. https://doi.org/10.1061/(asce)0733-9410(1991)117:3(467).

Szyszkiewicz-Warzecha, K., Jasielec, J. J., Fausek, J. and Filipek, R. Determination of Diffusion Coefficients in Cement-Based Materials: An Inverse Problem for The Nernst-Planck And Poisson Models. Journal of Materials Engineering And Performance, 2016. 25(8): p. 3291-3295. https://doi.org/10.1007/s11665-016-2167-4.

Takewaka, K. and Mastumoto, S. Quality and Cover Thickness of Concrete Based on The Estimation of Chloride Penetration in Marine Environments. Concrete in Marine Environment: Proceedings, 1988. 109: p. 381-400.

Tang, L.P. and Nilsson, L.O. Chloride Binding-Capacity and Binding Isotherms of opt Pastes And Mortars. Cement and Concrete Research, 1993. 23(2): p. 247-253.

The MathWorks Inc., MATLAB. 2018.

Truc, O., Ollivier, J.P. and Nilsson, L.O. Numerical Simulation of Multi-Species Diffusion. Materials and Structures, 2000. 33(233): p. 566-573. https://doi.org/10.1007/bf02480537.

Uji, K., Matsuoka, Y., and Maruya, T. Formulation of An Equation for Surface Chloride Content of Concrete Due to Permeation of Chloride. Corrosion of Reinforcement in Concrete, 1990: p. 258-267.

Wang, Y., Li, L.Y. and Page, C.L. Modelling of Chloride Ingress Into Concrete from A Saline Environment. Building and Environment, 2005. 40(12): p. 1573-1582. https://doi.org/10.1016/j.buildenv.2005.02.001.

Xia, J. and Li, L.-y. Numerical Simulation of Ionic Transport in Cement Paste Under The Action of Externally Applied Electric Field. Construction and Building Materials, 2013. 39: p. 51-59. https://doi.org/https://doi.org/10.1016/j.conbuildmat.2012.05.036.

Yeh, G.T. and Tripathi, V.S. A Critical-Evaluation of Recent Developments in Hydrogeochemical Transport Models of Reactive Multichemical Components. Water Resources Research, 1989. 25(1): p. 93-108. https://doi.org/10.1029/WR025i001p00093.

Yu, Y.G., Zhang, Y.X., and Khennane, A. Numerical Modelling of Degradation of Cement-Based Materials Under Leaching and External Sulfate Attack. Computers & Structures, 2015. 158: p. 1-14.. https://doi.org/10.1016/j.compstruc.2015.05.030.

Zienkiewicz, O.C., The Finite Element Method Its Basis and Fundamentals, R.L. Taylor, et al., Editors. 1977, Elsevier Butterworth-Heinemann.

Table 2.1: Summary of recent research using NPP in modeling chloride diffusion in concrete structures

Research work	Diffusion mechanisms			Charges interaction			Chemical reactions		Year
	Molecular	Electro-migration	Chemical activity	Poisson's	Electro-neutrality	Null current	Binding isotherms	Chemical equilibrium	
Truc et al. [21]	✓	✓			✓	✓	✓		2000
Page et al. [16]	✓	✓			✓		✓		2000
Wang et al. [17]	✓	✓			✓		✓		2005
Pivonka et al. [24]	✓	✓			✓		✓		2006
Johannesson et al. [19]	✓	✓			✓			✓	2007
Krabbenhøft et al. [25]	✓	✓			✓		✓		2008
Samson et al. [23]	✓	✓	✓	✓				✓	2008
Damrongwiriyanupap et al. [20]	✓	✓			✓		✓		2012
Xia et al, [26]	✓	✓			✓		✓		2013
Yu et al. [22]	✓	✓	✓	✓				✓	2015
Szyszkiewicz et al [18]	✓	✓		✓			Finding lumped D_i from experimental data		2016

Table 2.2: Parameter a_i value for common ions in the concrete pore solution:

Ion	$\boldsymbol{a_i}$ (m) x 10^{-10}	Ion	$\boldsymbol{a_i}$ (m) x 10^{-10}
OH^-	3	SO_4^{2-}	1
Na^+	3	Ca^{2+}	1 x 10^{-3}
K^+	3.3	Cl^-	2

Table 2.3: Chemical equilibrium constants for different solid phases

Solid Phase	Equilibrium relationship	$-\boldsymbol{log}(\boldsymbol{K_m})$
Portlandite	$K_{sp} = \{Ca\}\{OH\}^2$	5.2
C-S-H	$K_{sp} = \{Ca\}\{OH\}^2$	6.2
Ettringite	$K_{sp} = \{Ca\}^6\{OH\}^4\{SO_4\}^3\{Al(OH)_4\}^2$	44
Monosulfate	$K_{sp} = \{Ca\}^4\{OH\}^4\{SO_4\}\{Al(OH)_4\}^2$	29.1
Gypsum	$K_{sp} = \{Ca\}\{SO_4\}$	4.6
Mirabilite	$K_{sp} = \{Na\}^2\{SO_4\}$	1.2
Friedel's salt*	$K_m = \{Cl\}^2[AFm]/\{SO_4\}[FS]$	-3

*ion exchange, $\{..\}$ indicates activity of species, $[..]$ indicates the solid content in mmol/g of concrete.

Table 2.4: Concrete properties and pore solution composition used in code verification

Property	**Value**	**Property**	**Value**
Cement type	CSA, T10	Porosity	13.4 %
w/c	0.65	Tortuosity	0.0368
Mixture proportions	**(kg/m^3)**	**Diffusion Coefficients**	**(x10^{-11} m^2/s)**
Cement	280	OH^-	19.4
Water	182	Na^+	4.9
Coarse aggregates	1065	K^+	7.2
Fine aggregates	833	SO_4^{2-}	3.9
Density	2360	Ca^{2+}	2.9
		$Al(OH)_4^-$	2.0
Cement composition	**(% mass)**	Cl^-	7.5
CaO	62.10		
SiO_2	20.40	**Initial pore solution**	**(mmol/L)**
Al_2O_3	4.30	OH^-	273.5
SO_3	3.20	Na^+	133.5
		K^+	140.1
Initial solids phases	**(g/kg)**	SO_4^{2-}	1.7
Portlandite (CH)	35.1	Ca^{2+}	1.7
C-S-H	73.5	$Al(OH)_4^-$	0.1
Ettringite (AFt)	2.9	Cl^-	0
Monosulfate (AFm)	25.2		

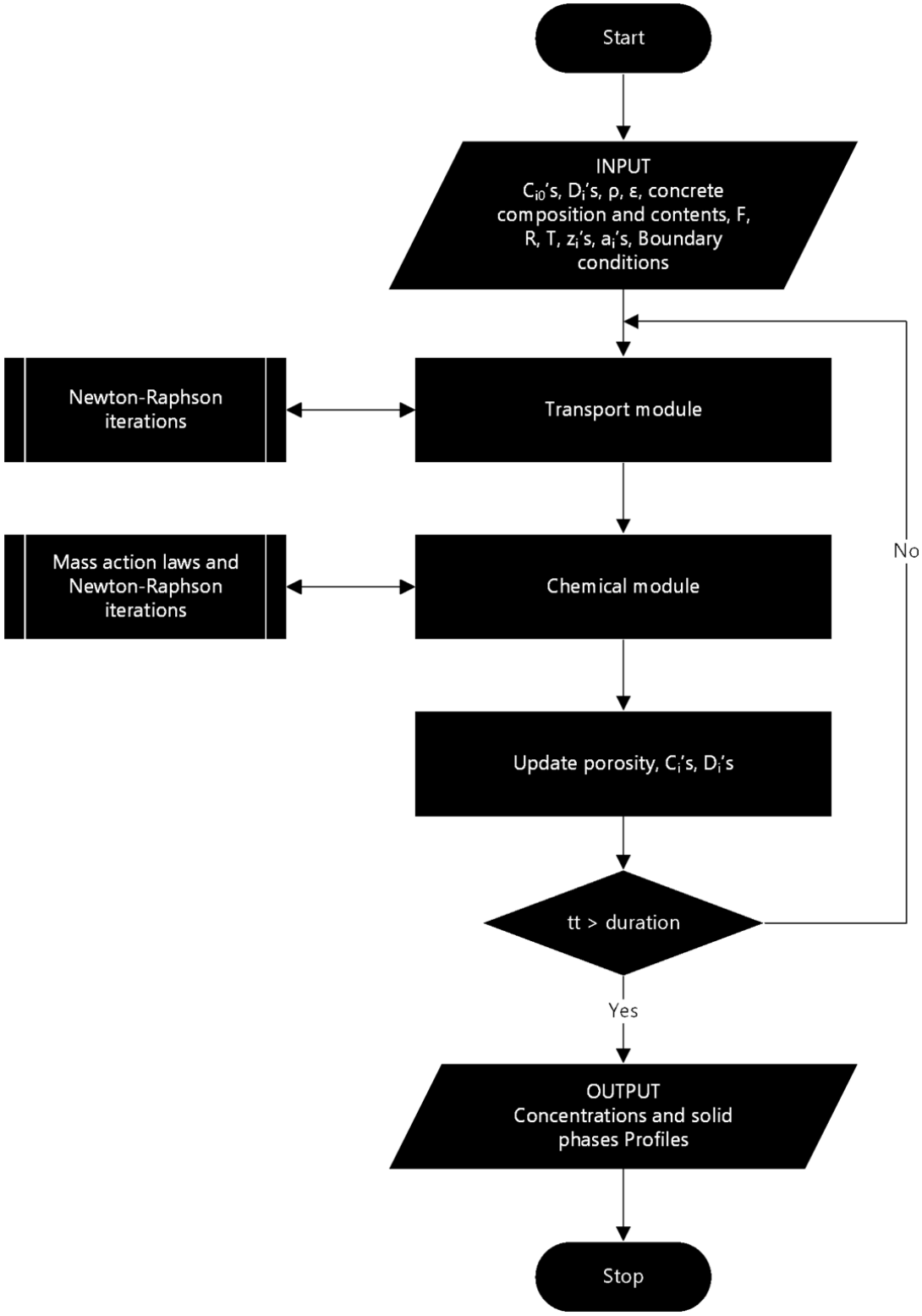

Fig. 2.1: Flowchart for the computer implementation of the model used

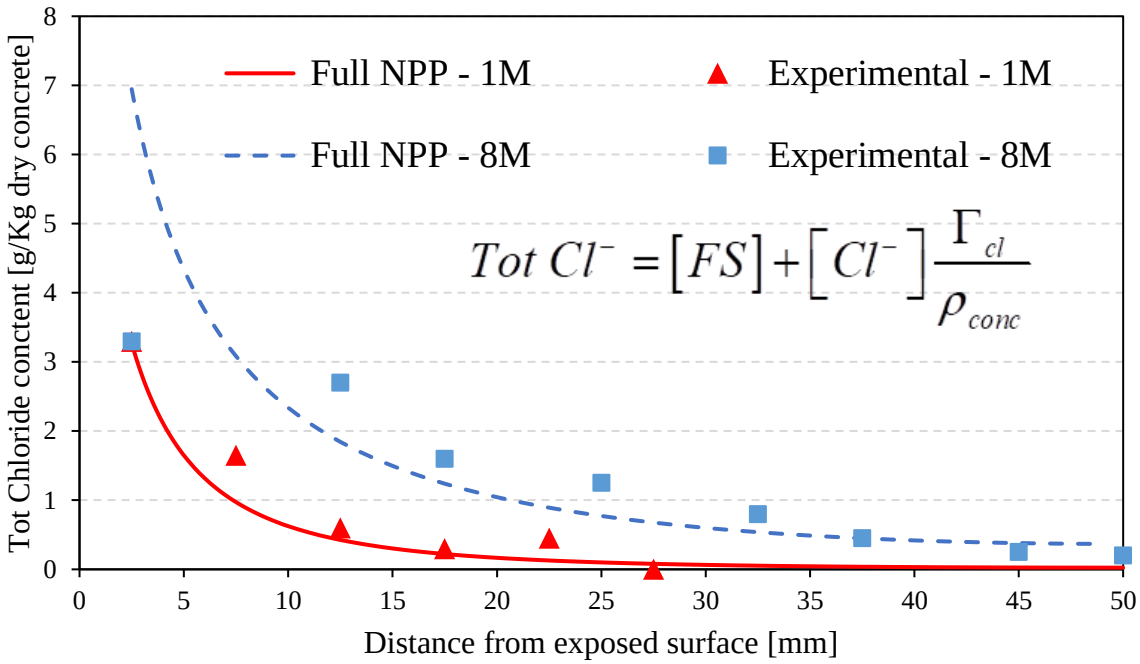

Fig. 2.2: Comparison of predicted and measured chloride concentrations after one month and eight months of exposure results

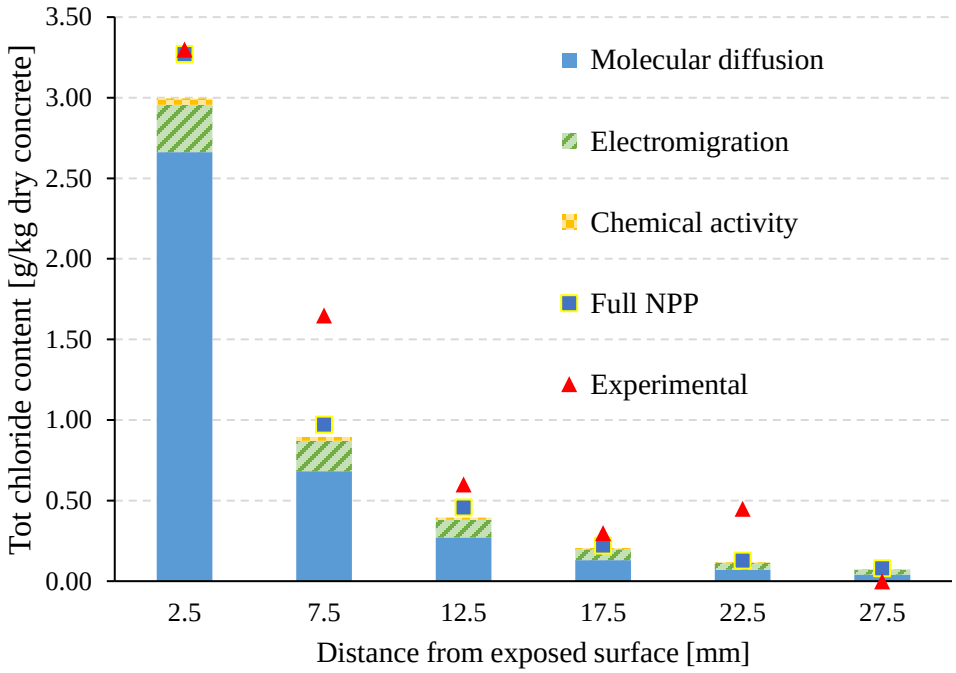

Fig. 2.3: Total chloride content profiles at one month

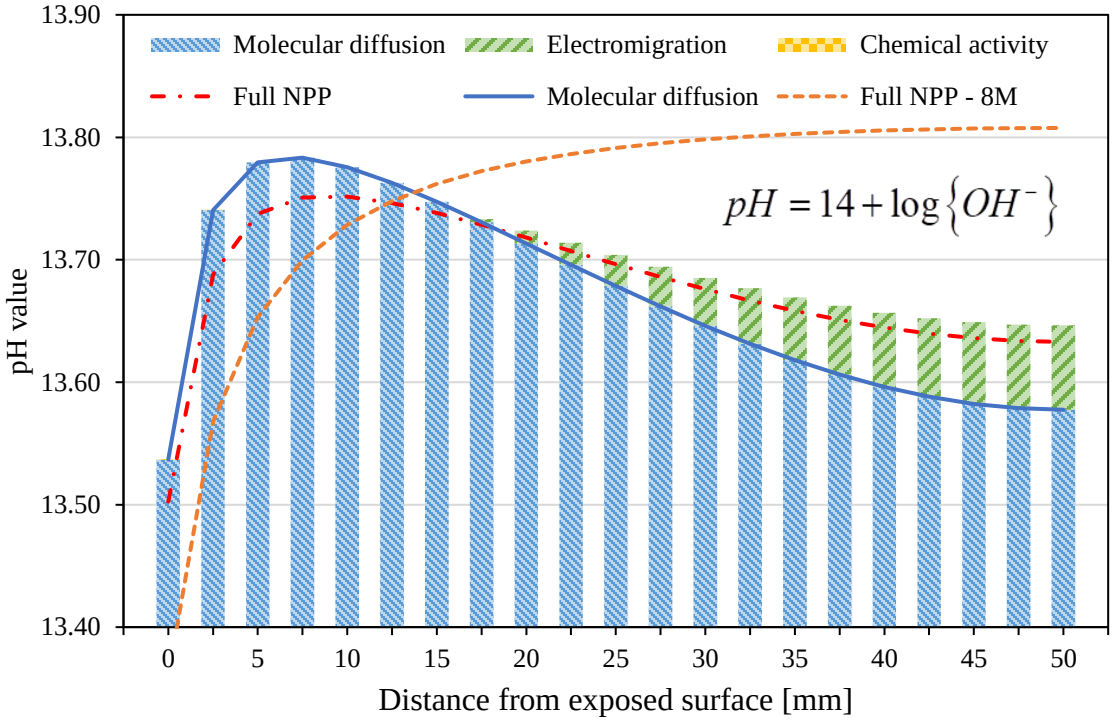

Fig. 2.4: Effect of the three transport modes on the pH profile at one month of Eq. 2.2

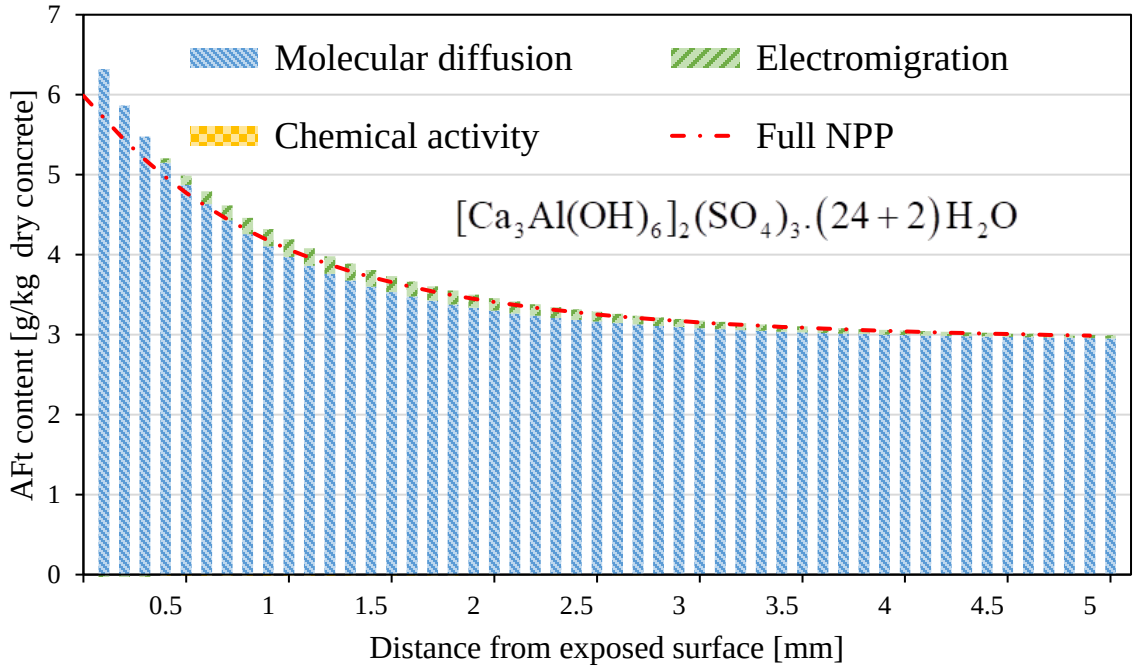

Fig. 2.5: Ettringite profile at one month due to different components of Eq. 2.2

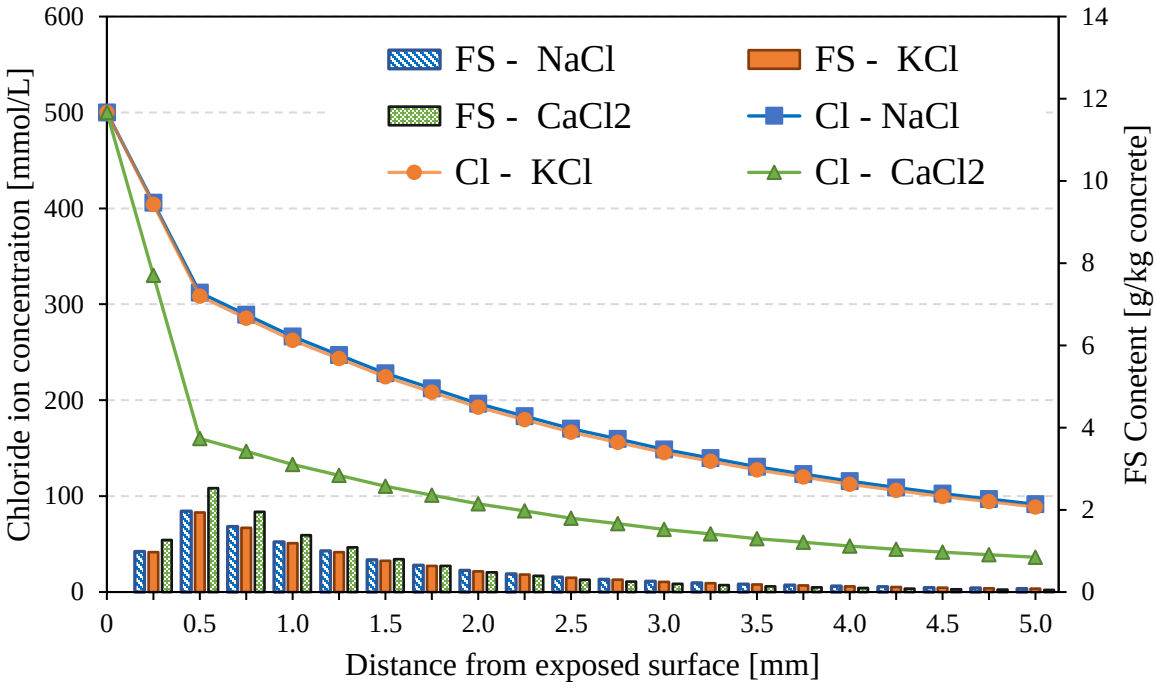

Fig. 2.6: Chloride ion concentration and Friedel's salt content for different salts at one month

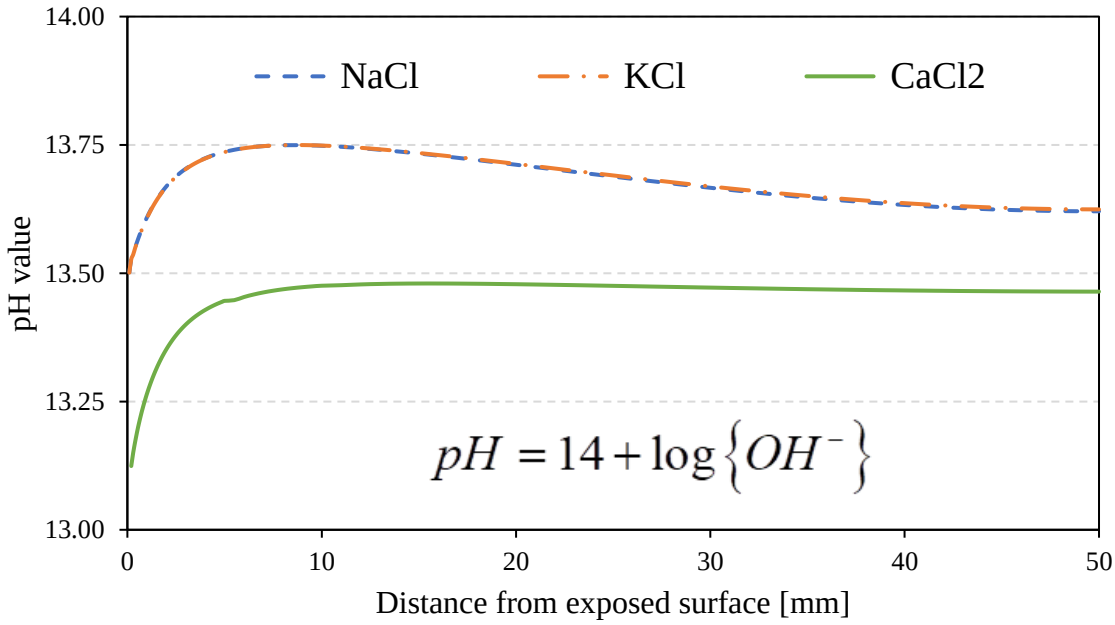

Fig. 2.7: pH profiles for different salts at one month

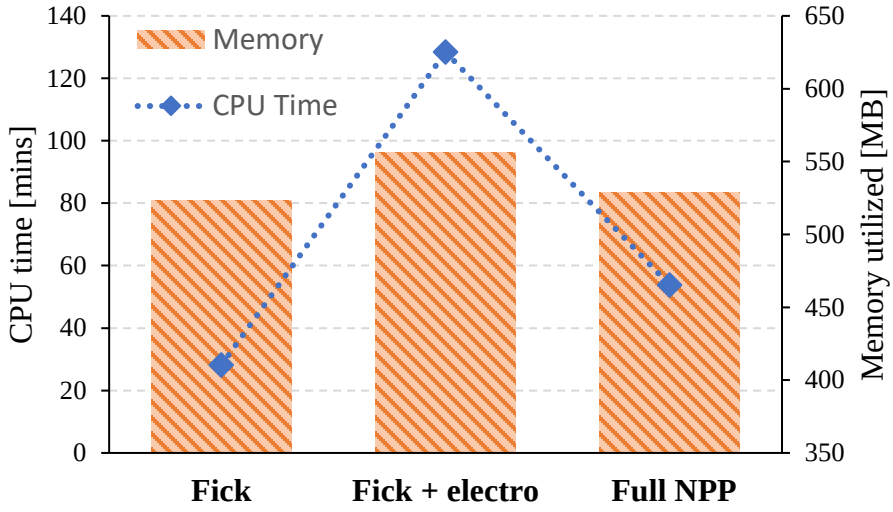

Fig. 2.8: CPU-time and memory utilized for different modeling techniques for one-month simulation

CHAPTER 3

MODELING OF CONCRETE CARBONATION AS A COUPLED NERNST-PLANCK-POISSON REACTIVE TRANSPORT PROCESS

3.1 ABSTRACT

Concrete carbonation is modeled as a reactive transport process which involves entry of gaseous CO_2 from the environment into the concrete, its partial dissolution into the multi-ionic concrete pore solution and its transport deeper into the concrete by Fickian diffusion, electromigration and ionic activity. In this study, the time-dependent transport process is modelled by coupling the Nernst-Planck equation with the Poisson's equation, with the latter equation relating the electric potential due to the electric field distribution created by the ions in the pore solution. To account for the reactions among the chemical species in the pore solution and their dissolution/precipitation, a detailed chemical module is implemented in the present work. The change in the concrete porosity and diffusion coefficients of the species involved due to the changes in the volumetric ratio of the solid phases within the cement paste are captured. The non-steady governing transport equations are solved using the Galerkin's finite element formulation and a backward (implicit) Euler scheme in the time domain. The model is validated by the reasonable agreement between its results and the corresponding experimental data in the literature as well as the results of another advanced numerical model developed by other researchers.

3.2 INTRODUCTION

A major concern with respect to concrete structures deterioration is reinforcement corrosion, which is accompanied by cracking, spalling of concrete cover, loss of strength and unsatisfactory serviceability. Reinforcement corrosion is often initiated by the penetration and accumulation of chlorides and/or carbon dioxide inside concrete and their transport within the multi-ionic concrete pore solution to the concrete-reinforcement interface. The focus of the present study is modelling of carbonation as a complex electrochemical process, with the ultimate goal of developing a tool for accurately predicting the service life and safety of reinforced concrete structures exposed to carbonation. The end of service life of structure means that at the end of this period the structure will not be able to function without extensive repair/rehabilitation.

Concrete service life prediction is important to ensure the satisfactory serviceability and safety of reinforced concrete infrastructure over time. As the time to corrosion initiation is normally considered the end of service life (Maage et al. 1996) and as this time is generally long (of the order of 15 to 25 years or more), it is not practically possible to accurately predict it by using results of short-term laboratory experiments, especially if the structure exposure conditions are substantially different from those in the experiment. Consequently, a practical approach is and has been to develop detailed numerical models based on fundamental principles of materials science and mechanics and validate them by comprehensive short-term laboratory tests. Once a model is sufficiently validated, it can be used to predict the long-term performance and durability of structures under variable exposure conditions. Such effort has been underway for a long time, but developments in

computational power and greater understanding of the fundamental mechanisms of materials deterioration and their governing principles allow one to enhance the robustness and accuracy of the models.

Early, carbonation models were based on the simple semi-empirical relation (Tuutti 1982)

$$x = K\sqrt{t} \tag{3.1}$$

where x is the distance from the exposed surface, t is the exposure time, and K is a coefficient which depends on the CO_2 concentration gradient, its diffusivity and on the concrete mixture composition.

The accuracy of this elementary model is strongly dependent on the robustness of the procedures used to estimate K and the scope of the experimental data, but it is unlikely to be able to predict the microstructural and chemical changes engendered by carbonation in all cases because it cannot account for the detailed chemical reactions and microstructural changes that occur during the carbonation process (Brieger 1986). Although the simple models are useful for preliminary design or in routine cases, in the case of iconic or expensive reinforced concrete structures, it may be warranted to perform more accurate analyses by using more detailed robust models. The latter models can be also used to delimit the scope of the simple models and guide designers in the selection of the appropriate model for specific purposes.

Research on more detailed models of the carbonation process in concrete has been conducted by many researchers in the past and a summary of the relatively recent representative works and their salient features is presented in Table 3.1.

Table 3.1: Some recent investigations on modeling concrete carbonation

Research work	Transport mechanisms		Chemical interaction module			Year
	Fick's law	NP	Simplified	Detailed	Comprehensive	
Wittmann et al (Brieger 1986)	✓		✓			1986
Papadakis et al (Papadakis et al. 1989)	✓			✓		1989
Saetta et al. (Saetta and Vitaliani 2005)	✓		✓			1995
Isgor and Razaqpur (Isgor and Razaqpur 2004)	✓			✓		2004
Peter et al (Peter et al. 2005)	✓			✓		2005
Thiery (Thiery 2005)	✓	✓			✓	2005
Hyvert et al. (Hyvert et al. 2010)	✓		✓			2010
Jeong et al. (Jeong et al. 2019)	✓			✓		2019

There are two key features that characterize each model. First, the laws governing the CO_2 transport within the concrete pore solution and second the type, nature, and products of the chemical reactions among the various species in the solution during carbonation. With the exception of Thiery, it can be observed that in all the works in Table 3.1**,** CO_2 transport is assumed to be governed by Fick's second law and in many cases either chemical interaction among the different chemical species in concrete is either ignored or selectively considered.

Some researchers (Papadaki et al. 1989; Hyvert et al. 2010) have striven to improve the elementary square root model by considering an increasing number of parameters in the empirical procedures for estimating the value of the coefficient K. Since ambient hygrothermal conditions affect the carbonation process, others (Jeong et al. 2019; Isgor and Razaqpur 2004) have coupled the diffusion of CO_2 with heat and moisture transport, but Saetta et al. (Saetta and Vitaliani 2005) argued that temperature does not have significant effect on the carbonation process in the usual temperature range to which structures are exposed, thus they recommended that thermal effects can be disregarded.

In terms of the breadth of the chemical reactions considered in the different models, past works can be classified into three groups, depending on the type and number of species included in the model. Here they are classified as (i) simplified (Brieger 1986; Saetta and Vitaliani 2005; Hyvert et al. 2010), (ii) detailed (Papadakis et al. 1989; Isgor and Razaqpur 2004; Peter et al. 2005; Jeong et l. 2019), and (iii) comprehensive (Thiery 2005). It should be stated that the seminal work of Papadakis et al. (Papadakis et al. 1989) forms the basis of several of models, including those of (Isgor and Razaqpur 2004; Peter et al. 2005; Jeong et al. 2019) due to the inclusion of the underlying chemistry of carbonation.

Briefly, the simplified chemical models reduce the carbonation of cement to that of Portlandite by considering only the following reaction

$$Ca(OH)_2 + CO_2 \rightarrow CaCO_3 + H_2O \tag{3.2}$$

However, experiments have shown (Papadakis et al. 1991) that other phases of the hydrated cement, including CSH, C_2S, and C_3S also undergo carbonation as indicated by reactions 3.3, 3.4,and 3.5, respectively.

$$\left(3CaO.2SiO_2.3H_2O\right)+3CO_2 \xrightarrow{r_{CSH}} \left(3CaCO_3.2SiO_2.3H_2O\right) \quad (3.3)$$

$$\left(3CaO.SiO_2\right)+3CO_2+\vartheta H_2O \xrightarrow{r_{C_3S}} 3CaCO_3+SiO_2.\vartheta H_2O \quad (3.4)$$

$$\left(2CaO.SiO_2\right)+2CO_2+\vartheta H_2O \xrightarrow{r_{C_2S}} 2CaCO_3+SiO_2.\vartheta H_2O \quad (3.5)$$

Despite the inclusion of reaction (3.2) to (3.5) in the detailed models, they do not follow the delicate mass and charge conservation laws governing the molecular level reactions and the interaction between the solids and the pore solution in concrete as well as the dissociation/precipitation of the solids.

The comprehensive model of (Thiery 2005) includes the latter chemical reactions per the mass action law. The model is more robust and better represents the chemistry of the carbonation process in Portland cement concrete. Moreover, the model can relatively easily accommodate the presence of new chemical species in the concrete, such as those contained in supplementary cementitious materials, and their effect on the carbonation process.

Although (Thiery 2005)'s model is conceptually comprehensive, in applying it, he reduced the number of chemical species directly involved in the carbonation process to four. This was made possible by making the reaction/production of the other species within the pore solution and the cement matrix as a function of those four. In the current investigation, such a simplification is not made rather the full suite of the chemical reactions are considered. Furthermore, he solved the system of equations following the kinetics of reaction without applying the operator splitting approach while in the current study the later approach is applied.

The operator splitting approach allows consideration of a more comprehensive set of chemical interactions and faster convergence of the numerical solution. The latter attributes would be helpful when considering the interaction of different physiochemical phenomena (e.g. chloride and carbonation attacks on concrete) where many more chemical reactions are involved. Moreover, it has been reported (Abreu et al. 2009) that reaction kinetics are usually experimentally estimated by making the numerical solution agree with experimental results rather than being based on well established theoretical knowledge or proper equilibrium reaction constants.

It should be pointed out that in the past implementation of the comprehensive model was rather challenging due to the slow convergence of the numerical process and the difficulty of calibrating the model as it requires fitting by inverse analysis of the various physical parameters, such as diffusivity, pore size distribution, and CO_2 interaction with the concrete pore solution. Advancements in the computational power of contemporary computers along with the development of efficient instruments and numerical techniques have paved the way for the application of comprehensive models as presented in the current work.

Although each type of model has been shown to give reasonably satisfactory estimate of the extent of carbonation in specific cases, theoretically, they lack generality because they are unable to account for the changes caused by the chemical reactions to the molar concentration of the various phases and species within the concrete matrix and their effect on the carbonation process. For example, precipitation/dissolution reactions will change the concrete porosity and diffusivity, which need to be considered to accurately evaluate the carbonation front advance. Similarly, the aqueous and gaseous phases of CO_2 in

concrete and their effects on carbonation must be individually considered via fundamental chemical principles.

In view of the above, the objective of this investigation is to develop a finite element model for the simulation of concrete carbonation based on detailed principles of material science, laws of chemistry and robust numerical methods. Due to the multi-ionic nature of the concrete pore solution, the proposed model is designed to track the transport of the major chemical species within the concrete pore solution by molecular diffusion, electromigration and ionic activity. Mass transport is modelled by solving the nonlinear Nernst-Planck-Poisson (NPP) equations using finite element analysis formulated within the framework of the Galerkin's weighted residual method in space and the implicit, or Euler backward difference, scheme in time. Unlike Thiery, who also used the NPP transport model, in the current study the assumption of electroneutrality will not be made, instead the fully coupled system of Nernst-Planck and Poisson equations will be solved. As pointed out by MacGillivray (MacGillivray 1968) and McGillivray and Hare (MacGillivray and Hare 1969) the assumption of electroneutrality or null current only applies to solutions with very high ionic concentration, which is generally not be the case in concrete pore solution. By determining the electric field via the Poisson equation, solutions with high or low concentration can be treated by the same model.

The NPP transport model is augmented by a detailed chemical module that includes the chemical equilibrium among the various species within the concrete pore solution and accounts for the dissolution/precipitation of the reactants or products. It also ensures both mass and charge conservation. Since diffusion in concrete is often treated as a one-

dimensional problem, the current formulation is one-dimensional, but in principle, it can be extended to two or three dimensions.

3.3 GOVERNING EQUATIONS OF MASS TRANSPORT

The different chemical species in the concrete pore solution include both ionic and non-ionic species. It is convenient to mathematically separate the transport of the two types species as shown below.

3.3.1 Modelling ionic species transport

The different chemical species in the concrete pore solution include both ionic and non-ionic species. It is convenient to mathematically separate the transport of the two types species as shown below.

The transport of ions in the pore solution can be modelled by the coupled Eqs. (3.6) and (3.7), known as NPP equations (Samson and Marchand 2007; Nguyen and Amiri 2016)

$$\frac{\partial c_i}{\partial t} = \frac{\partial}{\partial x}\left[D_i \left(\underbrace{\frac{\partial c_i}{\partial x}}_{molecular} + \underbrace{\frac{z_i F}{RT} c_i \frac{d\psi}{dx}}_{electromigration} + \underbrace{c_i \frac{d \ln \gamma_i}{dx}}_{chemical\ activity} \right) \right] + r_i \qquad (3.6)$$

where c_i , z_i and γ_i, respectively, are the concentration, valence number and activity coefficient of species i , F is the Faraday constant = 96,488.46 (C/mol), R is the ideal gas constant = 8.3143 (J/mol/K), T is temperature of the solution (^{o}K), ψ is the electric

potential (V), r_i : source/sink term, accounting for the production/consumption of species i. The first term in the curly bracket on the right-hand side of Eq. 3.6 represents Fickian or concentration driven diffusion, the second term ionic migration due to the electric field created by the charged ions within the pore solution and the last term transport due to chemical activity, which reflects the effective concentration of a species in a multi-ionic solution.

For a chemical solution containing i $(i = 1, n)$ ionic species, Eq. 3.6 can be applied to each species at a time, resulting in n equations, but due to the presence of the electric potential term in these equations, they will contain $(n+1)$ unknowns. Therefore, to obtain a unique solution, another relation is necessary among the unknowns of the problem. The additional relation is provided by the Poisson equation which relates the electric potential to the charge distribution in the medium as (Christopher and Shipman 1968)

$$\frac{d^2\psi}{dx^2} + \frac{F}{\varepsilon}\left(\sum_i z_i c_i\right) = 0 \tag{3.7}$$

3.3.2 Modelling non-ionic species transport

Since certain species do not ionize in the pore solution, e.g. water, carbon dioxide, they are electrically neutral, therefore, their transport is governed by Fick's second law

$$\frac{\partial c}{\partial t} = \frac{\partial}{\partial x}\left(D\left(\frac{\partial c}{\partial x}\right)\right) + r \tag{3.8}$$

where c is the molar concentration of the species, D is its diffusion coefficient modified by tortuosity, and r is the source/sink term.

3.3.3 Modelling moisture transport in non-saturated concrete

Moisture transport in non-saturated porous media is governed by Richard's equation (Taigbenu 1999) as follows

$$\frac{\partial w}{\partial t} = \frac{\partial}{\partial x}\left(D_w \left(\frac{\partial w}{\partial x} \right) \right) + r \tag{3.9}$$

where w represents the volumetric water content, and D_w is the moisture diffusivity. Note, Eq. (3.9) has the same form as Eq. (3.8) and they are both captured by the first term on the right-hand side of Eq. (3.6).

The quantity w can be related to the atmospheric relative humidity using the BET desorption isotherm (Xi et al. 1994):

$$w_e = \frac{C k_m V_m h}{\left(1 - k_m h\right)\left[1 + \left(C - 1\right) k_m h\right]} \tag{3.10}$$

where w_e is the evaporable water content expressed in terms of water per grams of cementitious material, h is the atmospheric relative humidity, V_m is the monolayer capacity, C and k_m are two parameters of the model. More information regarding these parameters and their experimental evaluation is provided by (Xi et al. 1994).

Finally, the volumetric water content can be related to the evaporable water content as

$$w = \frac{w_e \, M_c}{\rho_w \, V_S} \tag{3.11}$$

where M_c is the cement content of the concrete (kg/m^3), ρ_w is the density of water at given temperature (kg/m^3), V_S is the volume of the solids, given by

$$V_S = \frac{M_c}{G_c\ \rho_w} + \frac{A}{G_a\ \rho_w} \tag{3.12}$$

where A is the total aggregates content of the concrete (kg/m^3), G_c is the specific gravity of cement , and G_a is the specific gravity of aggregates.

The calculated volumetric water content w_∞ can be imposed as a convective flux, q_w, at the boundary as

$$q_w = h_w \left(w_{(0,t)} - w_{\infty,1} \right) \tag{3.13}$$

where $w_{(0,t)}$ is the volumetric water content at the exposed surface, h_w is the convection coefficient and can be taken as 3×10^{-8} (m/s) (Sakata 1983). Adding the convection term modifies both the stiffness (conductance) matrix and loading vector of the element with the specified flux.

The preceding scheme allows one to split the transport mechanisms into two types: one for molecules governed by Fick's 2nd law of diffusion and the other for charged particles (ions) following NPP.

The chemical activity coefficient can be evaluated using different models, varying in complexity from simple, e.g. Debye-Hückel and Davies (Moore 1998), to complex, e.g. Pitzer (Pitzer 1991). According to (Samson et al. 1999), the modified Davies relationship given in Eq. 3.14(a) yields good results for a wide range of ionic strengths, hence it is adopted in the current work

$$\ln \gamma_i = A z_i^2 \left(\frac{\sqrt{I}}{1 + a_i B \sqrt{I}} - \frac{\left(0.2 - 4.17 x 10^{-5} I \right) I}{\sqrt{1000}} \right) \tag{3.14a}$$

where I is the ionic strength (mM) given by Eq. (3.14b), A and B are temperature dependent parameters given by equations Eqs. (3.14c and d), and a_i is a fitting parameter (m) whose values for the common ions in concrete are shown in Table 3.2.

$$I = 0.5 \sum_i z_i^2 C_i \tag{3.14b}$$

$$A = \frac{\sqrt{2} F^2 e_0}{8\pi (\varepsilon RT)^{3/2}} \tag{3.14c}$$

$$B = \sqrt{\frac{2F^2}{\varepsilon RT}} \tag{3.14d}$$

where e_0 = 1.602x10^{-19} C is the electron charge.

Water activity in a solution can be determined using (Garrels and Christ 1965)

$$\{H_2O\} = 1 - 0.017 \sum_i C_i \tag{3.15}$$

where C_i is the concentration of the ith ionic species in the pore solution.

Table 3.2: Parameter a_i value for common ions in the concrete pore solution: (Samson et al. 1999)

Ion	a_i (m) x 10^{-10}	Ion	a_i (m) x 10^{-10}
OH^-	3	SO_4^{2-}	1
Na^+	3	Ca^{2+}	1 x 10^{-3}
K^+	3.3	Cl^-	2

3.4 APPLICATION OF NPP TO CONCRETE AS A POROUS MEDIUM MODELLING

The system of Eqs. 3.6 and 3.7 is strictly applicable to diffusion in chemical solutions. However, concrete is considered as a reactive porous medium; consequently, the latter

equations need to be modified to account for the characteristics of concrete. Accordingly, following (Samson and Marchand 2007) the modified equations based on mass balance can be written as

$$\frac{\partial\left(w_s c_i^s\right)}{\partial t}+\frac{\partial\left(wc_i\right)}{\partial t}-\frac{\partial}{\partial x}\left(wD_i\left(\underbrace{\frac{dc_i}{dx}}_{molecular}+\underbrace{\frac{z_i F}{RT}c_i\frac{d\psi}{dx}}_{electro-migration}+\underbrace{c_i\frac{d\ln\gamma_i}{dx}}_{chemical\ activity}\right)\right)+wr_i=0 \tag{3.16a}$$

$$\frac{d}{dx}\left(\tau w\frac{d\psi}{dx}\right)+\frac{F}{\varepsilon}w\left(\sum_{i=1}^{n}z_i c_i\right)=0 \tag{3.16b}$$

where c_i^s is the concentration of the solid phase (mol/m^3), w_s is the volumetric solid phase content (m^3/m^3), w is the volumetric water content (m^3/m^3), τ is the apparent tortuosity of the concrete pore structure, which includes the effect of tortuosity and constrictiveness of the porous medium, n is the number of species, and r_i is the source/sink term to account for the production/consumption of species i during the reaction.

The porosity reduction due to carbonation can be approximated by a bi-linear decay function (Isgor and Razaqpur 2004) as

$$f\left(d\right)=\left(a_{car}-1\right)*\alpha_c/b_{car} \tag{3.17}$$

where a_{car}, b_{car} are fitting parameters, α_c is the carbonation degree which can be expressed as:

$$\alpha_c=\frac{\left[CaCO_3\right]}{\left[CSH\right]+\left[CH\right]} \tag{3.18}$$

Hence, the porosity of the concrete matrix modified by carbonation can be expressed as

$$\phi_i^{'} = f(d)\phi_i \tag{3.19}$$

where $\phi_i^{'}$ is the modified porosity due to carbonation and ϕ_i is the original porosity.

The diffusivity of any species i, D_i, in concrete is function of concrete porosity and the capillary pores tortuosity and can be expressed as

$$D_i = \tau D_i^0 f(d) \tag{3.20}$$

where, D_i^0 is the diffusion coefficient of species i in free-water (m^2/sec), and $f(d)$ is a coefficient that reflects the effect of the medium porosity change due to carbonation.

3.4.1 Modeling of transport modes

Local chemical equilibrium can be assumed at each point in the medium for the majority of ionic transport problems (Barbarulo et al. 2000). This allows one to separate the physical transport of the ions from the chemical equilibrium. Consequently, for each species i the conservation of mass can be expressed as

$$\frac{\partial(wc_i)}{\partial t} - \frac{\partial}{\partial x}\left(wD_i \left(\underbrace{\frac{dc_i}{dx}}_{molecular} + \underbrace{\frac{z_i F}{RT} c_i \frac{d\psi}{dx}}_{electric\ coupling} + \underbrace{c_i \frac{d\ln\gamma_i}{dx}}_{chemical\ activity} \right) \right) = -wr_i - \frac{\partial\left(w_s c_i^s\right)}{\partial t} \tag{3.21}$$

in which the right-hand terms can be evaluated in a separate chemical module after solving the physical transport problem represented by the left-hand side of Eq. 3.21. The chemical module will account for the precipitation/dissolution of each solid phase within the pore

solution. This technique for separating the local chemical equilibrium from the mass transport phenomenon is known as the operator-splitting approach and is applied here due to its computational efficiency (Yeh and Tripathi 1989). The validity of the local equilibrium assumption in concrete was established by (Samson and Marchand 2007). Moreover, this assumption allows one to enforce chemical equilibrium via a set of algebraic equations rather than using the kinetics of reactions.

The numerical implementation of the split operator technique involves two computational modules, the transport module and chemical module, which are applied sequentially either through a sequential iterative approach (SIA) or sequential non-iterative approach (SNIA). The SNIA was selected here due to its computational advantages, as it will be shown, and it gives good results when compared to available experimental results.

3.4.2 Modeling of the chemical reactions in concrete carbonation

Chemical reactions can be classified into heterogenous (solid – aqueous) and homogeneous (aqueous – aqueous) reactions. Both types of reaction take place during carbonation which lead to a simultaneous equilibria problem. The list of reactions occurring during concrete carbonation includes (Thiery 2005):

$$CaCO_{3(s)} \rightleftarrows Ca^{2+} + CO_3^{2-} \tag{3.22-a}$$

$$Ca\left(OH\right)_{2(s)} \rightleftarrows Ca^{2+} + 2OH^{-} \tag{3.22-b}$$

$$CSH_{(s)} \rightleftarrows Ca^{2+} + 2OH^{-} \tag{3.22-c}$$

$$CO_{2(aq)} + H_2O \rightleftarrows H_2CO_3 \quad (3.22\text{-d})$$

$$H_2CO_3 \rightleftarrows HCO_3^- + H^+ \quad (3.22\text{-e})$$

$$HCO_3^- \rightleftarrows CO_3^{2-} + H^+ \quad (3.22\text{-f})$$

$$H_2O \rightleftarrows OH^- + H^+ \quad (3.22\text{-g})$$

The balance between the gaseous and aqueous phases of carbon dioxide can be modelled using Henry's law. Thus, the source/sink term can include the gaseous-aqueous equilibrium as (Peter et al. 2005)

$$r_{Henry} = C^{ex}\left(C^{Henry}C_{CO_{2(g)}} - C_{CO_2}\right) \quad (3.23)$$

where C^{ex} is the interfacial mass-transfer coefficient and C^{Henry} is Henry's constant.

The heterogeneous reaction involving the solid phases are modeled using the mass action equation, which has the conservation of charge embedded within it (Moore 1998), and is expressed as

$$K_m = \prod_m^N c_i^{\nu mi}\gamma_j^{\nu mi} \quad ;m = 1,...,M \quad (3.24)$$

where c_i is the molar concentration of ionic species (M), ν_{mi} is the stoichiometric coefficient of species i in the m^{th} solid, and K_m is the solubility constant of the m^{th} solid. The value of the solubility constant for the solids participating in the carbonation process in the proposed model is listed in Table 3.3.

Table 3.3: Solubility constants for different solid phases

Solid Phase	Equilibrium relationship	$-\boldsymbol{log(K_m)}$
Portlandite	$K_{sp_1} = \{Ca\}\{OH\}^2$	5.2
C-S-H	$K_{sp_2} = \{Ca\}\{OH\}^2$	6.2
Calcium carbonate	$K_{sp_3} = \{Ca\}\{CO_3\}$	8.48

The homogeneous reactions are modeled using the equilibrium constants. For a typical chemical reaction of the following form:

$$aA + bB \rightleftharpoons cC + dD$$

the equilibrium constant is expressed as (Moore 1998):

$$K_C = \frac{[C]^c [D]^d}{[A]^a [B]^b} \tag{3.25}$$

where $[\ ]$ is the molar concentration of ionic species (M), a,b,c,d are the stoichiometric coefficient of species i in the reaction, and K_C is the equilibrium constant of the reaction. The values of equilibrium constants used in reactions (3.22-d) to (3.22-e) are listed in Table 3.4.

Table 3.4: Equilibrium constants for different homogeneous reactions (Soli and Byrne 2002)

Reaction #	Equilibrium relationship	$-log(K_c)$
(3.22-d)	$K_{C_1} = \{H_2CO_3\} / \{CO_{2(aq)}\}\{H_2O\}$	2.52
(3.22-e)	$K_{C_2} = \{HCO_3^-\}\{H^+\} / \{H_2CO_3\}$	3.70
(3.22-f)	$K_{C_3} = \{CO_3^{2-}\}\{H^+\} / \{HCO_3^-\}$	10.22
(3.22-g)	$K_{C_4} = \{OH^-\}\{H^+\} / \{H_2O\}$	14.00

The set of equations from solid phases and homogeneous equilibria need to be solved simultaneously. This produces a system of nonlinear algebraic equations whose solution requires an iterative procedure as discussed in the sequel.

3.5 FINITE ELEMENT FORMULATION

3.5.1 Numerical formulation of the governing equations of species transport

Equations (3.16a) and (3.16b) are solved by applying the Galerkin's weighted residual method (Zienkiewicz et al. 2013). For clarity, without loss of generality, the details of the formulation are presented for two ionic species, but in the developed computer program more species are considered as demonstrated later.

For two ionic species, the unknowns of the problem are the species concentrations, C_1, C_2, and their electrostatic potential, ψ. As Eqs. (3.16a) and (3.16b) are second order differential equations, in one-dimensional transport, a two-node linear finite element would suffice. The element nodal degrees of freedom (DOF) are the foregoing three unknowns.

Let $u_i(x)$ represent a typical trial function for field variable C_i or ψ, then

$$u_i(x) = N_1 u_{i1} + N_2 u_{i2} \tag{3.26}$$

where u_{i1}, u_{i2}, are the element nodal degrees of freedom and N_1, N_2 are shape functions

$$\begin{bmatrix} N_1 & N_2 \end{bmatrix} = \begin{bmatrix} 1 - \frac{x}{l} & \frac{x}{l} \end{bmatrix} \tag{3.27}$$

with x being a local coordinate, with its origin at node 1, and l the element length. Substituting the trial functions for c_1, c_2 and ψ per Eq. 3.26 into the governing Eqs. (3.16a) and (3.16b), leads to the following residuals

$$R_1 = \frac{\partial(wc_1)}{\partial t} - \frac{\partial}{\partial x}\left(wD_1\left(\frac{\partial c_1}{dx} + \frac{z_1 F}{RT} c_1 \frac{d\psi}{dx} + c_1 \frac{d\ln\gamma_1}{dx} \right)\right) \tag{3.28}$$

$$R_2 = \frac{\partial(wc_2)}{\partial t} - \frac{\partial}{\partial x}\left(wD_2\left(\frac{\partial c_2}{dx} + \frac{z_2 F}{RT} c_2 \frac{d\psi}{dx} + c_2 \frac{d\ln\gamma_2}{dx} \right)\right) \tag{3.29}$$

$$R_3 = \frac{d}{dx}\left(\tau w \frac{d\psi}{dx} \right) + \frac{F}{\varepsilon} w\left(\sum_{i=1}^{N} z_i c_i \right) \tag{3.30}$$

Based on the Galerkin's method (Logan 2012; Segerlind 1984) the weighted sum of the residuals, *I*, over the domain (element volume V) can be minimized as

$$I = \int_V N_i R_i(x) dV = 0 \qquad ;(\text{i} = 1,2,3) \tag{3.31}$$

where the shape function N_i serves as the weighing function.

In expanded form, Eq. 3.31 is written as

$$I = A\int_l \begin{bmatrix} N_1 & N_2 & N_3 \end{bmatrix} \begin{bmatrix} w & 0 & 0 \\ 0 & w & 0 \\ 0 & 0 & 0 \end{bmatrix} \begin{bmatrix} \dot{c}_1 \\ \dot{c}_2 \\ \dot{\psi} \end{bmatrix} dx +$$

$$+A\int_l \begin{bmatrix} \frac{dN_1}{dx} & \frac{dN_2}{dx} & \frac{dN_3}{dx} \end{bmatrix} \begin{bmatrix} wD_1 & 0 & \frac{D_1 z_1 F}{RT} wc_1 \\ 0 & wD_2 & \frac{D_2 z_2 F}{RT} wc_2 \\ 0 & 0 & \tau w \end{bmatrix} \begin{bmatrix} c_{1,x} \\ c_{2,x} \\ \psi_{,x} \end{bmatrix} dx +$$

$$+A\int_l \begin{bmatrix} \frac{dN_1}{dx} & \frac{dN_2}{dx} & \frac{dN_3}{dx} \end{bmatrix} \begin{bmatrix} wD_1 \frac{d\ln\gamma_1}{dx} & 0 & 0 \\ 0 & wD_2 \frac{d\ln\gamma_2}{dx} & 0 \\ 0 & 0 & 0 \end{bmatrix} \begin{bmatrix} c_1 \\ c_2 \\ \psi \end{bmatrix} dx + \quad (3.32)$$

$$+A\int_l \begin{bmatrix} N_1 & N_2 & N_3 \end{bmatrix} \begin{bmatrix} 0 & 0 & 0 \\ 0 & 0 & 0 \\ -\frac{F}{\varepsilon} wz_1 & -\frac{F}{\varepsilon} wz_2 & 0 \end{bmatrix} \begin{bmatrix} c_1 \\ c_2 \\ \psi \end{bmatrix} dx + B.I. = 0$$

where A is the cross section of the element and $B.I.$ are the boundary terms which are omitted as only Dirichlet-type boundary conditions are specified.

Since in the Galerkin's method, the weighing function at each node is set equal to the nodal shape function, for a two-node linear element one obtains,

$$\begin{bmatrix} c_1 \\ c_2 \\ \psi \end{bmatrix} = [N][U_n] \quad (3.33)$$

$$[N]=\begin{bmatrix} N_1 & 0 & 0 & N_2 & 0 & 0 \\ 0 & N_1 & 0 & 0 & N_2 & 0 \\ 0 & 0 & N_1 & 0 & 0 & N_2 \end{bmatrix} \tag{3.34}$$

$$\left[U_n^e\right]=\begin{bmatrix} c_{11} & c_{21} & \psi_1 & c_{12} & c_{22} & \psi_2 \end{bmatrix}^T \tag{3.35}$$

where c_{ij} is the concentration of species i at node j of the element. Setting the weighted residual integral to zero and after integration by parts to reduce the second derivatives to first derivatives, –one can write

$$[M]^e = A\int_l [N]^T [C][N]dx \tag{3.36}$$

$$[K]^e = A\int_l [B]^T [k_I][B]dx + A\int_l [N]^T [k_{II}][N]dx + A\int_l [B]^T [k_{III}][N]dx \tag{3.37}$$

where

$$[C]=\begin{bmatrix} w & 0 & 0 \\ 0 & w & 0 \\ 0 & 0 & 0 \end{bmatrix} \tag{3.38}$$

$$[B]=\begin{bmatrix} N_{1,x} & 0 & 0 & N_{2,x} & 0 & 0 \\ 0 & N_{1,x} & 0 & 0 & N_{2,x} & 0 \\ 0 & 0 & N_{1,x} & 0 & 0 & N_{2,x} \end{bmatrix} \tag{3.39}$$

$$\left[k_I\right]=\begin{bmatrix} wD_1 & 0 & \dfrac{D_1 z_1 F}{RT} wc_1 \\ 0 & wD_2 & \dfrac{D_2 z_2 F}{RT} wc_2 \\ 0 & 0 & \tau w \end{bmatrix} \tag{3.40}$$

$$\left[k_{II}\right]=\begin{bmatrix} wD_1 \dfrac{d\ln\gamma_1}{dx} & 0 & 0 \\ 0 & wD_2 \dfrac{d\ln\gamma_2}{dx} & 0 \\ 0 & 0 & 0 \end{bmatrix} \tag{3.41}$$

$$\left[k_{III}\right]=\begin{bmatrix} 0 & 0 & 0 \\ 0 & 0 & 0 \\ -\dfrac{F}{\varepsilon} wz_1 & -\dfrac{F}{\varepsilon} wz_2 & 0 \end{bmatrix} \tag{3.42}$$

After assembling the elements $\left[M\right]^e$ and $\left[K\right]^e$ matrices, the following system of equations is obtained:

$$\left[M\right]\left[\dot{U}\right]+\left[K\right]\left[U\right]=0 \tag{3.43}$$

The equations are semi-discretized in space. Thus, time-discretization of the quasi-harmonic Nernst-Plank equation can be performed following a first-order single time-step algorithm with implicit Euler scheme as follows:

$$[M_t]\left[\frac{U_t - U_{t-\Delta t}}{\Delta t}\right] + [K_t][U_t] = 0 \tag{3.44}$$

$$\left(M_t + \Delta t\ K_t\right)U_t = \left[M_t U_{t-\Delta t}\right] \tag{3.45}$$

$$\left[\widehat{K}\right][U_t] = \left[\widehat{F}\right] \tag{3.46}$$

where U_t are the unknowns values at current time step, $U_{t-\Delta t}$ are the values from previous time step, Δt is the time-step, and $[M]$ is a lumped matrix by summation of rows method. This improves the convergence of the selected time-discretization scheme.

Equation 3.46 provides a system of nonlinear algebraic equations which need to be solved at each time-step. Several methods can be used to solve this system (Heath 2018); here the Newton-Raphson's method was applied. The nonlinear terms in the tangent matrix make small contribution to the convergence rate, thus, the tangent matrix without the nonlinear terms is shown in Eq. 3.47.

$$\left[K_T^e\right] = \left[M^e\right] + \Delta t\left[K^e\right] \tag{3.47}$$

All the variables appearing in Eqs. 3.40, 3.41, and 3.42 are evaluated at the integration points using two-point Gauss quadrature.

As stated earlier, since the movement of molecules is not influenced by an electric field, their transport in porous media follows Fick's second law as given in Eq. 3.8. Such molecules in the carbonation process include carbon dioxide (both gaseous and dissolved), carbonic acid, and moisture. In this research, the relevant concentration of these species must be determined before applying the NPP model, because w is an input to the NPP

model. The finite element formulation for Fick's law is not presented here as it is readily available in the literature (Logan 2012; Reddy and Gartling 2010; Peter et al. 2005). It must be pointed out that any water that is produced/consumed during the carbonation reactions is determined within the chemical module and the volumetric water content of the concrete for the NPP model is accordingly adjusted. Moreover, applying the convection boundary condition in Eq. 3.13 for volumetric water content involves updating the stiffness matrix and forcing term for the first element (Logan 2012).

3.5.2 Formulation of chemical equilibrium and mass conservation

Applying the mass action equation to the different solid phases and the chemical equilibrium expressions to the homogeneous reactions yields a system of nonlinear algebraic equations which need to be solved simultaneously.

The unknowns of the problem are the progress of the reactions, denoted as ξ_I, ξ_{II}, ξ_{III}, ξ_{IV}, ξ_V, ξ_{VI} and ξ_{VII} as described below. The Newton-Raphson method is applied to solve the relevant system of equations. The chemical balance equations included in the present model are

$$\Delta_I = [Ca][OH]^2 - K'_{CH} \tag{3.48}$$

$$\Delta_{II} = [Ca][OH]^2 - K'_{CSH} \tag{3.49}$$

$$\Delta_{III} = [Ca][CO_3] - K'_{CaCO_3} \tag{3.50}$$

$$\Delta_{IV} = \left(\left[H_2CO_3 \right] / \left[CO_{2(aq)} \right] \left[H_2O \right] \right) - K'_{C,IV} \tag{3.51}$$

$$\Delta_V = \left(\left[HCO_3^- \right] \left[H^+ \right] / \left[H_2CO_3 \right] \right) - K'_{C,V} \tag{3.52}$$

$$\Delta_{VI} = \left(\left[CO_3^{2-} \right] \left[H^+ \right] / \left[HCO_3^- \right] \right) - K'_{C,VI} \tag{3.53}$$

$$\Delta_{VII} = \left(\left[OH^- \right] \left[H^+ \right] / \left[H_2O \right] \right) - K'_{C,VII} \tag{3.54}$$

where the square brackets denote molar concentration and the K'_C represent mixed equilibrium constants, which are given by:

$$K'_C = \frac{\gamma_{reac}}{\gamma_{prod}} K_C \tag{3.55}$$

The concentration of the ions can be represented in terms of the amount of the solids dissolution/precipitation necessary to restore equilibrium of $\xi_m \ (i = 1, m)$.

$$\left[Ca^{2+} \right] = \left[Ca^{2+} \right]_0 + \xi_I + \xi_{II} + \xi_{III} \tag{3.56}$$

$$\left[CO_3^{2-} \right] = \left[CO_3^{2-} \right]_0 + \xi_{III} + \xi_{VI} \tag{3.57}$$

$$\left[OH^- \right] = \left[OH^- \right]_0 + 2\xi_I + 2\xi_{II} + \xi_{VII} \tag{3.58}$$

$$\left[H^+ \right] = \left[H^+ \right]_0 + \xi_V + \xi_{VI} + \xi_{VII} \tag{3.59}$$

$$\left[H_2CO_3 \right] = \left[H_2CO_3 \right]_0 + \xi_{IV} - \xi_V \tag{3.60}$$

$$\left[HCO_3^- \right] = \left[HCO_3^- \right]_0 + \xi_V - \xi_{VI} \tag{3.61}$$

$$\left[CO_{2(aq)} \right] = \left[CO_{2(aq)} \right]_0 - \xi_{IV} \tag{3.62}$$

$$\left[H_2O\right] = \left[H_2O\right]_0 - \xi_{VII} - \xi_{IV} \tag{3.63}$$

where the magnitude of the quantities inside the $\left[\ \right]^0$ brackets is computed by the transport module, and they may not satisfy equilibrium, hence they need to be corrected to satisfy equilibrium. At each iteration, the chemical activity is evaluated according to Eq. 3.14.

It is worth mentioning that water is produced in each chemical balancing equation at every time step, hence, the moisture balance is restored in the following step in the transport model. Due to the short time-steps used in the present analyses, authors believe this approach is reasonable.

The Jacobian matrix used in the Newton-Raphson method is given by Eq. 3.64 and is derived by assuming chemical activity to be constant in each iteration.

$$\left[K_T\right] = \begin{bmatrix} \frac{\partial \Delta_I}{\partial \xi_I} & \frac{\partial \Delta_I}{\partial \xi_{II}} & \cdots & \frac{\partial \Delta_I}{\partial \xi_{VII}} \\ \frac{\partial \Delta_{II}}{\partial \xi_I} & \ddots & & \frac{\partial \Delta_{II}}{\partial \xi_{VII}} \\ \vdots & & \ddots & \vdots \\ \frac{\partial \Delta_{VII}}{\partial \xi_I} & \cdots & & \frac{\partial \Delta_{VII}}{\partial \xi_{VII}} \end{bmatrix} \tag{3.64}$$

Note, substitution of Eqs. 3.56-3.63 into Eqs. 3.48-3.54 allows for the differentiation of Δ_i in terms of ξ_i. For more details, the reader can refer to (Samson and Marchand 2006).

3.6 MODEL VERIFICATION

3.6.1 Problem description and its numerical simulation details

The finite element model is developed within the MATLAB platform (The MathWorks Inc. 2018) and is verified by comparing its results with Peter et al. (Peter et al. 2005) numerical simulation results, which are based on Papadakis et al. (Papadakis et al. 1991) chemical reaction model.

Measurement of the concentration of all solid phases and the pH at different locations within a concrete specimen is time consuming. The writers are not aware of any experimental work which has measured and reported these quantities for tests involving carbonation, including the seminal works in (Papadakis et al. 1989; Saetta and Vitaliani 2005). The latter studies only report the carbonation depth in the specimen, measured by using the phenolphthalein indicator. (Peter et al. 2005) computed the relevant concentrations and pH through the depth by numerically simulating (Papadakis et al. 1989)'s experiments. Consequently, the quantities of the species and the pH values predicted for specimens S2 and S3 of Papadakis et al. will be compared with the corresponding values calculated by Peter et al. Figure 3.1 shows schematically Papadakis et al.'s experimental set-up.

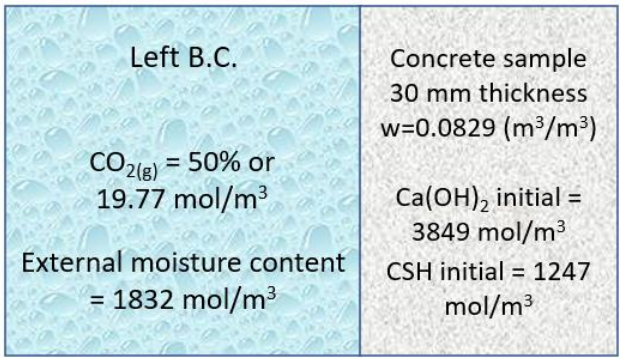

Fig. 3.1: Initial and boundary conditions for simulating carbonation of specimen S2

The test samples were 30 mm thick concrete disks. They were moist cured for 90 days and thereafter one face of each disk was kept exposed while its other surfaces were covered with a gas-tight paint. The paint-free surface was subjected to replenished 50% carbon dioxide gas (19.77 mol/m^3) and 50% air mixture. The experiments were conducted in a temperature-controlled environment; hence, temperature effect is neglected in the current analysis.

The concrete mixture proportions, porosity and the cement and concrete pore solution initial compositions are given in Table 3.5. Note that S2 and S3 have different w/c ratio. The table also gives the diffusion coefficients of the ions present in the pore solution and the initial concentration of the three solid phases, viz. Portlandite, CSH, and Calcite. Carbonation depth was measured at 20 mm increments through the disk thickness in accordance with (RILEM 1988).

In the current finite element simulation, a non-uniform mesh of 100 two-node linear finite elements is used to model the carbonation front advance through the thickness of each specimen. The element length is chosen as 0.1 mm for the first 5 mm from the exposed

surface, 0.5 mm for the region located from 5 to 10 mm from the exposed surface, and 1 mm for the remining depth. The time step is selected as 900 sec.

Table 3.5: Concrete properties and pore solution composition used in the current simulation of Papadakis et al. specimens S2 and S3

Property	**Value**	**Property**	**Value**
Cement type	Type I	Porosity	S2: 18 %, S3: 20%
w/c	S2: 0.5, S3: 0.65	Tortuosity	S2: 0.0033, S3: 0.0072
RH	0.65	w	0.0829 (m^3/m^3)
Cement composition	**(% mass)**	**Free Diffusion Coefficients**	**($x10^{-9}$ m^2/s)**
CaO	65.28	H^+	9.310
SiO_2	23.55	Ca^{2+}	0.793
Al_2O_3	6.12	CO_3^{2-}	0.955
SO_3	0.47	OH^-	5.270
		HCO_3^-	1.180
Initial solids phases	**(mol/m^3)**	$CO_{2(g)}$	13.889
Portlandite (CH)	S2: 3849, S3: 1470	$CO_{2(aq)}$	0.0011628
C-S-H	S2: 1247, S3: 786	H_2CO_3	0.028935
$CaCO_3$	0	H_2O	0.011574
C_2S	S2: 159.1, S3: 196		
C_3S	S2: 24.3, S3: 55	**Initial pore solution**	**(mol/m^3)**
		H^+	$4.7075x10^{-10}$
Porosity change parameters		Ca^{2+}	14.578
a_{car}	0.5	CO_3^{2-}	0
b_{car}	0.9	OH^-	33.645
		HCO_3^-	0
Boundary conditions		$CO_{2(g)}$	0
External moisture content	1832 mol/m^3	$CO_{2(aq)}$	0
$CO_{2(g)}$ external	19.77 mol/m^3	H_2CO_3	0
C^{Henry}	0.85		
C^{ex}	0.0116 1/s	pH	12.33

Figure 3.2 illustrates for specimens S2 and S3 the carbonation depth from the exposed surface versus the exposure time. The results of the current model are compared with the experimentally measured values and with the values calculated by Peter et al. It can be

observed that the current model results agree closely with the corresponding experimental values.

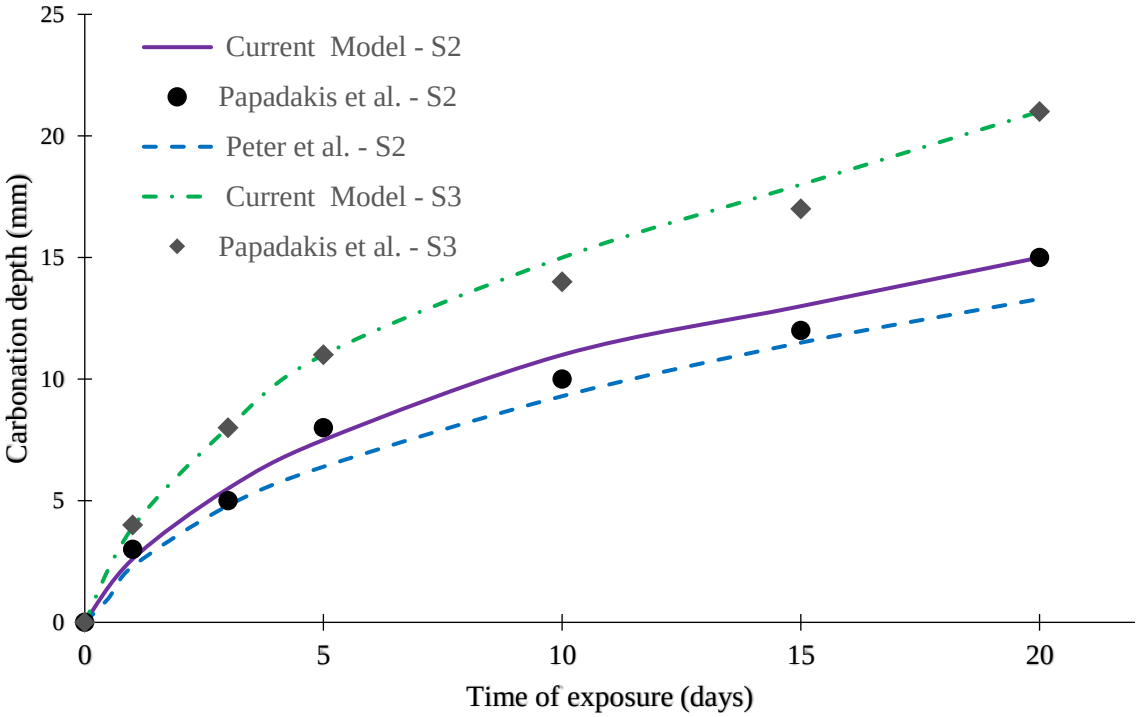

Fig. 3.2: Comparison of the carbonation depth computed by the current model with the experimental values of Papadakis et al. and the calculated values of Peter et al.

3.6.2 Comparison of carbonated species concentration with the calculated values by (Peter et al. 2005)

In the following, the computed concentrations of the various species in (Papadakis et al. 1989)'s experiments are compared with the corresponding values calculated by (Peter et al. 2005). Following the latter investigators, at the given depths, the concentration profile of each species is plotted as fraction of the maximum concentration of the same species computed as

$$[CH]_{\max} = [CH]_{ini} + 0.5[C_2S]_{ini} + 1.5[C_3S]_{ini} \quad (3.65)$$

$$[CaCO_3]_{\max} = [CH]_{\max} + 3[CSH]_{ini} + 2[C_2S]_{ini} + 3[C_3S]_{ini} \quad (3.66)$$

where subscript "ini" and subscript "$\max$" means initial and maximum concentration of the species, respectively.

Carbonation depth is defined as the region where the $CaCO_3$ concentration is greater than 10% of maximum $CaCO_3$ given by Eq. 3.66.

Figure 3.3 shows the normalized calcite concentration variation through the thickness of specimen S2.

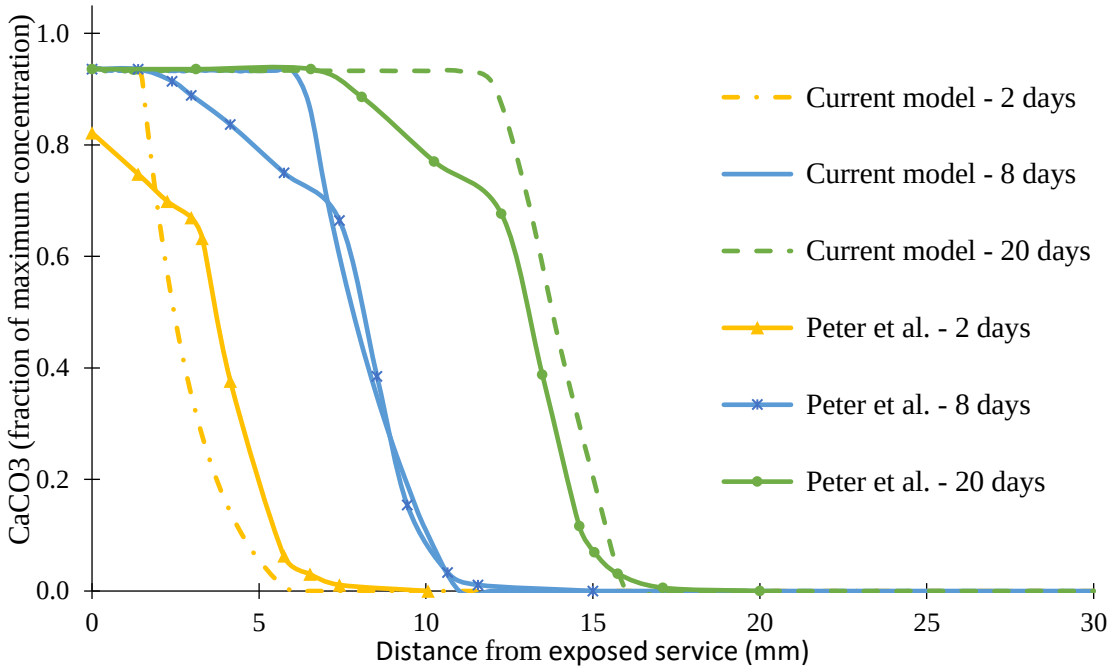

Fig. 3.3: Comparison of S2 specimen Calcite concentration computed by the current model with that calculated by Peter et al.

It can be observed that contrary to Peter et al.'s computed profiles, the ones given by the current model do not exhibit initially a gradual reduction from the peak, followed by a steep reduction. The lack of the two-stage reduction can be attributed to allowing the concurrent carbonation of CH and CSH in the current model while the Peter et al. model does not permit carbonation of CSH until all the CH has completely carbonated. The authors believe that the approach adopted in the current model conforms better to the real situation.

Figure 3.4 shows the normalized CH concentration variation through the S2 specimen thickness.

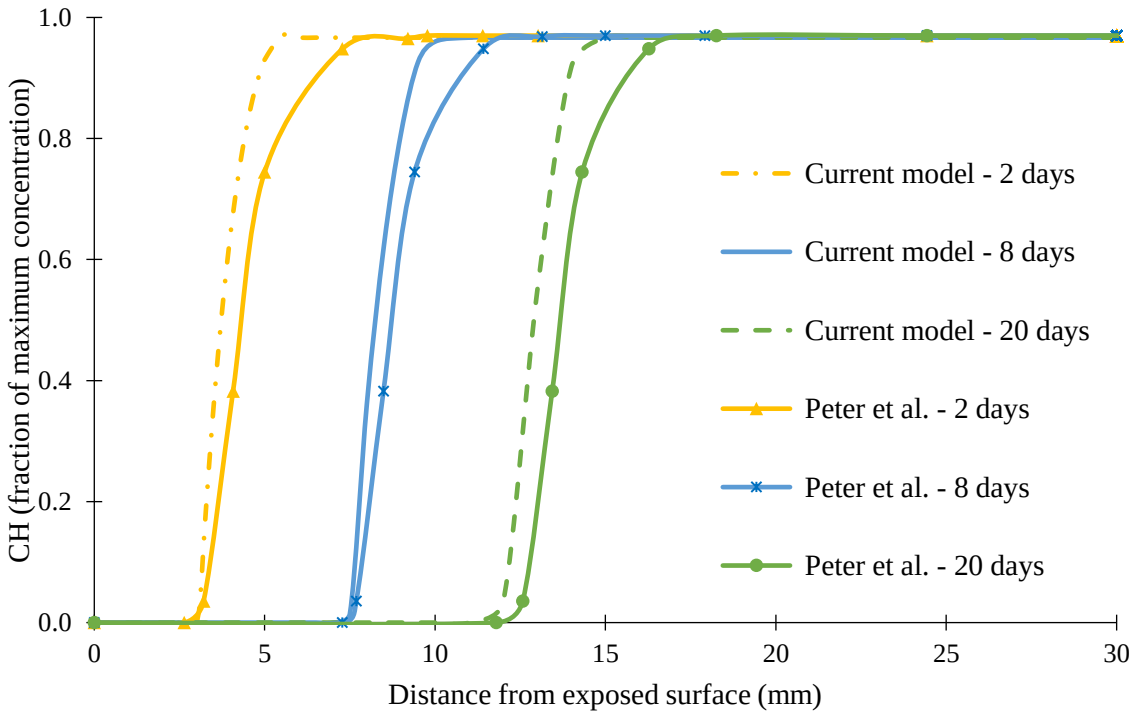

Fig. 3.4: Comparison of Portlandite fraction computed by the current model with that calculated by Peter et al. for S2 specimen

The difference between the Peter et al. model and the current analysis values is again ascribed to the sequence of carbonation of CH and CSH, as described earlier, and to the manner in which the interaction between the solid phases and the pore solution is dealt with in the current model.

The profile of the normalized concentration of the gaseous phase of CO_2 through the specimen thickness is illustrated in Figure 3.5, which shows that the current model predicts deeper penetration, but less concentration of the gas compared to Peter et al.'s model. The differences can be ascribed to the manner that chemical equilibrium is established in the two models.

Finally, the pH variation through the thickness of the specimen is plotted in Figure. 3.6.

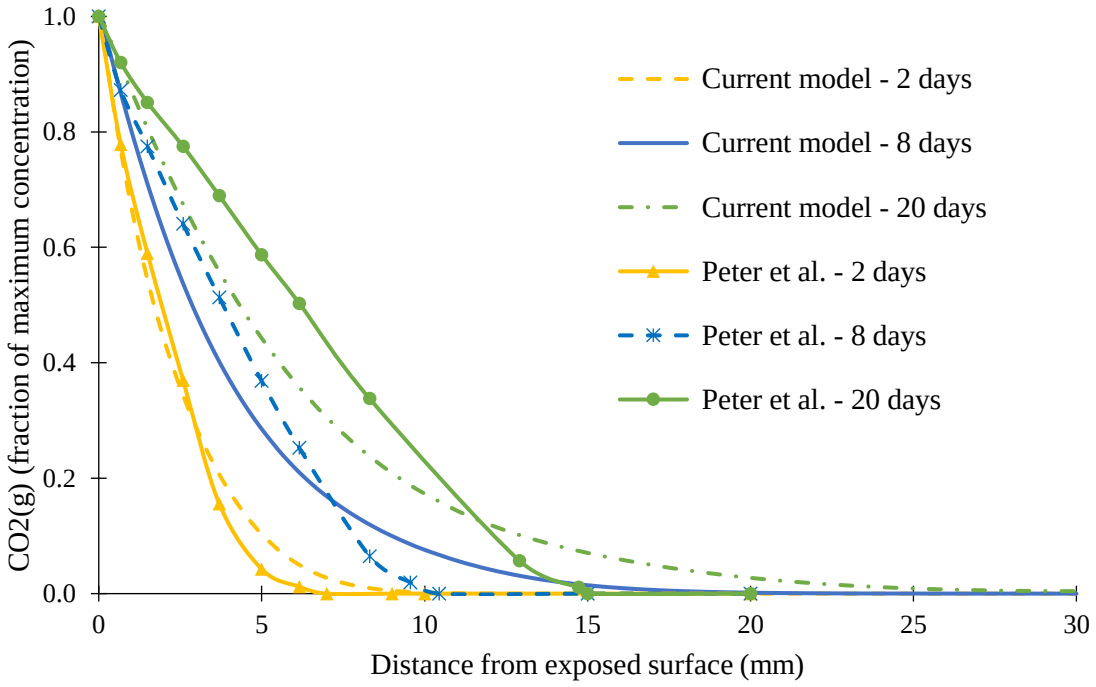

Fig. 3.5: Comparison of CO_2(g) fraction computed by the current model with that calculated by Peter et al. for S2 specimen

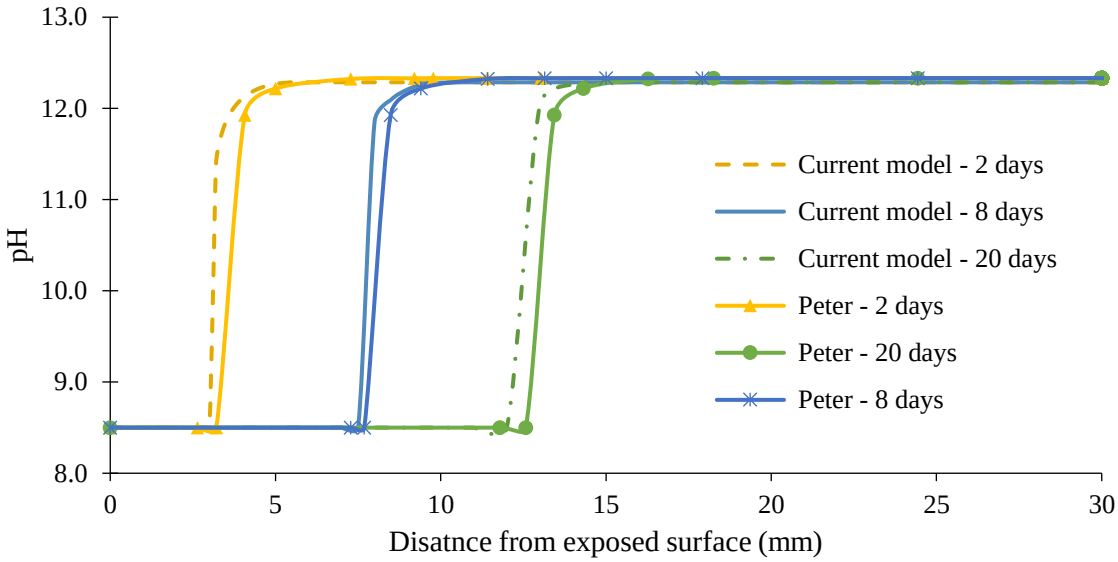

Fig. 3.6: Comparison of pH values computed by the current model with those computed by Peter et al. of S2 specimen

The difference in the pH values between the two predicted profiles by the two models can be attributed to the difference between the predicted CH values by the two models, as suggested by Papadakis et al.

$$pH = 14 + \log\left(2\left[CH\right]\right) \tag{3.67}$$

where $\left[CH\right]$ is the molarity of Portlandite

3.7 CONCLUSIONS

The coupled Nernst-Planck-Poisson equations governing carbon dioxide transport in portland cement concrete by Fickian diffusion, electromigration and ionic activity are solved using the Galerkin's finite element method. Mass and charge conservation are

preserved by considering the chemical equilibrium among the various species within the concrete pore solution. Results of the study support the following conclusions:

1. As indicated by the close agreement between the results of the current model and the corresponding experimental data, the model can accurately predict the coupled effect of carbonation and chloride attack.
2. Compared to an existing detailed carbonation model, the current model appears to more accurately determine the CH and CSH concentrations as well as the concrete pH variation through the thickness of a specimen subjected to one-dimensional carbonation.
3. Detailed consideration of the chemical reactions among the various species within the concrete pore solution and establishing their equilibrium based on laws of chemistry, as performed in the current model, lead to accurate estimation of the concrete pH, after exposure to CO_2.

3.8 ACKNOWLEDGMENTS

The first author gratefully acknowledges the financial support of McMaster University and the Natural Sciences and Engineering Research Council Canada (NSERC) in support of this research. The second author wishes to thank NSERC for its financial support of the investigation through its Discovery Grant program. The second author is also grateful for the financial assistance of Tianjin government, the Ministry of Science and Technology of China and Nankai University in support of the preparation of this paper.

3.9 REFERENCES

Abreu, E., Douglas, J., Furtado, E. and Pereira E.. 2009. “Operator Splitting for Three-Phase Flow in Heterogeneous Porous Media.” *Communications in Computational Physics* 6 (1): 72–84. https://doi.org/10.4208/cicp.2009.v6.p72.

Barbarulo, R., Marchand, J., Snyder, K. A. and Prené, S.. 2000. “Dimensional Analysis of Ionic Transport Problems in Hydrated Cement Systems - Part 1. Theoretical Considerations.” *Cement and Concrete Research* 30 (12): 1955–60. https://doi.org/10.1016/S0008-8846(00)00383-5.

Brieger, L M. 1986. “Numerical Simulation of Carbonation of Concrete.” In *Werkstoffwissenschaften Und Bausanierung, Berishtsband Zum 2. Internationalen Kolloquium*, 635–40. Technische Akademie Esslingen.

Christopher, H. A., and Shipman, C. W.. 1968. “Poisson’s Equation as a Condition of Equilibrium in Electrochemical Systems.” *Journal of The Electrochemical Society* 115 (5): 501. https://doi.org/10.1149/1.2411292.

Garrels, R. M., and Christ, C. L.. 1965. *Solutions, Minerals, and Equilibria*. New York: Harper & Row.

Heath, M. T. 2018. *Scientific Computing: An Introductory Survey*. *SIAM*. Philadelphia: McGraw-Hill.

Hyvert, N., Sellier, A., Duprat, F., Rougeau, P. and Francisco, P.. 2010. “Dependency of C–S–H Carbonation Rate on CO2 Pressure to Explain Transition from Accelerated

Tests to Natural Carbonation." *Cement and Concrete Research* 40 (11): 1582–89. https://doi.org/https://doi.org/10.1016/j.cemconres.2010.06.010.

Isgor, B.O., and Razaqpur, A.G.. 2004. "Finite Element Modeling of Coupled Heat Transfer, Moisture Transport and Carbonation Processes in Concrete Structures." *Cement and Concrete Composites* 26 (1): 57–73. https://doi.org/https://doi.org/10.1016/S0958-9465(02)00125-7.

Jeong, J., Ramezani, H., and Chuta, E.. 2019. "Reactive Transport Numerical Modeling of Mortar Carbonation: Atmospheric and Accelerated Carbonation." *Journal of Building Engineering* 23: 351–68. https://doi.org/10.1016/j.jobe.2019.01.038.

Logan, D. L. 2012. *A First Course in the Finite Element Method*. Fifth Edit. Stamford, CT: Cengage Learning.

Maage, M., Helland, S., Poulsen, E., Vennesland, Ø. and Carlsen, J. E.. 1996. "Service Life Prediction of Existing Concrete Structures Exposed to Marine Environment." *ACI Materials Journal* 93 (6): 602–8. https://doi.org/10.14359/9866.

MacGillivray, A. D. 1968. "Nernst-Planck Equations and the Electroneutrality and Donnan Equilibrium Assumptions." *The Journal of Chemical Physics* 48 (7): 2903–7.

MacGillivray, A. D., and Hare, D.. 1969. "Applicability of Goldman's Constant Field Assumption to Biological Systems." *Journal of Theoretical Biology* 25 (1): 113–26.

Moore, W. J.. 1998. *Physical Chemistry*. Fifth edit. Beccles and London, Great Britain: Longman.

Nguyen, P. T., and Amiri, O.. 2016. “Study of the Chloride Transport in Unsaturated Concrete: Highlighting of Electrical Double Layer, Temperature and Hysteresis Effects.” *Construction and Building Materials* 122: 284–93. https://doi.org/10.1016/j.conbuildmat.2016.05.154.

Papadakis, V. G., Vayenas, C. G., and Fardis, M. N.. 1989. “A Reaction Engineering Approach to the Problem of Concrete Carbonation.” *AIChE Journal* 35 (10): 1639–50. https://doi.org/10.1002/aic.690351008.

Papadakis, V. G., Vayenas, C. G. and Fardis, M. N.. 1991. “Fundamental Modeling and Experimental Investigation of Concrete Carbonation.” *ACI Materials Journal* 88 (4): 363–73.

Peter, A. M., Muntean, A., Meier, A. S., and Bohm, M.. 2005. “Modelling and Simulation of Concrete Carbonation: Competition of Several Carbonation Reactions.” Bremen: Universität Bremen.

Pitzer, K. S. 1991. *Activity Coefficients in Electrolyte Solutions*. Boca Raton, FL: CRC Press.

Reddy, J. N., and Gartling, D. K.. 2010. *The Finite Element Method in Heat Transfer and Fluid Dynamics*. *The Finite Element Method in Heat Transfer and Fluid Dynamics*. Third Ed. CRC Press.

Rilem. 1988. “CPC-18 Measurement of Hardened Concrete Carbonation Depth.” *RILEM Recommendations TC56-MHM Hydrocarbon Materials*.

https://doi.org/10.1007/BF02472327.

Saetta, A. V., and Vitaliani, R. V.. 2005. "Experimental Investigation and Numerical Modeling of Carbonation Process in Reinforced Concrete Structures Part II. Practical Applications." *Cement and Concrete Research* 35 (5): 958–67. https://doi.org/10.1016/j.cemconres.2004.06.023.

Sakata, K. 1983. "A Study on Moisture Diffusion in Drying and Drying Shrinkage of Concrete." *Cement and Concrete Research* 13 (2): 216–24. https://doi.org/10.1016/0008-8846(83)90104-7.

Samson, E., Lemaire, G., Marchand, J., and Beaudoin, J.J.. 1999. "Modeling Chemical Activity Effects in Strong Ionic Solutions." *Computational Materials Science* 15 (3): 285–94. https://doi.org/10.1016/s0927-0256(99)00017-8.

Samson, E., and Marchand, J.. 2007. "Modeling the Transport of Ions in Unsaturated Cement-Based Materials." *Computers & Structures* 85 (23–24): 1740–56. https://doi.org/10.1016/j.compstruc.2007.04.008.

Samson, E., and Marchand, J.. 2006. "Multiionic Approaches to Model Chloride Binding in Cementitious Metrials." In *2nd International RILEM Symposium on Advances in Concrete through Science and Engineering*, edited by M. Jolin and F. Paradis J. Marchand, B. Bissonnette, R. Gagné, 101–122. Quebec City, Canada: RILEM Publication SARL. https://doi.org/10.1617/2351580028.008.

Segerlind, L. J. 1984. *Applied Finite Element Analysis*. Second Ed. United States of

America: John Wiley and Sons.

Soli, A. L., and Byrne,R. H.. 2002. "CO_2 System Hydration and Dehydration Kinetics and the Equilibrium CO_2/H_2CO_3 Ratio in Aqueous NaCl Solution." Marine Chemistry 78 (2–3): 65–73. https://doi.org/10.1016/S0304-4203(02)00010-5.

Taigbenu, A. E. 1999. "Unsaturated Flow (Richards Equation)." In *The Green Element Method*, edited by Akpofure E Taigbenu, 217–30. Boston, MA: Springer US. https://doi.org/10.1007/978-1-4757-6738-4_8.

The MathWorks Inc. 2018. "MATLAB." https://www.mathworks.com/.

Thiery, M.. 2005. "Modélisation de La Carbonatation Atmosphérique Des Matériaux Cimentaires : Prise En Compte Des Effets Cinétiques et Des Modifications Microstructurales et Hydriques." Ecole Nationale Des Ponts et Chaussees.

Tuutti, K.. 1982. "Corrosion of Steel in Concrete." Edited by betong Svenska forskningsinstitutet för cement och. *Swedish Cement and Concrete Research Institute*. Stockholm: Swedish Cement and Concrete Research Institute.

Xi, Y. P., Bazant, Z. P., and Jennings, H. M.. 1994. "Moisture Diffusion in Cementitious Materials - Adsorption Isotherms." *Advanced Cement Based Materials* 1 (6): 248–57. https://doi.org/10.1016/1065-7355(94)90033-7.

Yeh, G. T., and Tripathi, V. S.. 1989. "A Critical Evaluation of Recent Developments in Hydrogeochemical Transport Models of Reactive Multichemical Components." *Water Resources Research* 25 (1): 93–108.

https://doi.org/10.1029/WR025i001p00093.

Zienkiewicz, O., Taylor,R. L., and Zhu, J. Z.. 2013. *The Finite Element Method: Its Basis and Fundamentals*. Seventh Ed. New York: Elsevier Butterworth-Heinemann.

CHAPTER 4

A REACTIVE TRANSPORT MODEL FOR CHLORIDE MOVEMENT IN PRE-CARBONATED CONCRETE

4.1 ABSTRACT

The time-dependent transport of chloride ions in pre-carbonated concrete is modelled as a sequential Nernst-Planck-Poisson (NPP) reactive transport process. First, the effects of carbonation on the concrete physical and chemical properties are determined. Next, the ingress of chlorides in the carbonated and non-carbonated portion of the concrete and the ensuing changes in the relevant concrete properties are determined. To account for the reactions among the chemical species in the pore solution and their dissolution/precipitation, the transport model is supplemented with a comprehensive chemical module that ensures chemical equilibrium among the species involved. By quantifying the amount of Friedel's salt formed during the chemical reactions, the free and bound chlorides proportions are evaluated without resorting to empirical isotherms. The changes in the pore solution pH, the concrete porosity, and the diffusion coefficients of the relevant species due to the changes in the volumetric ratio of the solid phases within the hydrated cement are also computed. The non-steady governing transport equations are solved using the Galerkin's finite element formulation and an implicit Euler scheme in the time domain. The model is validated by the reasonable agreement between its results and the corresponding experimental data in the literature for both non-carbonated and carbonated concretes.

4.2 INTRODUCTION

The corrosion of the steel reinforcement bars (rebars) is a major cause of the deterioration of reinforced concrete (RC) structures exposed to aggressive environments. It shortens their expected service-life and endangers their safety, unless timely and effective maintenance and repair works are undertaken. The two main causes of steel corrosion in RC structures are known to be chloride attack and carbonation. Once the concentration of free chloride ions exceeds a certain threshold or the pH of concrete drops below a certain level at the surface of the steel, the conditions for corrosion initiation are created (Papadakis et al. 1991). Hence, the key to predicting the service life of the structure and to undertaking timely and effective repair is one's ability to accurately estimate, spatially and temporally, the extent of carbonation and chloride concentration in the structure. The end of service life means that the structure at the end of this period may not be able to properly function without extensive repair/rehabilitation. Although one could take core samples from the structure to make these determinations, it would be intrusive and likely expensive. Furthermore, the gathered information cannot be confidently extrapolated to the future or to all other locations within the structure without a sound theoretical basis. Alternatively, one can develop robust and validated theoretical models which can be applied by themselves, or supplemented with limited test data, to assess the current condition and the future status of the structure under prescribed exposure conditions.

Application of theoretical models for estimating chloride diffusion in concrete based on Fick's second law of diffusion date back to almost half a century ago, and they have undergone gradual improvements over the years through the inclusion of the effects of

temperature, relative humidity, degree of cement hydration and chloride binding on the chlorides apparent diffusion coefficient (Collepardi et al. 1972; Saetta et al. 1993; Martín-Pérez et al. 2001). Other models have been developed based on the Nernst-Planck-Poisson (NPP) equations coupled with the enforcement of chemical equilibrium among the species in the concrete pore solution (Samson and Marchand 2007a; Samson et al. 2005; Alsheet and Razaqpur 2020b). The latter are often termed reactive transport models and follow procedures similar to those used in other fields such as hydrogeology (Xu et al. 1999).

Similar developments have taken place with respect to modelling carbonation of concrete. Fickian diffusion models for ingress of CO_2 and its interaction with the chemical species in the concrete pore solution and the solid phases in the hydrate cement were applied by several investigators (Papadakis et al. 1991; Isgor and Razaqpur 2004). A more advanced NPP reactive transport model, including detailed consideration of the dissolution/precipitation reactions, was developed by (Alsheet and Razaqpur 2020a).

While chloride diffusion and carbonation in concrete have been individually extensively investigated, their synergetic effect on concrete has received less attention, both experimentally and analytically. Since exposure of concrete to the atmosphere leads to its immediate carbonation, it is important to determine chloride diffusion in carbonated concrete and to investigate the effects of carbonation on chloride diffusion properties in concrete and on the durability of concrete structures.

The CO_2 diffuses into the concrete via the concrete pore solution, forms carbonic acid and the acid reacts with the calcium hydroxide in the concrete and lowers its pH. The drop in pH render the rebars vulnerable to corrosion (Papadakis et al. 1991). On the other hand,

chlorides from deicing salts or marine water/vapor penetrate into the concrete and upon reaching the surface of rebars, attack them by destroying their protective passive layer and eventually causing corrosion (Hirao et al. 2005).

Carbonation can affect the concrete physically and chemically. Experimental evidence (Suryavanshi and Swamy 1996; Goñi and Guerrero 2003; Geng et al. 2016; Zibara 2001) reveals that carbonation of concrete samples previously subjected to chloride attack causes increase in the concentration of free chloride in the concrete pore solution, thus bound chlorides are released by carbonation (Zhu et al. 2016). Carbonation also causes reduction in the porosity of portland cement concrete (Jeong et al. 2019), which impedes subsequent diffusion of chlorides. It should be mentioned that in practice, chloride attack and carbonation are more likely to happen sequentially rather than concurrently. As soon as concrete/cement comes in contact with air bearing CO2, it is carbonated, but the diffusion of CO2 into concrete is relatively slow compared to that of chloride. Hence, due to the different rates of diffusion of the two phenomena, practically it is less likely that the two will occur concurrently.

Available literature shows some numerical models that deal with combined chloride diffusion and carbonation. (Zhu et al. 2016) used the traditional Fickian diffusion model, while other researchers (Wang and Baroghel-Bouny 2012; Mai-Nhu and Sellier 2013; Achour et al. 2019) applied the Nernst-Planck (NP) transport model under the assumption of electroneutrality. Irrespective of the type of transport model, these researchers employed some semi-empirical isotherms to model chloride binding. The effect of carbonation on chloride ions diffusion was considered by modifying their diffusion coefficient as function

of the reduction in concrete porosity and/or degree of moisture saturation induced by carbonation. In some cases, the binding isotherm parameters were also empirically adjusted to account for the effects of carbonation.

Wang and Baroghel-Bouny (2012) considered chloride binding in carbonated concrete to be negligible. The effect of carbonation on chloride transport was modeled by scaling the diffusion coefficient of chloride by the ratio of the porosity of carbonated concrete to the porosity of the non-carbonated concrete. Mai-Nhu and Sellier (2013), on the other hand, treated the chloride diffusion coefficient as a nonlinear function of the degree of saturation of concrete. Moreover, they reduced the concrete chloride binding capacity as a function of the amount of calcite ($CaCO_3$) produced by carbonation. Finally, they considered the change in porosity as a function of the change in the volume of the solid phases due to carbonation.

Achour et al. (2019) adopted the nonlinear relationship between the degree of saturation and the diffusion coefficient in the saturated state as suggested by Mai-Nhu and Sellier. They also used the latter researchers approach to adjustment of the chloride diffusion coefficient based on the change in the concrete porosity. Furthermore, they modified the values of the binding isotherm parameters to account for the lower binding capacity of carbonated concrete. Finally, due to carbonation, Zhu et al. (2016) modified (a) the porosity of concrete, (b) the binding isotherm parameters values, (c) the chloride diffusion coefficient as function of the ratio of the tortuosity and constructiveness of the non-carbonated to those of the carbonated concrete. Table 4.1 provides a summary of the key features of the afore-mentioned models.

The use of empirical isotherms in conjunction with the NP model and the assumption of electroneutrality make the above models semi-empirical and the accuracy of their results will depend on the selected binding isotherm and the selected values of its parameters. To avoid this issue, in this study, first the NPP transport model will be applied to track the

Table 4.1: Key features of some recent investigations on modeling combined chloride diffusion and carbonation

Research work	Transport mechanisms		Chloride binding		Year
	Fick's law	NP	Isotherms	Chemical Equilibrium	
Wang and Baroghel-Bouny (2012)		✓	✓		2012
Mai-Nhu and Sellier (2013)		✓	✓		2013
Zhu et al. (2016)	✓		✓		2016
Achour et al. (2019)		✓	✓		2019

transport of the ionic species in both the carbonated and the non-carbonated concrete. Since in the NPP model the electric field created by the ions in the pore solution will be determined by solving the Poisson's equation, the assumption of electroneutrality is dispensed within this investigation. Furthermore, chloride binding will be modelled by monitoring the formation of Friedel's salt and the associated dissolution/precipitation reactions rather than applying any empirical isotherm. Chemical equilibrium among the various species within the concrete pore solution will be satisfied and any change in the species concentration caused by chloride diffusion or carbonation will be quantified. The

change in concrete porosity will be evaluated by tracking the changes in the solid phases volume due to the chemical reactions within the concrete pore structure.

The writers believe that the fundamental and novel approach followed in the proposed model minimizes empiricism and it can be extended to other chemical interaction phenomena in concrete, such as combined chloride and sulfate attack. It is important to mention that in its present form, the proposed model treats carbonation and chloride diffusion as sequential, rather than concurrent, processes. Although here carbonated concrete was subjected to chloride diffusion, the model is able to simulate the two phenomena occurring in reverse order. Since carbonation does not occur under fully saturated condition while chloride diffusion often occurs in the saturated state, the preceding limitation may not pose a serious practical problem.

4.3 GOVERNING EQUATIONS OF THE PROBLEM

4.3.1 Modeling ionic species transport

The transport of ions in the porous media, such as concrete, can be modelled as a reactive transport process using the Nernst-Planck-Poisson's (NPP) system of equations (Alsheet and Razaqpur 2020b; Samson and Marchand 2007b), coupled with the relevant chemical equilibrium equations. In their general form, the NPP equations are basically the conservation of mass and charge equations that can be written for any chemical species *i* as

$$\frac{\partial wc_i}{\partial t}+\frac{\partial w_s c_i^s}{\partial t}-\nabla.\left(D_i w\nabla c_i+\frac{D_i w z_i F}{RT}\nabla\psi+D_i wc_i\nabla\left(ln\gamma_i\right)+D_w c_i\nabla w\right)+wr_i=0 \quad (4.1)$$

$$\nabla.\left(\tau w\nabla\psi\right)+\frac{F}{\varepsilon}w\left(\sum_{i=1}^{n}z_i c_i\right)=0 \quad (4.2)$$

In addition, Eq. 4.1 is coupled to Richards equation, Eq. 4.3 (Samson and Marchand 2007b; Taigbenu 1999), for determining the moisture transport in concrete as

$$\frac{\partial w}{\partial t}-\nabla.\left(D_w\nabla w\right)=0 \quad (4.3)$$

where c_i , z_i, D_i and γ_i, respectively, are the concentration, valence number, diffusion coefficient (m^2/sec) and activity coefficient of species i, F is Faraday constant = 96,488.46 (C/mol), τ is the apparent tortuosity of the concrete pore structure, which includes the tortuosity and constrictiveness of the porous medium, c_i^s is the concentration of the solid phase *i* (mol/m^3), w_s is the volumetric solid phase content (m^3/m^3), w is the volumetric water content (m^3/m^3), n is the number of species, R is the ideal gas constant = 8.3143 (J/mol/K), T is temperature of the solution (K), ψ is the electric potential (V), r_i: source/sink term, accounting for the production/consumption of species i. Note, in the current work moisture transport is assumed to take place in liquid form only.

Equations. 4.1 to 4.3 are general and can be applied to model three dimensional transport processes, but in the field of concrete science, it is common practice to treat chemical diffusion and other permeation phenomena as one-dimensional transport processes, from

the member exposed surface into its thickness, in which case, the above equations can be written in expanded form as Eqs. 4.4 to 4.6, respectively.

$$\frac{\partial\left(wc_i\right)}{\partial t}-\frac{\partial}{\partial x}\left(\underbrace{D_i w\frac{\partial c_i}{\partial x}}_{molecular}+\underbrace{\frac{D_i w z_i F}{RT}c_i\frac{\partial \psi}{\partial x}}_{electromigration}+\underbrace{D_i w c_i\frac{\partial \ln\gamma_i}{\partial x}}_{chemical\ activity}+\underbrace{D_w c_i\frac{\partial w}{\partial x}}_{advection}\right)=-wr_i-\frac{\partial\left(w_s c_i^s\right)}{\partial t} \tag{4.4}$$

$$\frac{d}{dx}\left(\tau w\frac{d\psi}{dx}\right)+\frac{F}{\varepsilon}w\left(\sum_{i=1}^{n}z_i c_i\right)=0 \tag{4.5}$$

$$\frac{\partial w}{\partial t}-\frac{\partial}{\partial x}\left(D_w\frac{\partial w}{\partial x}\right)=0 \tag{4.6}$$

The first term in the curly bracket on the left-hand side of Eq. 4.4 represents Fickian or concentration driven diffusion, the second term ionic migration due to the electric field created by the ions within the concrete pore solution, the third transport due to chemical activity, which reflects the effective concentration of a species in a multi-ionic solution, and the last term represents transport by advection (Achour et al. 2019; Samson and Marchand 2007b). In the present study, it is assumed that transport of chemical species occurs under constant temperature and humidity conditions, therefore, transport by advection is neglected. Moreover, for determining non-ionic species transport, e.g. $CO_{2(g)}$ and H_2CO_3, considering the molecular diffusion term in Eq. 4.4 alone will be sufficient.

For a chemical solution containing $i\,(i=1,n)$ ionic species, applying Eq. 4.4 to each species at a time, results in *n* equations, but due to the presence of the electric potential and advection terms, the system of equations will contain $(n+2)$ unknowns. Therefore, to

obtain a unique solution, another two relation are necessary among the unknowns of the problem. The additional relations are provided by the Poisson's equation (i.e. Eq. 4.5), which relates the electric potential to the charge distribution in the medium (Christopher and Shipman 1968), and Richard's equation, which provides the moisture distribution through the concrete thickness.

The right-hand side of Eq. 4.4 is related to the solid phases in the hydrated cement and their chemical reactions while the left-hand side is related to the transport of the relevant ionic species. By applying the operator-splitting approach, one can solve Eq. 4.4 in two separate modules (i.e. transport module and chemical module). The two modules are solved following a sequential non-iterative approach (SNIA). Local chemical equilibrium can be assumed at each point in the medium for the majority of the ionic transport problems (Samson and Marchand 2007b). Thus, the SNIA approach can be applied to the reactive transport of porous media.

Under the assumption of constant temperature and humidity, the diffusion coefficient in porous media can be written as function of the porosity and the tortuosity of its pore structure as (Samson and Marchand 2007b)

$$D_i = \tau D_i^0 P(D) \tag{4.7}$$

where D_i^0 is the diffusion coefficient of species i in free-water (m^2/sec). Value of D_i^0 for all the species involved in chloride ingress and carbonation are given in Table 4.2 (Rumble et al. 2019). $P(D)$ is a coefficient that accounts for the change in porosity due to

dissolution/precipitation of solids during the diffusion process and can be evaluated as proposed by Samson and Marchand (2007b), i.e.

$$P(D) = \frac{e^{4.3\phi/V_p}}{e^{4.3\phi_o/V_p}} \tag{4.8}$$

where ϕ_o is the initial porosity of concrete, ϕ is the porosity of concrete at a given age, per Eq. 4.9, and v_p is the volumetric paste content (m^3/m^3) of concrete

$$\phi = \phi_o + \sum_{m=1}^{M} \left(V_m^{ini} - V_m \right) \tag{4.9}$$

where V_m^{ini} and V_m, respectively, are the initial and instantaneous volumetric content of a given solid phase (m^3/m^3), and M is the total number of solid phases. The quantity V_m is determined by enforcing mass balance after each dissolution/precipitation reaction while V_m^{ini} is found by determining the quantity of each solid phase prior to the commencement of diffusion.

The diffusion coefficient of gaseous CO_2 is given by Papadakis et al. (1991) as follows:

$$D_{CO_{2(g)}}^0 = 1.64\,\phi^{1.8}\left(1 - RH/100\right)^{2.2} \times 10^{-6} \tag{4.10}$$

where RH is the relative humidity (%)

Table 4.2: Diffusion coefficient in free water, D_i^0, for species i in the concrete pore solution (Rumble et al. 2019; Papadakis et al. 1991)

Species	D_i^0 **(m²/sec) x 10⁻⁹**	**Species**	D_i^0 **(m²/sec) x 10⁻⁹**	**Species**	D_i^0 **(m²/sec) x 10⁻⁹**
OH^-	5.27	SO_4^{2-}	1.07	$CO_{2(aq)}$	1.1628
Na^+	1.33	Ca^{2+}	0.792	CO_3^{2-}	0.96
K^+	1.96	Cl^-	2.03	HCO_3^-	1.18
$Al(OH)_4^-$	0.54	H_2CO_3	0.0289	H^+	9.31

4.3.2 Modeling chemical activity

The chemical activity coefficient can be evaluated using different models, varying in complexity from simple, e.g. Debye-Hückel and Davies (Moore 1998), to complex, e.g. Pitzer (Pitzer 1991). According to Samson et al. (1999), the modified Davies relationship given by Eq. 4.11 yields good results for a wide range of ionic strengths, hence it is adopted in the current work

$$\ln \gamma_i = Az_i^2 \left(\frac{\sqrt{I}}{1 + a_i B\sqrt{I}} - \frac{\left(0.2 - 4.17x10^{-5} I\right) I}{\sqrt{1000}} \right) \tag{4.11}$$

where I, is the ionic strength (mM), given by Eq. 4.12, A and B are temperature dependent parameters given by equations Eqs. 4.13 and 4.14, and a_i is a fitting parameter (m) given in Table 4.3

$$I = 0.5 \sum_i z_i^2 c_i \tag{4.12}$$

$$A = \frac{\sqrt{2} F^2 e_0}{8\pi \left(\varepsilon RT\right)^{3/2}} \tag{4.13}$$

$$B = \sqrt{\frac{2F^2}{\varepsilon RT}} \tag{4.14}$$

where e_0 is the electric charge of one electron 1.602x10^{-19} C. For the common ions present in the concrete pore solution and those involved in chloride diffusion and carbonation, values of parameter a_i are shown in Table 4.3.

Table 4.3: Parameter a_i value for common ions in the concrete pore solution: (Samson et al. 1999; Gustafsson 2014)

Ion	a_i **(m) x 10^{-10}**	**Ion**	a_i **(m) x 10^{-10}**	**Ion**	a_i **(m) x 10^{-10}**	**Ion**	a_i **(m) x 10^{-10}**	**Ion**	a_i **(m) x 10^{-10}**
OH^-	3	SO_4^{2-}	1	K^+	3.3	$Al(OH)_4^-$	1.5	CO_3^{2-}	5.4
Na^+	3	Ca^{2+}	1 x 10^{-3}	Cl^-	2	$HCO3^-$	5.4	H^+	1

a_i for HCO_3^-, CO_3^{2-}, and H^+ were not given in by (Samson et al. 1999), hence they were determined here using the Debye-Hückel's model.

4.3.3 Modeling chemical reactions

There are two sets of chemical reactions involved in the current investigation, and each set may involve two types of reactions, viz. dissolution/precipitation and ion exchange. The first set pertains to concrete carbonation reactions, which is assumed to precede chloride diffusion, and the second set to chloride ingress into carbonated and non-carbonate concrete. The pertinent reactions are summarized below.

4.3.3.1 Carbonation reactions

The concrete carbonation involves the following set of reactions (Alsheet and Razaqpur 2020a; Thiery 2005; Revert et al. 2019)

$$CaCO_{3(s)} \rightleftarrows Ca^{2+} + CO_3^{2-} \quad (4.15\text{-a})$$

$$Ca(OH)_{2(s)} \rightleftarrows Ca^{2+} + 2OH^- \quad (4.15\text{-b})$$

$$AFt \rightleftarrows 6Ca^{2+} + 4OH^- + 3SO_4^{2-} + 2Al(OH)_4^- \quad (4.15\text{-c})$$

$$AFm \rightleftarrows 4Ca^{2+} + 4OH^- + SO_4^{2-} + 2Al(OH)_4^- \quad (4.15\text{-d})$$

$$CO_{2(aq)} + H_2O \rightleftarrows H_2CO_3 \quad (4.15\text{-e})$$

$$H_2CO_3 \rightleftarrows HCO_3^- + H^+ \quad (4.15\text{-f})$$

$$HCO_3^- \rightleftarrows CO_3^{2-} + H^+ \quad (4.15\text{-g})$$

$$H_2O \rightleftarrows OH^- + H^+ \quad (4.15\text{-h})$$

In addition, Berner (Berner 1992) reported that CSH also partially decalcifies in the given C/S (Ca/Silica) ratio, which was expressed as

$$CSH \rightarrow CaH_2SiO_4 + 0.65Ca(OH)_2 \quad (4.16)$$

Hence, the latter decomposition increases the portlandite concentration in the pore solution. However, Berner also noted that the portlandite in Eq. 4.16 dissolves with a solubility

constant of $10^{-6.2}$ for the given C/S ratio versus the $10^{-5.2}$ for the portlandite produced during the cement hydration.

The balance between the gaseous and aqueous phases of carbon dioxide can be modelled using Henry's law (Peter et al. 2005)

$$r_{Henry} = C^{ex}\left(C^{Henry}C_{CO_{2(g)}} - C_{CO_2}\right) \tag{4.17}$$

where C^{ex} is the interfacial mass-transfer coefficient (taken as 0.0116 1/s) and C^{Henry} is Henry's constant (taken as 0.85) as per (Peter et al. 2005) suggestion.

4.3.3.2 Chloride diffusion reactions

Friedel's salt forms by the ion exchange process between the chloride and the sulfate ions in Alumina-Ferric Oxide-Monosulfate (AFm) phases in hydrated cement (Johannesson et al. 2007; Jones et al. 2003), which follows the series of reactions below (Alsheet and Razaqpur 2020b; Samson and Marchand 2007b)

$$Ca(OH)_{2(s)} \rightleftarrows Ca^{2+} + 2OH^- \tag{4.18}$$

$$AFt \rightleftarrows 6Ca^{2+} + 4OH^- + 3SO_4^{2-} + 2Al(OH)_4^- \tag{4.19}$$

$$AFm \rightleftarrows 4Ca^{2+} + 4OH^- + SO_4^{2-} + 2Al(OH)_4^- \tag{4.20}$$

$$\left[\underbrace{AFm^+ - SO_4^{2-}}_{monosulfate}\right] + 2Cl^- \rightleftarrows \left[\underbrace{AFm^+ - 2Cl^-}_{Friedel's\ salt}\right] + SO_4^{2-} \tag{4.21}$$

Chemical reactions are modelled by applying the law of mass action per Eq. 4.22, which embodies the law of conservation of mass and charge (Moore 1998)

$$K_m = \prod_{i=1}^{N} c_i^{\nu mi} \gamma_j^{\nu mi} \quad ; m = 1,...,M \tag{4.22}$$

where c_i and γ_i are the molar concentration and ionic activity coefficient of ion *i*, K_m is the solubility constant of the m^{th} solid, and ν_{mi} is the stoichiometric coefficient of species i in the m^{th} solid, *M* is the total number of solids, and *N* is the total number of ions in the solution. Values of K_m for the common solid phases in concrete are given in Table 4.4 (Samson and Marchand 2007b).

Table 4.4: Solubility constants for different solid phases

Solid Phase	**Equilibrium relationship**	$-log(K_m)$
Portlandite	$K_{sp_1} = \{Ca\}\{OH\}^2$	5.2
CH (due to CSH decalcification)	$K_{sp_2} = \{Ca\}\{OH\}^2$	6.2
Calcium carbonate	$K_{sp_3} = \{Ca\}\{CO_3\}$	8.48
Ettringite	$K_{sp_4} = \{Ca\}^6\{OH\}^4\{SO_4\}^3\{Al(OH)_4\}^2$	44
Monosulfate	$K_{sp_5} = \{Ca\}^4\{OH\}^4\{SO_4\}\{Al(OH)_4\}^2$	29.4
Friedel's salt	$K_m = \{Cl\}^2[AFm]/\{SO_4\}[FS]$	-3

$\{..\}$ indicates activity of species, $[..]$ indicates the solid content in mmol/g of concrete.

4.4 FINITE ELEMENT FORMULATION

4.4.1 Numerical formulation of transport governing equation

The system of Eqs. 4.4, 4.5 and 4.6 are solved to model the transport of the chemicals within the concrete pore solution. The Galerkin's weighted residual method (Zienkiewicz et al. 2013) is applied to convert the governing partial differential equations Eqs. 4.4 to 4.6 into a set of algebraic equations within the finite element method framework. As the governing equations are all second order, in one dimension, a linear finite element (FE), with two end nodes, suffices to satisfy the continuity requirements. The details of the Galerkin's FE formulation is presented elsewhere by the authors and others (Alsheet and Razaqpur 2020b; Samson and Marchand 2007b); it results in the following set of algebraic equations

$$\left[C\right]\left\{\dot{U}\right\}+\left[K\right]\left\{U\right\}=0 \tag{4.23}$$

where $\left[C\right]$ and $\left[K\right]$ are the global capacitance and conductance matrices and {U} is the vector of the nodal degrees of freedom or unknowns. The global matrices are obtained by assembling the corresponding element matrices, designated by the superscript *e*, and are computed as

$$\left[C\right]^{e}=A\int_{l}\left[N\right]^{T}\left[W\right]\left[N\right]dx \tag{4.24}$$

$$\left[K\right]^{e}=A\int_{l}\left[B\right]^{T}\left[k_{DE}\right]\left[B\right]dx+A\int_{l}\left[N\right]^{T}\left[k_{CA}\right]\left[N\right]dx+A\int_{l}\left[B\right]^{T}\left[k_{p}\right]\left[N\right]dx \tag{4.25}$$

where

$$[W]=\begin{bmatrix} w & 0 & 0 \\ 0 & w & 0 \\ 0 & 0 & 0 \end{bmatrix} \tag{4.26}$$

$$[N]=[N_1 \quad N_2]=\begin{bmatrix} 1-\frac{x}{\ell} & \frac{x}{\ell} \end{bmatrix} \tag{4.27}$$

$$[B]=\begin{bmatrix} N_{1,x} & 0 & 0 & N_{2,x} & 0 & 0 \\ 0 & N_{1,x} & 0 & 0 & N_{2,x} & 0 \\ 0 & 0 & N_{1,x} & 0 & 0 & N_{2,x} \end{bmatrix} \tag{4.28}$$

$$[k_{DE}]=\begin{bmatrix} wD_1 & 0 & \frac{D_1 z_1 F}{RT} wc_1 \\ 0 & wD_2 & \frac{D_2 z_2 F}{RT} wc_2 \\ 0 & 0 & \tau w \end{bmatrix} \tag{4.29}$$

$$[k_{CA}]=\begin{bmatrix} wD_1 \frac{d\ln\gamma_1}{dx} & 0 & 0 \\ 0 & wD_2 \frac{d\ln\gamma_2}{dx} & 0 \\ 0 & 0 & 0 \end{bmatrix} \tag{4.30}$$

$$[k_P]=\begin{bmatrix} 0 & 0 & 0 \\ 0 & 0 & 0 \\ -\frac{F}{\varepsilon} wz_1 & -\frac{F}{\varepsilon} wz_2 & 0 \end{bmatrix} \tag{4.31}$$

where x is a local coordinate (x = 0 at node 1 and x = ℓ at node 2), ℓ is the element length and *A* is its cross-sectional area. The matrices $[k_{DE}], [k_{CA}], [k_P]$ are constitutive matrices for diffusion plus electromigration, chemical activity, and electric potential, respectively. A two-point Gauss quadrature is used to perform the integrations numerically.

So far, only the procedure for the discretization of the continuum in spatial domain is shown. The time domain discretization of the quasi-harmonic Nernst-Plank-Poisson's equations are performed following a first-order single time-step algorithm with implicit Euler scheme as follows (Zienkiewicz et al. 2013):

$$[C_t]\left[\frac{\{U_t\}-\{U_{t-\Delta t}\}}{\Delta t}\right]+[K_t][U_t]=0 \tag{4.32}$$

which can be re-arranged as

$$\left([C_t]+\Delta t\,[K_t]\right)\{U_t\}=[C_t]\{U_{t-\Delta t}\} \tag{4.33}$$

where the subscript *t* represents time. The vector $\{U_t\}$ contains nodal unknowns values at the current time step, while $\{U_{t-\Delta t}\}$ contains their values at the previous time step, Δt is the time-step, and $[C_t]$ is the lumped capacitance matrix by summation of rows method, a process which improves the convergence of the selected time-discretization scheme.

Equation 4.33 represents a system of nonlinear equations, which need to be solved at each time-step. Several methods can be used to solve this system (Heath 2018); here, the Newton-Raphson's scheme is applied

4.4.2 Numerical formulation of the chemical equilibrium relations

The mass action law stated in Eq. 4.22 can be applied to each of the chemical reactions 4.15 to 4.21, and the concentration of each of the ions and solids involved at a given time in the analysis can be expressed in terms of its concentration at the beginning of the time step and any change in its value during the given time increment. For the carbonation analysis, the relevant chemical equilibrium equations are expressed as

$$\left[Ca^{2+}\right] = \left[Ca^{2+}\right]_0 + \xi_I + \xi_{II} + 6\xi_{III} + 4\xi_{IV} \tag{4.34}$$

$$\left[CO_3^{2-}\right] = \left[CO_3^{2-}\right]_0 + \xi_I + \xi_{VII} \tag{4.35}$$

$$\left[OH^-\right] = \left[OH^-\right]_0 + 2\xi_{II} + 4\xi_{III} + 4\xi_{IV} + \xi_{VIII} \tag{4.36}$$

$$\left[H^+\right] = \left[H^+\right]_0 + \xi_{VI} + \xi_{VII} + \xi_{VIII} \tag{4.37}$$

$$\left[H_2CO_3\right] = \left[H_2CO_3\right]_0 + \xi_V - \xi_{VI} \tag{4.38}$$

$$\left[HCO_3^-\right] = \left[HCO_3^-\right]_0 + \xi_{VI} - \xi_{VII} \tag{4.39}$$

$$\left[CO_{2(aq)}\right] = \left[CO_{2(aq)}\right]_0 - \xi_V \tag{4.40}$$

$$\left[H_2O\right] = \left[H_2O\right]_0 - \xi_V - \xi_{VIII} \tag{4.41}$$

while for the chloride analysis, involving chloride diffusion in carbonated or non-carbonated concrete, the pertinent equations are

$$\left[Ca\right] = \left[Ca\right]^0 + \xi_{CH} + 6\xi_{AFt} + 4\xi_{AFm} \tag{4.42}$$

$$[OH] = [OH]^0 + 2\xi_{CH} + 4\xi_{AFt} + 4\xi_{AFm} \quad (4.43)$$

$$[SO_4] = [SO_4]^0 + 3\xi_{AFt} + \xi_{AFm} - \xi_{FS} \quad (4.44)$$

$$[Al(OH)_4] = [Al(OH)_4]^0 + 2\xi_{AFt} + 2\xi_{AFm} \quad (4.45)$$

$$[Cl] = [Cl]^0 + 2\xi_{FS} \quad (4.46)$$

where $[\ ]^0$ represents the concentration at the end of a time step obtained from the solution of the transport equations, which may not satisfy chemical equilibrium. Hence, to restore chemical equilibrium, the concentrations must be adjusted according to the latter two sets of chemical equilibria.

In the above equations, the symbol ξ_s refers to the unknown amount of species *s* that must dissociate or precipitate to restore chemical equilibrium in the pore solution. With reference to the solubility constants in Table 4.4, the relevant concentrations from Eqs. 4.34 to 4.46 can be substituted in the second column of Table 4.4, but because the latter concentrations will not automatically satisfy equilibrium, for the case of chloride diffusion, for example, the equations will produce residuals as shown below

$$R_{CH} = \{Ca\}\{OH\}^2 - K_{sp1} \quad (4.47)$$

$$R_{AFt} = \{Ca\}^6\{OH\}^4\{SO_4\}^3\{Al(OH)_4\}^2 - K_{sp4} \quad (4.48)$$

$$R_{AFm} = \{Ca\}^4\{OH\}^4\{SO_4\}\{Al(OH)_4\}^2 - K_{sp5} \quad (4.49)$$

$$R_{FS} = \{Cl\}^2[AFm]/\{SO_4\}[FS] - K_m \quad (4.50)$$

Following Samson and Marchand (2006), determination of the unknow ξ_s values involve a set of nonlinear equations that must be solved iteratively until equilibrium is satisfied, or the R_s become negligibly small, based on a prescribed tolerance. This process can be expressed as

$$\left[K_T^{j-1}\right]\left\{\Delta\xi^j\right\} = -\left\{R^{j-1}\right\} \tag{4.51}$$

$$\left\{\xi^j\right\} = \left\{\xi^{j-1}\right\} + \left\{\Delta\xi^j\right\} \tag{4.52}$$

where $[K_T]$ is the tangent matrix, j is the iteration number and $\Delta\xi$ is the correction applied to restore equilibrium. For example, for the species involved in chloride diffusion, the tangent matrix is given as

$$\left[K_T\right] = \begin{bmatrix} \frac{\partial R_{CH}}{\partial \xi_{CH}} & \frac{\partial R_{CH}}{\partial \xi_{AFt}} & \frac{\partial R_{CH}}{\partial \xi_{AFm}} & \frac{\partial R_{CH}}{\partial \xi_{FS}} \\ \frac{\partial R_{AFt}}{\partial \xi_{CH}} & \frac{\partial R_{AFt}}{\partial \xi_{AFt}} & \frac{\partial R_{AFt}}{\partial \xi_{AFm}} & \frac{\partial R_{AFt}}{\partial \xi_{FS}} \\ \frac{\partial R_{AFm}}{\partial \xi_{CH}} & \frac{\partial R_{AFm}}{\partial \xi_{AFt}} & \frac{\partial R_{AFm}}{\partial \xi_{AFm}} & \frac{\partial R_{AFm}}{\partial \xi_{FS}} \\ \frac{\partial R_{FS}}{\partial \xi_{CH}} & \frac{\partial R_{FS}}{\partial \xi_{AFt}} & \frac{\partial R_{FS}}{\partial \xi_{AFm}} & \frac{\partial R_{FS}}{\partial \xi_{FS}} \end{bmatrix} \tag{4.53}$$

Once equilibrium is satisfied, the solid phases contents are updated using

$$S_m^t = S_m^{t-1} - w\xi_m\Gamma_m / \rho \tag{4.54}$$

where S_m is the content of solid phase m [g/kg of concrete], Γ_m is the molar mass of the solid m [g/mol], ρ is the density of saturated concrete [kg/m^3], and superscript t indicates the time-step. It should be mentioned that the change in the solid content is accompanied

by change in volumetric water content, but in the current model the later change is assumed to be negligible. The validity of this assumption may need further investigation.

Figure 4.1 schematically summarises the key steps in the numerical model for determining chloride diffusion through carbonated concrete.

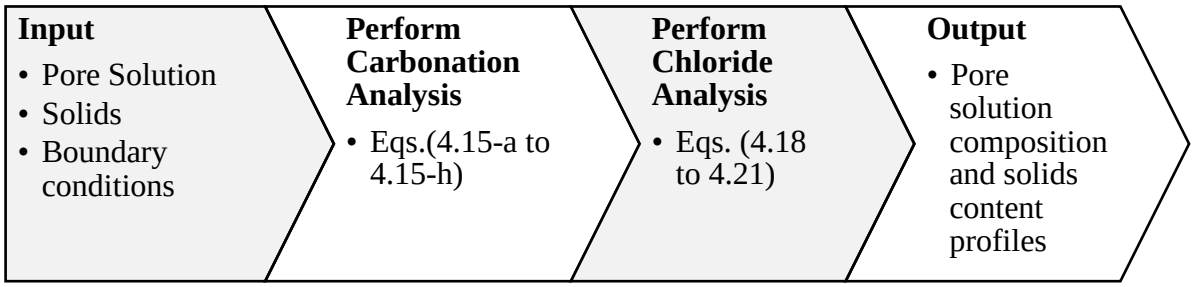

Fig. 4.1: Process of applying chloride analysis on carbonated sample adopted in this paper

The overall flowchart for the implementation of the time-dependent NPP reactive transport model in the current study is illustrated in Figure 4.2.

4.5 MODEL VERIFICATION

The implementation and expected accuracy of the foregoing NPP reactive transport model is demonstrated by comparing its results with available test data in the literature (Yuan et al. 2013).

4.5.1 Physical tests description and associated material properties

The experimental work of (Yuan et al. 2013) is selected to check the validity of the model and the accuracy of its result. Their tests involved chloride diffusion, carbonation and combined chloride diffusion and carbonation on a number of concrete samples. The tests were performed in two phases: in Phase I, one set of samples was subjected to unidirectional chloride diffusion for two months while the other set was exposed to unidirectional carbonation for 14 days. In Phase II, the carbonated samples from Phase I were subjected to chloride diffusion for two months under identical environmental and exposure conditions as in Phase I diffusion tests. These tests are simulated here using the proposed model and the results are compared with the corresponding experimentally measured pH values, carbonation depth and chloride profiles. In addition, detailed changes in the hydrated cement solid phase content precipitated by the intrusion of the above agents and their interaction are shown.

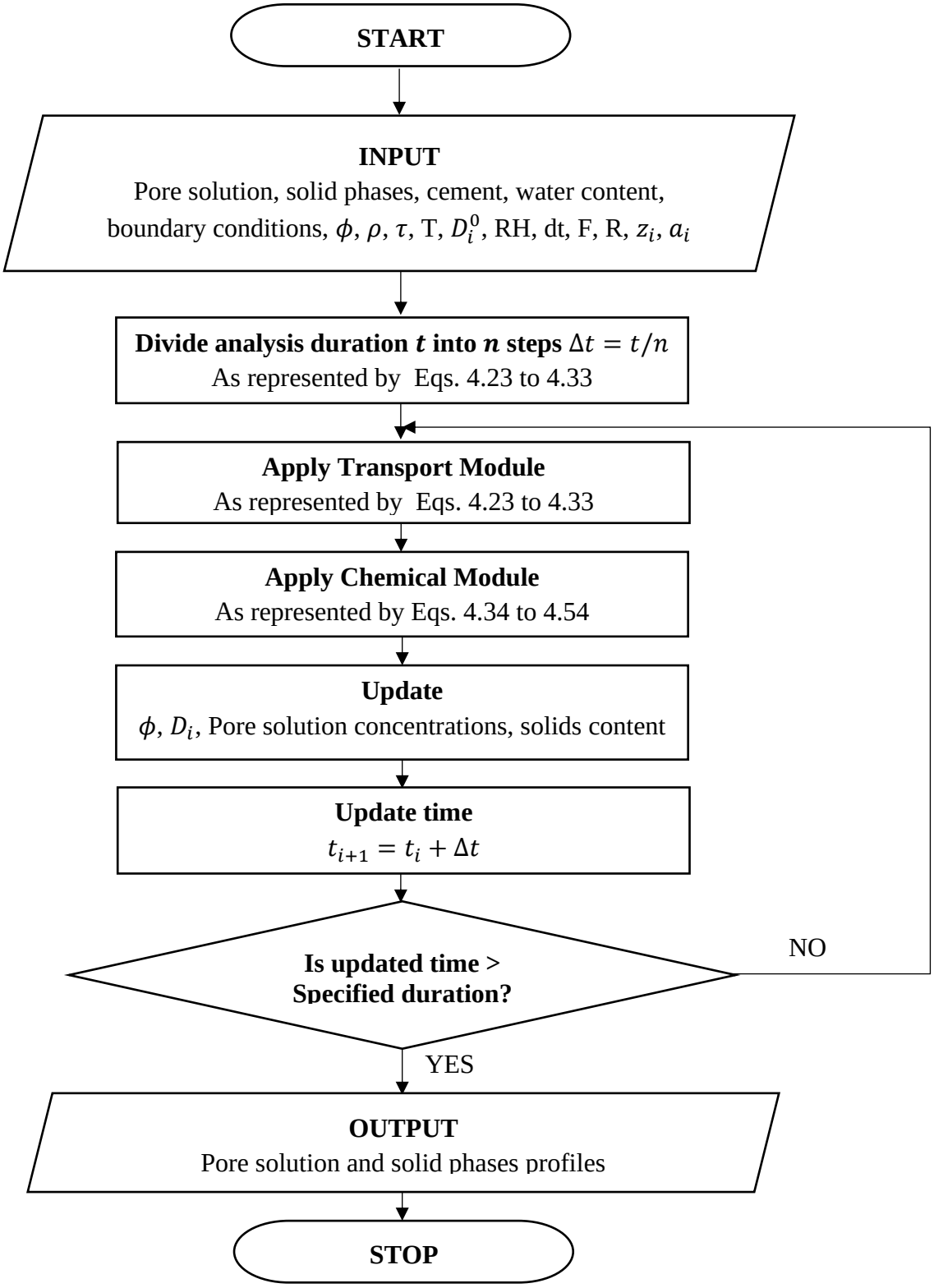

Fig. 4.2: Flowchart for the finite element implementation of the model.

It is important to point out that the proposed model requires detailed input data about the anhydrous cement composition and the hydrated concrete microstructure and diffusion properties. Since the full suite of required data is rarely reported in experimental works, it becomes necessary to make reasonable assumptions and estimate the missing values of the required parameters. This approach was followed to perform the present simulations.

The experiments by Yuan et al. (2013) involved sets of concrete cubes 100 mm on side, made with ordinary portland cement (OPC) and having different mixture proportions as shown in Table 4.5.

Table 4.5: Mix proportions of samples used by Yuan et al. (Yuan et al. 2013)

Concrete Mix	**Cement** (kg/m^3)	**Water** (kg/m^3)	**Gravel** (kg/m^3)	**Sand** (kg/m3)	**W/C** (-/-)	**A/C** (-/-)	**Superplasticizer** (%)	**Density** (kg/m^3)
I	457	160	1,159	624	0.35	3.90	0.5	2400
II	355	160	1,210	675	0.45	5.31	0.5	2400
III	290	160	1,267	683	0.55	6.72	0.5	2400

Since (Yuan et al. 2013) did not provide the chemical composition of the OPC in their mixes, it was estimated based on the guidelines in (Kosmatka et al. 2002), with SiO_2, CaO, Al_2O_3, and SO_3 being 20.2%wt, 63.2%wt, 4.3%wt, and 3.2%wt, respectively. The porosity ϕ of the test samples, shown in Table 4.6, were reported by the latter investigators, but their initial tortuosity τ was not, hence the tortuosity values in Table 4.6 were estimated using a trial-and error approach. Note, the subscripts "*o"* and "*c"* in the latter table designate the virgin and the carbonated concrete, respectively.

For estimating τ, different values were assumed until the computed concentration at one point near the exterior surface closely agreed with the corresponding experimentally measured chloride concentrations at the same location. Since the current model is not designed to track the evolution of the concrete microstructure, the preceding approach for estimating tortuosity, albeit semi-empirical, was found to give reasonable results in the present simulations. It should be mentioned that proprietary computational models already exist for the evaluation of concrete porosity, tortuosity and microstructure evolution (Bullard et al. 2018).

Table 4.6: Tortuosity and porosity of the samples under consideration

Sample	ϕ_0 **(%)**	ϕ_c **(%)**	τ_0 **(-)**	τ_c **(-)**
I	10.86	8.82	0.1797	0.1348
II	11.59	7.53	0.2400	0.0218
III	16.72	10.2	0.1282	0.0160

The amount of carbonatable solid phases in hydrated cement was estimated per Papadakis et al. (2000) recommendation as

$$CH = 0.29\,C - 0.5\,P \tag{4.55}$$

$$CSH = 0.57\,C - 0.79\,P \tag{4.56}$$

where: C, P ,respectively, denote cement and SCM (Supplementary Cementing Materials) mass content (kg/m^3 of concrete).

To calculate the molar concentration (mol/m^3 of concrete) of Ettringite (AFt) and Monosulfate (AFm), a modified form of Samson and Marchand's (2007b) proposed equations were used as shown below

$$3\frac{\Gamma_S}{\rho_c}\left[AFt\right]_0 + \frac{\Gamma_S}{\rho_c}\left[AFm\right]_0 = 10SO_3\frac{\Gamma_S}{\Gamma_{SO_3}} \quad (4.57)$$

$$2\frac{\Gamma_{Al}}{\rho_c}\left[AFt\right]_0 + 2\frac{\Gamma_{Al}}{\rho_c}\left[AFm\right]_0 = 10Al_2O_3\frac{2\Gamma_{Al}}{\Gamma_{Al_2O_3}} - 2\xi_{Al_2O_3}\frac{\Gamma_{Al}}{\Gamma_{Al_2O_3}}\left[CSH\right]_0\frac{\Gamma_{CSH}}{\rho_c} \quad (4.58)$$

where Γ_i is the molar weight of substance i (g/mol), $\xi_{Al_2O_3}$ is the amount of Al_2O_3 which substitute in the CSH, taken here to be 1% (Planel 2002; Samson and Marchand 2006), SO_3 and Al_2O_3 are the %wt of these compounds in the concrete while ρ_c is the density (kg/m^3) of concrete.

The computed hydrated solid phases in the concrete samples are summarized in Table 4.7. The solid phases of the carbonated samples were calculated using the carbonation model developed by the writers (Alsheet and Razaqpur 2020a).

Table 4.7: Initial hydrated solid phases for both carbonated and non-carbonated samples

Mix	CH		CSH		AFt		AFm		AFm^{Carb}
	mol/m^3	g/kg	mol/m^3	g/kg	mol/m^3	g/kg	mol/m^3	g/kg	g/ kg
I	1,788.8	55.2	2,039.5	108.5	4.9	2.5	160.1	41.5	34.1
II	1,389.5	42.9	1,584.3	84.3	3.8	2.0	124.4	32.2	26.6
III	1,135.1	35.0	1,294.2	68.9	3.1	1.6	101.6	26.3	21.7

AFm^{Carb} indicates the concentration of AFm in fully carbonated samples

In the fully carbonated zone, having carbonation degree, α_c, equal to 100% as per Eq. 4.59 (Matsushita et al. 2000), the concentration of CH is deemed negligible. Moreover, by comparing the AFm solid phase in carbonated and non-carbonated samples in Table 4.7, the carbonated samples have lower AFm content, thus they have lower binding capacity as

binding is based on ion-exchange between Cl^- and SO_4^{-2} in AFm phases, which results in the formation of Friedel's salt as per Eq. 4.21.

$$\alpha_C = \frac{(CO_2) - (CO_2)_0}{(CO_2)_{MAX} - (CO_2)_0} \times 100 \tag{4.59}$$

where $(..)$ is molar concentration (M), subscript "*0"* and "*MAX"* correspond to initial CO_2 concentration in the sample and maximum (ambient) concentration, respectively.

The initial pore solution composition for non-carbonated samples was estimated based on data reported by Samson and Marchand (2006) for a mix with similar composition, but for the carbonated pore solution, it was obtained by analysis using the carbonation model of Alsheet and Razaqpur (2020a). The pore solution composition for the non-carbonated concrete is shown in Table 4.8.

Table 4.8: Pore solution composition for non-carbonated zones of samples analyzed

Species	**OH^-**	**Na^+**	**K^+**	**SO_4^{2-}**	**Ca^{2+}**	**Cl^-**	**$Al(OH)^-_4$**
	mole/m^3 of pore solution						
Concentration	273.5	133.5	140.1	1.7	1.7	0	0.1

As the carbonation degree through the sample thickness varies (being 100% at exterior surface, 0% at the interface of the carbonated and non-carbonated concrete inside the test sample), for simplicity certain properties of the carbonated concrete layer were assumed to vary linearly through the carbonated layer thickness. These include porosity, tortuosity, and the diffusion coefficient. Using the model in (Alsheet and Razaqpur 2020a), the depth of

the carbonated zone was found to be 12 mm, which agrees with the estimated values based on the experimentally observed concrete pH variation through the sample thickness.

4.5.2 Finite element discretization

For the finite element modelling, only half of each concrete cube thickness, i.e. 50 mm, was discretized because the experimental results indicated chloride diffusion through less than 20 mm of the thickness in the non-carbonated and the carbonated samples. The same finite element mesh was used for modelling all the test specimens, and it comprised elements of length 0.1 mm for the first 5 mm from the exposed surface, 0.5 mm for the elements located from 5 to 10 mm from the surface, and 1 mm for the elements within the remaining 40 mm. The time step was selected to be 900 sec based on the suggestion in the literature (Samson and Marchand 2007b), the writers own experience (Alsheet and Razaqpur 2020b; 2020a) and after performing a sensitivity analysis.

In Phase I, following the relevant Chinese standard (GB National Standard 2010), the test samples were subjected to either accelerated carbonation for 14 days or to salt spray for two months. In Phase II, the pre-carbonated samples were subjected to salt spray for two months. The exposure conditions for the tests are shown in Table 4.9. Note, the chloride diffusion tests on the virgin and the carbonated concrete were performed under similar exposure conditions.

Table 4.9: Exposure conditions for the carbonation and chloride diffusion tests (Yuan et al. 2013)

Property	Carbonation Test	All Chloride Tests	Unit
Temperature	20	35	°C
Humidity	75%	100%	--
CO_2 Concentration	20% (7.9)	--	-- (mol/m^3 of pore solution)
NaCl Concentration	--	5% (856)	-- (mol/m^3 of pore solution)

4.5.3 Model results and comparison with experimental data

First, to gauge the correct implementation of the model and the relative accuracy of its results, the model results are compared with the corresponding experimental quantities. Next, additional results are presented which show the changes in the solid phases contents caused by the synergetic effects of carbonation and chloride diffusion.

Figure 4.3 shows the experimentally measured and presently computed pH variation through the thickness of the carbonated concrete samples after 14 days of exposure to carbonation. It can be observed that the model results are in reasonable agreement with the experimental data.

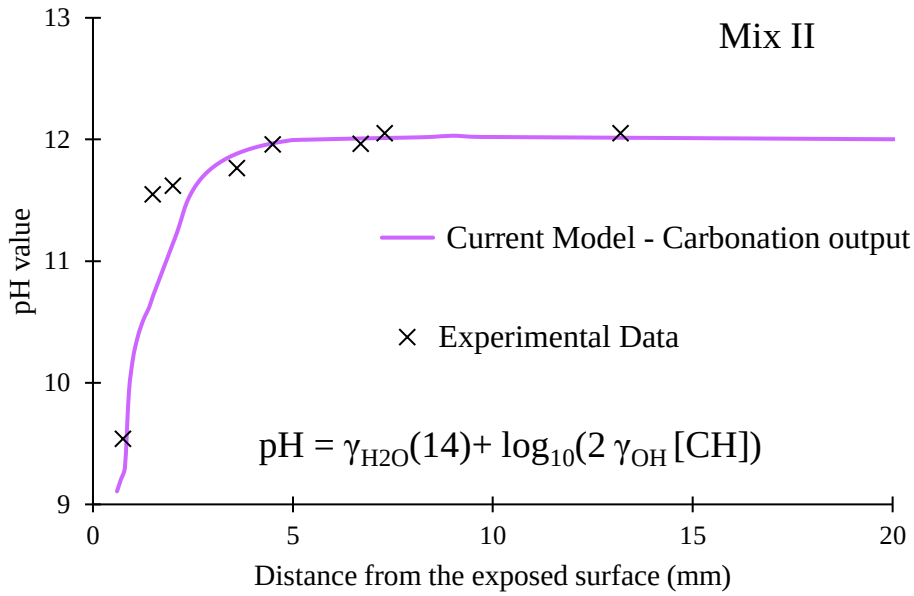

Fig. 4.3: pH variation with distance from the exposed surface for carbonation test of cubes of concrete mix II after 14 days of carbonation

It should be mentioned that the pH was calculated using the following chemical equation (Papadakis et al. 1991)

$$pH = \gamma_{H_2O}(14) + \log_{10}\left(2\gamma_{OH}[CH]\right) \tag{4.60}$$

The portlandite and CO_2 gas concentrations through the samples were obtained using the carbonation model. These concentrations are illustrated in Fig. 4.4, where one can observe that the carbonation front is approximately 12 mm, which is in agreement with the reported value by (Yuan et al. 2013).

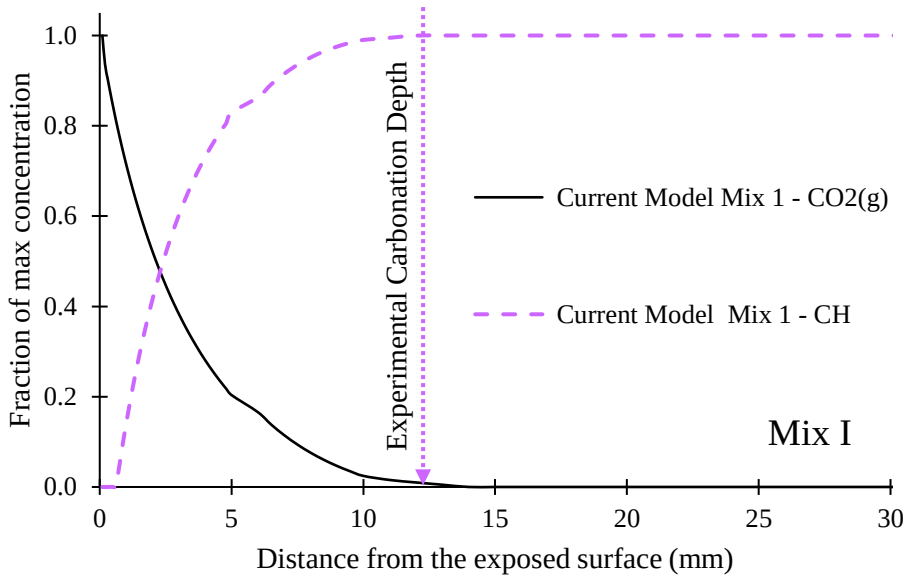

Fig. 4.4: Computed CO_2 and CH profiles for Mix I samples at 14 days of exposure

Figures 4.5 to 4.7 show the computed and measured free chloride concentration profiles of carbonated and non-carbonated samples made of concrete Mix I to III, respectively. The shown concentrations were reached at the end of the two months of salt exposure. These figures, together with Figs. 4.3 and 4.4, demonstrate good agreement between the experimental and computed values for both the non-carbonated (virgin) and carbonated samples, which verifies the basic theory of the proposed model and its numerical implementation.

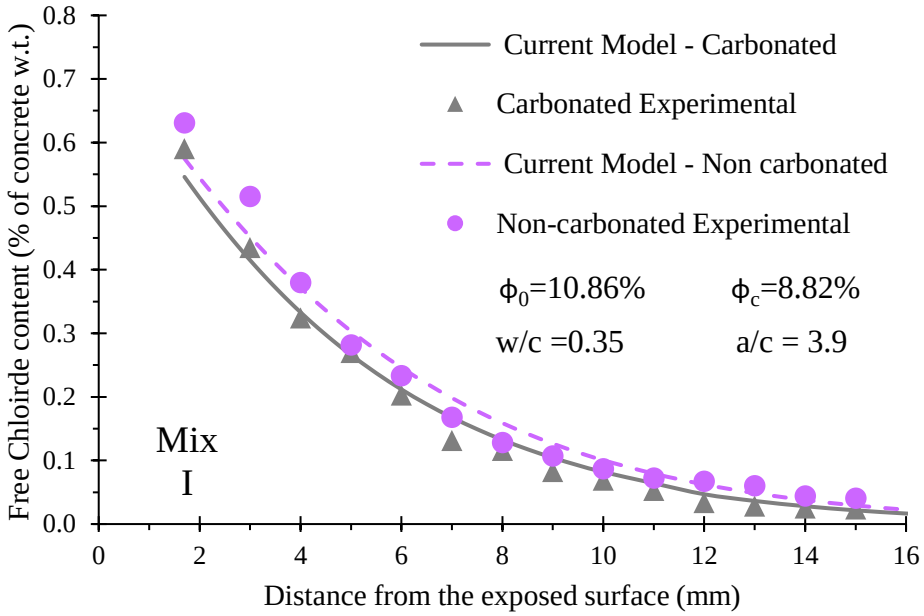

Fig. 4.5: Experimental and computed free chloride content of carbonated and non-carbonated Mix I samples after two months of salt exposure

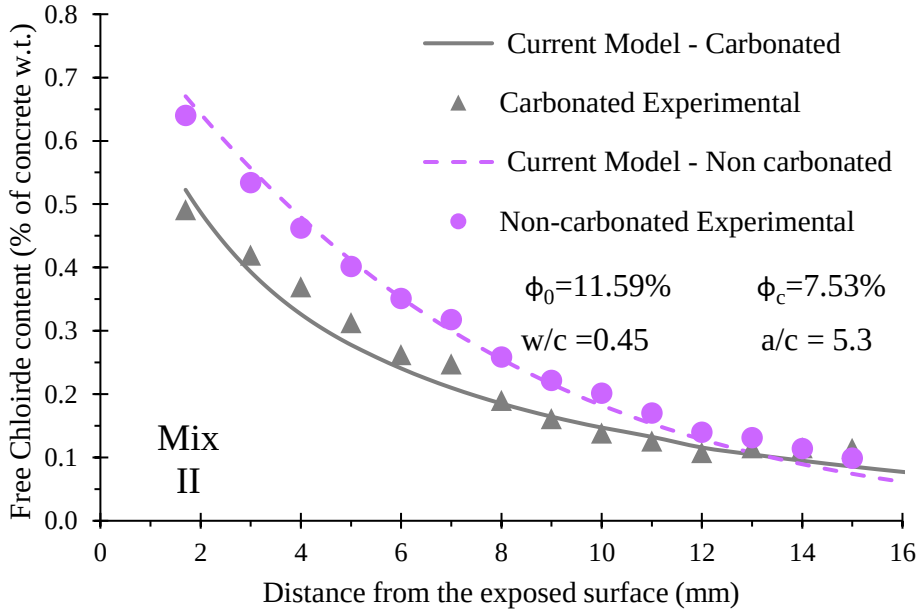

Fig. 4.6: Experimental and computed free chloride content of carbonated and non-carbonated Mix II samples after two months of salt exposure

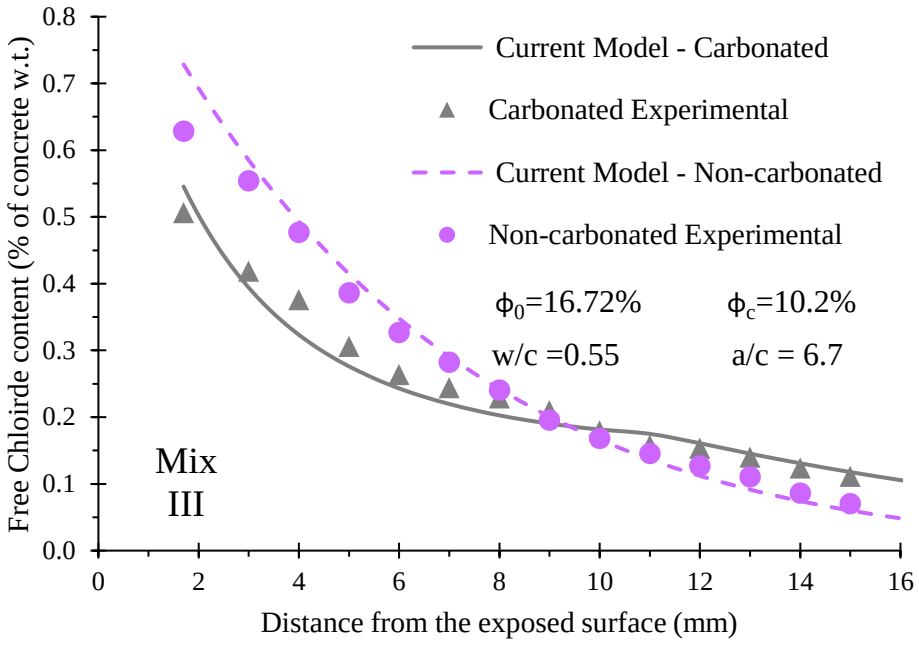

Fig. 4.7: Experimental and computed free chloride content of carbonated and non-carbonated Mix I samples after two months of salt exposure

As stated earlier, the model can capture changes in the hydrated cement solid phases caused by the ingress of chlorides or CO_2. Figures 4.8 to 4.10 illustrate the changes in the Freidel salt (FS) and Monosulfate (AFm) contents of the samples made of Mix I to III, respectively. It can be observed that in all three mixes, carbonation causes reduction in the concrete chloride binding capacity and in the formation of the Monosulfates. As expected, the binding capacity decreases with increased W/C ratio or alternatively with the reduction in the cement content of the mix. The reduction is approximately 25% for samples of Mix I and more than 50% for those of Mix III.

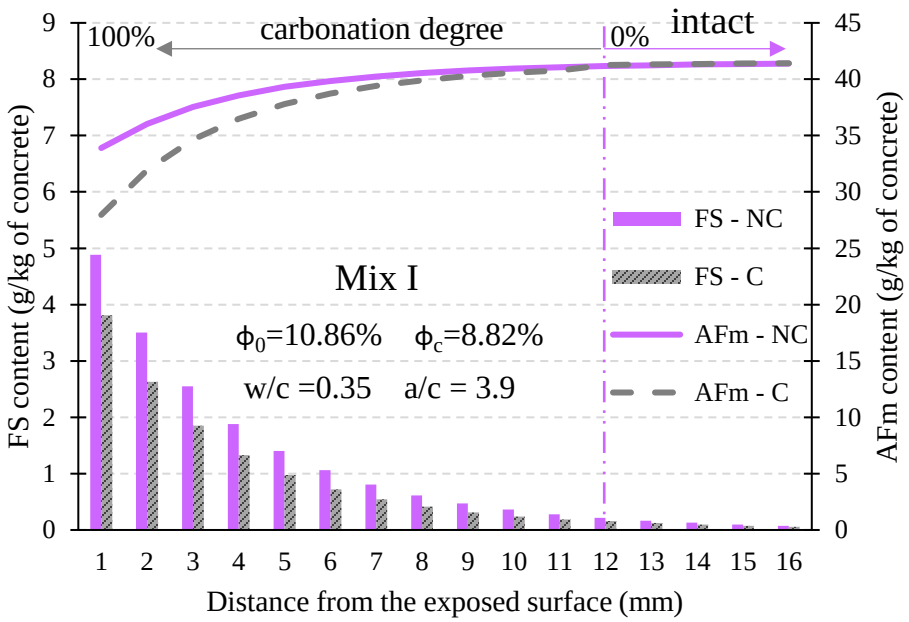

Fig. 4.8: FS and AFm contents of carbonated (C) and non-carbonated (NC) samples of concrete Mix I after two months of exposure to salt

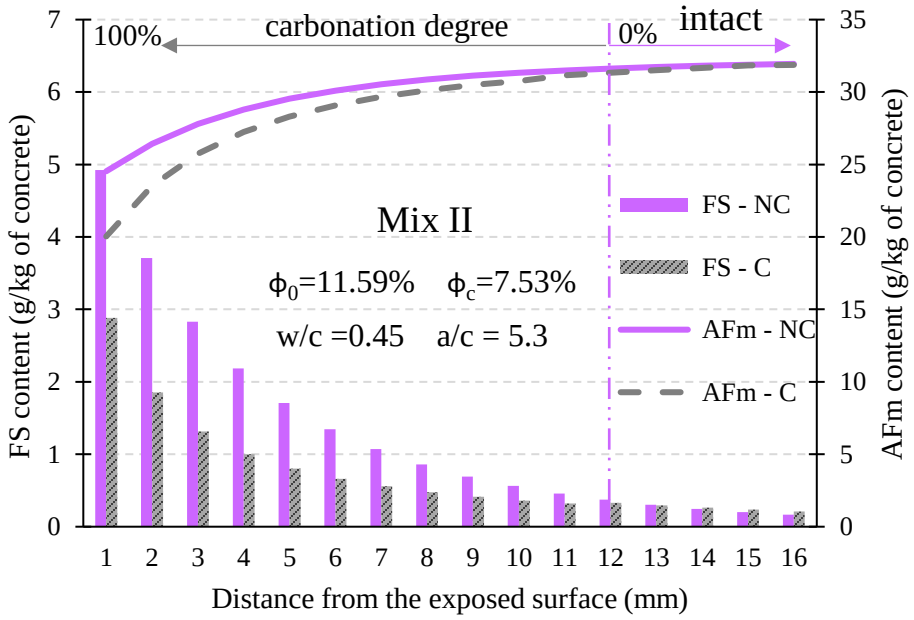

Fig. 4.9: FS and AFm contents of carbonated (C) and non-carbonated (NC) samples of concrete Mix II after two months of exposure to salt

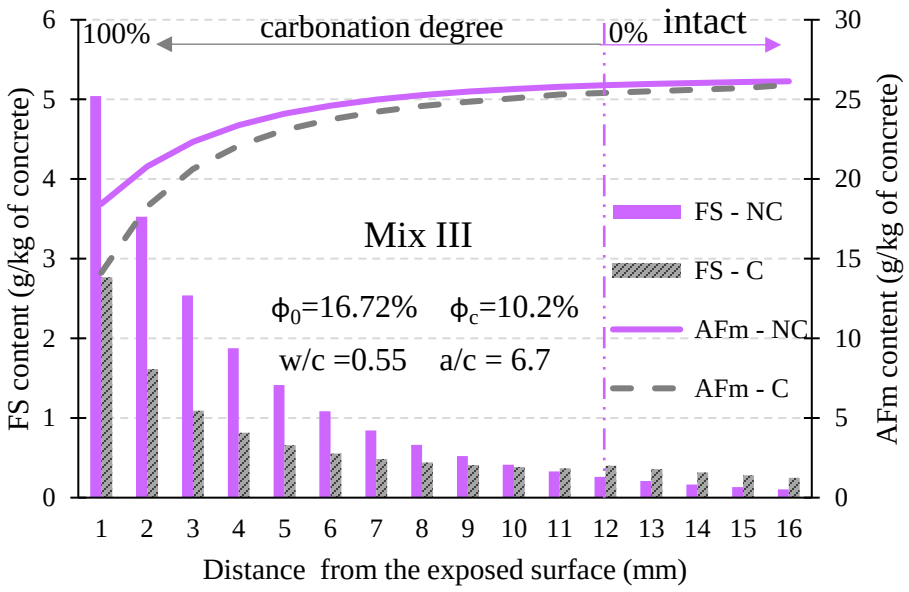

Fig. 4.10: FS and AFm contents of carbonated (C) and non-carbonated (NC) samples of concrete Mix III after two months of exposure to salt

Figure 4.11 shows the change in the Ettringite (Aft) content and the porosity of the carbonated and non-carbonated samples made of Mix I after two months of exposure to salt. The figure shows that chloride ingress by itself causes practically negligible reduction in porosity, but carbonation causes significant reduction. In Fig. 4.11, the reduction caused in the fully carbonated zone is approximately 18%.

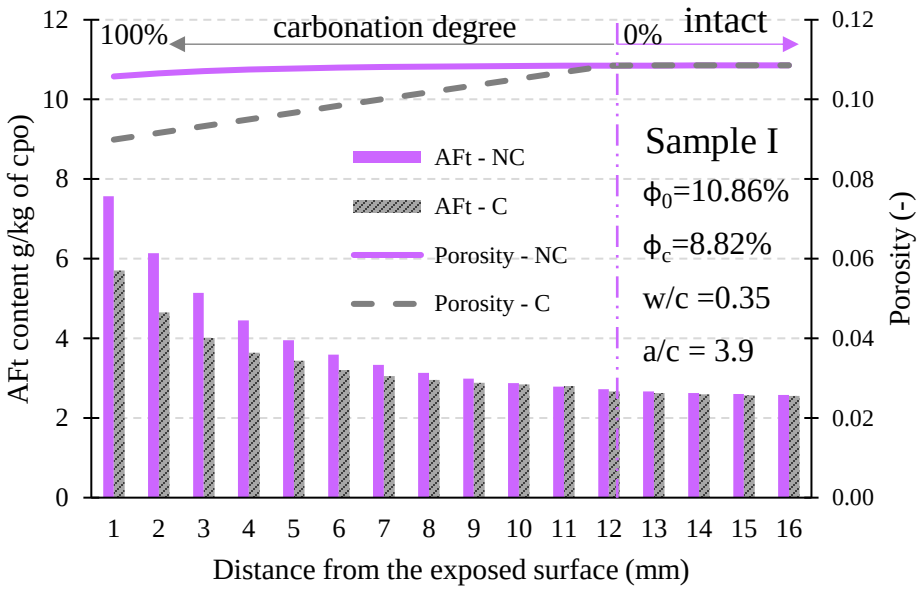

Fig. 4.11: AFt content and porosity profiles of carbonated (C) and non-carbonated (NC) samples made of Mix I after two months of salt exposure

Figure 4.11 also shows that the reduction in the AFm content in the carbonated samples results in the diminuition of its AFt content.

Finally, the pH profiles in Figure 4.12 for the carbonated and the non-carbonated samples exposed to salt spray show that chloride diffusion in the non-carbonated sample causes a small reduction in pH while carbonation results in a significant drop from approximately 12 to 8.5.

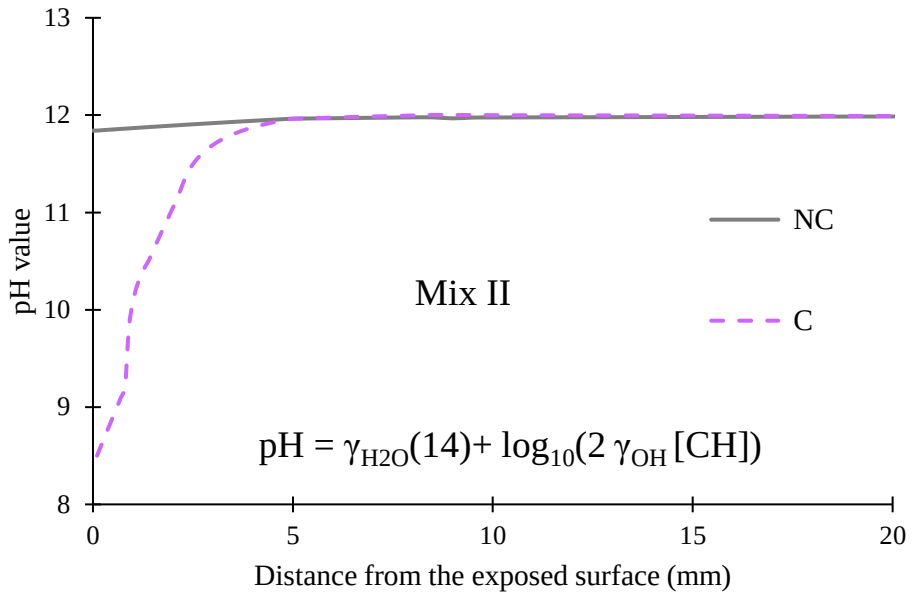

Fig. 4.12: pH variation with distance from the exposed surface in carbonated (C) and non-carbonated (NC) cubes of concrete mix II after two months of chloride exposure

The above results demonstrate that the current model can provide detailed information about the chemical and physical changes occuring in concrete due to chloride diffusion, carbonation or their combined action. Analyses of this kind can provide a more quatitative basis for assessing the effects of chemicals intruding into concretes of known composition and enables one to more rationally estimate the expected or remaining service life of a reinforced concrete structure exposed to variable environmental and exposure conditions.

4.6 CONCLUSIONS

The coupled Nernst-Planck-Poisson (NPP) equations governing the transport of ionic and non-ionic species in portland cement concrete by Fickian diffusion, electromigration and ionic activity were solved using the Galerkin's finite element method. Chemical equilibrium and mass conservation were satisfied via a dedicated chemical module in the model. The synergetic effects of chloride diffusion and carbonation on the changes in the physical and chemical composition of concrete were investigated and compared with available experimental data. Results of the model support the following conclusions:

1. It is possible to accurately model chloride diffusion and carbonation in virgin concrete and to predict the expected changes in the concrete physical and chemical properties caused by these actions.

2. The inclusion of a robust chemical module in the NPP model makes it possible to evaluate the synergetic effects of chloride diffusion and carbonation on the concrete physical and chemical properties and on the associated structure service life.

3. Although the NPP reactive transport model requires more detailed information about the chemical composition and microstructural properties of concrete than a typical Fickean diffusion model, and the accuracy of its results will depend on the availability of such data, it may still be possible to obtain reasonably accurate results via judicious estimation of the missing data.

4. The model provides a more accurate estimate of the chemical chloride binding capacity of concretes with different compositions than the empirical isotherm

approach because it can simulate dissolution/precipitation reactions in the concrete pore solution caused by the changes in the chemical composition of the solution.

5. The model can be theoretically more accurate and predict the reduction in the concrete pH and porosity due to carbonation.

4.7 ACKNOWLEDGMENTS

The first author gratefully acknowledges the financial support of McMaster University and the Natural Sciences and Engineering Research Council Canada (NSERC) in support of this research. The second author wishes to thank NSERC for its financial support of the investigation through its Discovery Grant program, the Tianjin government, the Ministry of Science and Technology of China, and Nankai University for financially supporting the preparation of this manuscript. Finally, we thank the Academic Research Computing Network (SHARCNET) of Ontario, a member of Compute Canada, for providing us free access to its supercomputer facilities.

4.8 REFERENCES

Achour, M., Amiri,O., Bignonnet, F. and Roziere, E.. 2019. “Influence of Carbonation on Ionic Transport in Unsaturated Concrete: Evolution of Porosity and Prediction of Service Life.” *European Journal of Environmental and Civil Engineering* 23 (5): 593–608. https://doi.org/10.1080/19648189.2018.1455609.

Alsheet, F., and Razaqpur, A. G.. 2020a. “Modeling of Concrete Carbonation as a Coupled Nernst-Planck-Poisson Reactive Transport Process.” *Cement and Concrete Research* (under rev.

Alsheet, F., and Razaqpur, A. G.. 2020b. “Quantification of Electromigration and Chemical Activity Effects on the Reactive Transport of Chloride Ions in the Concrete Pore Solution.” *ACI Material Journal* (in press).

Berner, U. R.. 1992. “Evolution of Pore Water Chemistry during Degradation of Cement in a Radioactive Waste Repository Environment.” *Waste Management* 12 (2): 201–19. https://doi.org/https://doi.org/10.1016/0956-053X(92)90049-O.

Bullard, J. W., Hagedorn, J., Ley, M. T., Hu, H., Griffin, W., and Terrill, J. E.. 2018. “A Critical Comparison of 3D Experiments and Simulations of Tricalcium Silicate Hydration.” *Journal of the American Ceramic Society* 101 (4): 1453–70. https://doi.org/10.1111/jace.15323.

Christopher, H. A., and Shipman, C. W.. 1968. “Poisson’s Equation as a Condition of Equilibrium in Electrochemical Systems.” *Journal of The Electrochemical Society* 115 (5): 501. https://doi.org/10.1149/1.2411292.

Collepardi, M., Marcialis, A., and Turriziani, R.. 1972. “Penetration of Chloride Ions into Cement Pastes and Concretes.” *Journal of the American Ceramic Society* 55 (10): 534–35. https://doi.org/10.1111/j.1151-2916.1972.tb13424.x.

GB National Standard. 2010. “GB/T 50082-2009 Standard for Test Methods of Long-

Term Performance and Durability of Ordinary Concrete." GB Chinese National Standards.

Geng, J., Easterbrook, D., Liu, Q-F., and Li, L-Y.. 2016. "Effect of Carbonation on Release of Bound Chlorides in Chloride-Contaminated Concrete." *Magazine of Concrete Research* 68 (7): 353–63. https://doi.org/10.1680/jmacr.15.00234.

Goñi, S., and Guerrero, A.. 2003. "Accelerated Carbonation of Friedel's Salt in Calcium Aluminate Cement Paste." *Cement and Concrete Research* 33 (1): 21–26. https://doi.org/https://doi.org/10.1016/S0008-8846(02)00910-9.

Gustafsson, J.P. 2014. "Visual MINTEQ 3.1." Sweden, Stockholm: KTH Royal Institute of Technology, Department of Land and Water Resource Engineering. http://vminteq.lwr.kth.se/.

Heath, M. T. 2018. *Scientific Computing: An Introductory Survey*. *SIAM*. Philadelphia: McGraw-Hill.

Hirao, H., Yamada, K., Takahashi, H. and Zibara, H.. 2005. "Chloride Binding of Cement Estimated by Binding Isotherms of Hydrates." *Journal of Advanced Concrete Technology* 3 (1): 77–84. https://doi.org/10.3151/jact.3.77.

Isgor, B. O., and Razaqpur, A. G.. 2004. "Finite Element Modeling of Coupled Heat Transfer, Moisture Transport and Carbonation Processes in Concrete Structures." *Cement and Concrete Composites* 26 (1): 57–73. https://doi.org/10.1016/S0958-9465(02)00125-7.

Jeong, J., Ramezani, H., and Chuta, E.. 2019. “Reactive Transport Numerical Modeling of Mortar Carbonation: Atmospheric and Accelerated Carbonation.” *Journal of Building Engineering* 23: 351–68. https://doi.org/10.1016/j.jobe.2019.01.038.

Johannesson, B., Yamada, K., Nilsson, L. O. and Hosokawa, Y.. 2007. “Multi-Species Ionic Diffusion in Concrete with Account to Interaction between Ions in the Pore Solution and the Cement Hydrates.” *Materials and Structures/Materiaux et Constructions* 40 (7): 651–65. https://doi.org/10.1617/s11527-006-9176-y.

Jones, M. R., Macphee, D. E., Chudek, J. A., Hunter, G., Lannegrand, R., Talero, R. and Scrimgeour, S. N.. 2003. “Studies Using 27Al MAS NMR of AFm and AFt Phases and the Formation of Friedel’s Salt.” *Cement and Concrete Research* 33 (2): 177–82. https://doi.org/https://doi.org/10.1016/S0008-8846(02)00901-8.

Kosmatka, S., Kerkhoff, B. and Panarese, W.. 2002. *Design and Control of Concrete Mixtures*. Fourteenth Edition. Skokie, Illinois, United States of America: Portland Cement Association.

Mai-Nhu, J., and Sellier, A.. 2013. “Corrosion Des Armatures Du Béton : Couplage Carbonatation-Chlorures En Présence de Cycles Hydriques.” http://www.theses.fr/2013TOU30124/document.

Martín-Pérez, B., Pantazopoulou, S. J., and Thomas, M. D.A.. 2001. “Numerical Solution of Mass Transport Equations in Concrete Structures.” *Computers and Structures* 79 (13): 1251–64. https://doi.org/10.1016/S0045-7949(01)00018-9.

Matsushita, F., Aono, Y., and Shibata, S.. 2000. "Carbonation Degree of Autoclaved Aerated Concrete." *Cement and Concrete Research* 30 (11): 1741–45. https://doi.org/https://doi.org/10.1016/S0008-8846(00)00424-5.

Moore, W. J. 1998. *Physical Chemistry*. Fifth edit. Beccles and London, Great Britain: Longman.

Papadakis, V. G., Vayenas, C. G., and Fardis, M. N.. 1991. "Fundamental Modeling and Experimental Investigation of Concrete Carbonation." *ACI Materials Journal* 88 (4): 363–73.

Papadakis, V. G., Vayenas, C. G., and Fardis, M. N.. 1991. "Physical and Chemical Characteristics Affecting the Durability of Concrete." *ACI Materials Journal* 88 (2): 186–96. https://doi.org/10.14359/1993.

Papadakis, V. G. 2000. "Effect of Supplementary Cementing Materials on Concrete Resistance against Carbonation and Chloride Ingress." *Cement and Concrete Research* 30 (2): 291–99. https://doi.org/https://doi.org/10.1016/S0008-8846(99)00249-5.

Peter, A M., Muntean, A., Meier, A. S., and Bohm, M.. 2005. "Modelling and Simulation of Concrete Carbonation: Competition of Several Carbonation Reactions." Bremen: Universität Bremen.

Pitzer, K. S. 1991. *Activity Coefficients in Electrolyte Solutions*. Boca Raton, FL: CRC Press.

Planel, D.. 2002. “Les Effets Couplés de La Précipitation d’espèces Secondaires Sur Le Comportement Mécanique et La Dégradation Chimique Des Bétons.” Université de Marne-la-Vallée . https://inis.iaea.org/collection/NCLCollectionStore/_Public/35/055/35055646.pdf.

Revert, A. B., Weerdt, K. D., Jakobsen, U. H. and Geiker, M. R.. 2019. “Impact of Accelerated Carbonation on Microstructure and Phase Assemblage.” *Nordic Concrete Research* 59 (1). https://doi.org/10.2478/ncr-2018-0018.

Rumble, J. R., Lide, D. R. and Bruno, T. J.. 2019. *CRC Handbook of Chemistry and Physics : A Ready-Reference Book of Chemical and Physical Data*. 100th edition. Boca Raton, FL: CRC Press.

Saetta, A. V., Schrefler, B. A. and Vitaliani, R. V.. 1993. “The Carbonation of Concrete and the Mechanism of Moisture, Heat and Carbon Dioxide Flow through Porous Materials.” *Cement and Concrete Research* 23 (4). https://doi.org/10.1016/0008-8846(93)90030-D.

Samson, E., Lemaire, G., Marchand, J., and Beaudoin, J. J.. 1999. “Modeling Chemical Activity Effects in Strong Ionic Solutions.” *Computational Materials Science* 15 (3): 285–94. https://doi.org/10.1016/s0927-0256(99)00017-8.

Samson, E., and Marchand, J.. 2007a. “Modeling the Effect of Temperature on Ionic Transport in Cementitious Materials.” *Cement and Concrete Research* 37 (3): 455–68. https://doi.org/https://doi.org/10.1016/j.cemconres.2006.11.008.

Samson, E., and Marchand, J.. 2007b. “Modeling the Transport of Ions in Unsaturated Cement-Based Materials.” *Computers & Structures* 85 (23): 1740–56. https://doi.org/https://doi.org/10.1016/j.compstruc.2007.04.008.

Samson, E., Marchand, J., Snyder, K. A., and Beaudoin, J. J.. 2005. “Modeling Ion and Fluid Transport in Unsaturated Cement Systems in Isothermal Conditions.” *Cement and Concrete Research* 35 (1): 141–53. https://doi.org/https://doi.org/10.1016/j.cemconres.2004.07.016.

Samson, E., and Marchand, J.. 2006. “Multiionic Approaches to Model Chloride Binding in Cementitious Metrials.” In *2nd International RILEM Symposium on Advances in Concrete through Science and Engineering*, edited by M. Jolin and F. Paradis J. Marchand, B. Bissonnette, R. Gagné, 101–122. Quebec City, Canada: RILEM Publication SARL. https://doi.org/10.1617/2351580028.008.

Suryavanshi, A. K., and Swamy, R. N.. 1996. “Stability of Friedel’s Salt in Carbonated Concrete Structural Elements.” *Cement and Concrete Research* 26 (5): 729–41. https://doi.org/https://doi.org/10.1016/S0008-8846(96)85010-1.

Taigbenu, A. E. 1999. “Unsaturated Flow (Richards Equation).” In *The Green Element Method*, edited by Akpofure E Taigbenu, 217–30. Boston, MA: Springer US. https://doi.org/10.1007/978-1-4757-6738-4_8.

Thiery, M.. 2005. “Modélisation de La Carbonatation Atmosphérique Des Matériaux Cimentaires : Prise En Compte Des Effets Cinétiques et Des Modifications Microstructurales et Hydriques.” Ecole Nationale Des Ponts et Chaussees.

Wang, X., and Baroghel-Bouny, V.. 2012. “Modélisation du Transport Multi-Espèces Dans Les Matériaux Cimentaires Saturés ou Non Saturés et Éventuellement Carbonatés.” http://www.theses.fr/2012PEST1037/document.

Xu, Tianfu, Samper, J., Ayora, C., Manzano, M. and Custodio, E.. 1999. “Modeling of Non-Isothermal Multi-Component Reactive Transport in Field Scale Porous Media Flow Systems.” *Journal of Hydrology* 214 (1–4): 144–64. https://doi.org/10.1016/S0022-1694(98)00283-2.

Yuan, C-F., Niu, D. and Qi, G-Z.. 2013. “Diffusion of Chloride Ions into Concrete under Joint Action of Carbonation and Salt Spray.” *Journal of JIangsu University(Natural Science Eidt)* 34 (5): 605–9. http://zzs.ujs.edu.cn/xbzkb/EN/Y2013/V34/I5/605.

Zhu, X., Zi, G., Cao, Z. and Cheng, X.. 2016. “Combined Effect of Carbonation and Chloride Ingress in Concrete.” *Construction and Building Materials* 110: 369–80. https://doi.org/https://doi.org/10.1016/j.conbuildmat.2016.02.034.

Zibara, H.. 2001. “Binding of External Chlorides by Cement Pastes.” University of Toronto. http://hdl.handle.net/1807/15366.

Zienkiewicz, O., Taylor, R. L. and Zhu, J. Z.. 2013. *The Finite Element Method: Its Basis and Fundamentals*. Seventh Ed. New York: Elsevier Butterworth-Heinemann.

CHAPTER 5
SUMMARY, CONCLUSIONS AND RECOMMENDATIONS

5.1 SUMMARY

This dissertation focuses on the modeling of concrete carbonation and the ingress of chlorides into non-carbonated and carbonated concrete. The objective is to determine the effect of the ingress of these deleterious agents on the concrete physical and chemical properties, with particular focus on its free chloride concentration and pH variation, which can be used to predict the corrosion initiation time in reinforced concrete structures. The Nernst-Planck-Poisson (NPP) transport model is coupled with the relevant chemical equilibrium equations of the various species in the concrete pore solution and the solid phases in the hydrated cement. For determining the transport of CO_2, which occurs in partially saturated concrete, Richard's equation is applied to find the moisture distribution in the concrete. The transient one-dimensional governing transport equations are solved numerically, using the Galerkin's finite element method in space and the Euler implicit scheme in the time domain. Results of the model are compared with available data that were obtained from the exposure of concrete test specimens to chlorides, CO_2 or to combined CO_2 and chlorides under prescribed exposure conditions. In all cases good agreement is observed between the model results and the corresponding experimental data.

In addition, the model is used to investigate the effect of the chemical composition of the deicing salts on the transport of the chloride ions and their chemical interaction with the

species in the concrete pore solution, and with the solid phases in the hydrated cement. In all cases, at each stage of the analysis, the hydrated cement solid phases contents, the pore solution chemical composition and pH, the amount of bound and free chlorides and the concrete porosity can be ascertained.

5.2 CONCLUSIONS

1. The Nernst-Planck-Poisson (NPP) reactive transport model can reasonably accurately capture the physical and chemical change caused by the ingress of chlorides and CO_2 in concrete.

2. The finite element method can be used to cast the transient one-dimensional governing differential of the NPP model into numerical form and solve the problem of chlorides and CO_2 transport in concrete under prescribed boundary and initial conditions.

3. The NPP model includes transport by Fickian diffusion, electromigration and ionic activity. Results of this study indicates that in the case of chlorides transport in fully saturated concrete, Fickian diffusion is the dominant transport mode, followed by electromigration while transport by ionic activity is negligible due to the dilute nature of the solution. Consequently, the latter can be neglected, without significant loss in the accuracy of the results. In the case of concrete under wet/dry cycles, advection can be important at depth close to the exposed surface.

4. The NPP transport model, coupled with the chemical equilibrium equations of the species in the concrete pore solution, the solid phases in the hydrated cement and the external chemical agents entering concrete, can provide detailed and reasonably accurate information about the pore solution chemical composition and pH, the concrete porosity and the hydrated cement solid phases contents.

5. The accuracy of the results of the current analyses not only depends on the accuracy of the finite element discretization and modelling, but more importantly, they depend on the precision of the chemical equilibrium equations utilized to capture the various chemical interactions in the concrete pore solution and structure. Notwithstanding the fact that similar to any other model, the accuracy of its results is dependent on the accuracy of its input data, in general its results are expected to be more accurate than those of the simple Fickian model because it accounts for the other relevant modes of chloride transport in concrete besides molecular diffusion.

6. The split operator technique that is employed in the current study to separate the transport part of the NPP model from its chemical equilibrium component makes the solution of the governing transport equations efficient and provides sufficiently accurate results for engineering practice.

7. Chloride binding by concrete can be reasonably accurately captured via the dissolution/precipitation ion exchange reactions involving the chloride ions and the AFm phase in the hydrate cement. This obviates the need for using empirical chloride binding isotherms.

8. The synergetic effect of chlorides and carbonation on drop in concrete pH is greater than the individual action of each species.

9. Concrete carbonation reduces its porosity, diffusion coefficient and chloride binding capacity, the consequence of which could be reduction or increase in the free chloride content of the carbonated versus the uncarbonated concrete.

10. The results of the current analyses showed that the use of the average annual temperature for calculating chloride diffusion in concrete structures may provide sufficiently accurate results for practical applications.

5.3 RECOMMENDATIONS FOR FUTURE RESEARCH

The research in this dissertation focused on the development of a robust reactive transport model for chlorides and carbon dioxide ingress in concrete and their reactions with the chemicals in the concrete pore solution and structure. The main motivation of the work was to develop a tool that can be used to accurately estimate the time to corrosion initiation steel reinforcement corrosion in concrete structures. The developed model provides a sound framework for further improvements and future changes to expand its applications and improve its accuracy. Some suggestions for future research in this regard are made below:

1. In the case of high-deicing salt concentrations, different solid phases than those in the case of low concentration are formed in the concrete. The chemical equilibrium constants

for these phases have not been quantified yet. Hence, experimental programs can be conducted to precisely identify these phases and establish their chemical equilibria.

2. Although the chemical module explained in this dissertation includes the main chemical reactions taking place in the pore solution and shows good agreement with the corresponding experimental data, for the ingress of other deleterious agents in concrete, such as sulfates, the current chemical module can be expanded to capture their effects on the physical and chemical properties of concrete.

3. As stated in Chapter 4 of this dissertation, there is paucity of detailed experimental data pertaining to chloride diffusion in carbonated concrete. This makes the validity of the NPP reactive transport model results less certain. So, there is need for experimental work which provides precise and comprehensive information about the cement composition, mix properties, temperature, humidity, porosity, tortuosity, pore solution composition, solid phases composition and content before the ingress of chlorides and CO_2 and the changes in the values of these parameters after exposure to the ingressing agents. Such data can greatly assist in validating the accuracy and robustness of the model.

4. In the present work, chloride binding in concrete was assumed to be due to chemical binding only while physical binding was neglected. Although consequence of this assumption was reasonable in the current work, nevertheless, a more detailed and sufficiently robust model for physical binding of the presented models show agreement to experimental data, quantifying the physical binding is necessary for inclusion in the model.

5. Although generally a one-dimensional transport model for chlorides and CO_2 is deemed to be adequate for engineering practice, there are situations where a one-dimensional model would not give sufficiently accurate results. Hence, the current NPP model can be extended to two and possibly three dimensions.

6. Cracks in concrete structures are a known reality, hence the model can be improved by considering the effect of cracks on the transport of chlorides and CO_2 ingress in concrete structures.

APPENDIX - A

EFFECT OF TIME-DEPENDENT CHLORIDE PROFILE AND TEMPERATURE VARIATION ON CHLORIDE DIFFUSION IN CONCRETE

ABSTRACT

Reinforcement corrosion due to chloride diffusion is one of the main problems in reinforced concrete structures exposed to certain environments. The diffusion rate is function of chloride surface concentration, concrete temperature, humidity, composition and microstructure. The intruded chlorides are partially chemically bound by the concrete and it is the unbound or free chloride which upon exceeding a defined threshold initiates corrosion. There is no general agreement about the magnitude of this threshold, but further discussion of it is beyond the scope of the current work. The time to corrosion initiation depends on the above variables; therefore, it is important to model their spatial and temporal variations in a manner that will yield a realistic estimate of the actual initiation period. In this study, the chloride surface concentration and temperature temporal variations are approximated in several ways to gauge the sensitivity of the chloride diffusion kinetics to them. Temperature profiles with constant 6-hours, daily, monthly, seasonally and yearly variations are used to approximate the actual temperature variation recorded for Toronto, Canada in a typical year. The surface chloride concentration is assumed either constant or allowed to vary monthly according to the reported values for Toronto. It is discovered that due to the limited temperature range encountered even in cold regions like Toronto, the

diffusion kinetics is not very sensitive to the temperature approximation method, but it is more sensitive to the way the surface chloride variation is approximated. For structures subjected to deicing salt applications, assuming constant seasonal temperature and monthly chloride variation in the analysis may yield a realistic estimate of the time to corrosion initiation and thus the prediction of the life-time of the structure.

INTRODUCTION

Reinforced concrete (RC) is the most popular construction material, but the deterioration of RC structures exposed to chlorides, which induce reinforcement corrosion and subsequent damage to concrete, is a serious and costly problem.

Chlorides enter concrete structures mainly through permeation of de-icing salts in cold regions or the ingress of sea salt along coastal area. The corrosion of the steel bars, termed steel reinforcement, begins when the chloride concentration at the level of reinforcement reaches a critical threshold. The kinetics of the chemical reactions, the rate of permeation of chlorides and the evolution of damage to the concrete microstructure are dependent on the prevailing hygrothermal conditions, which are in turn affected by the ambient conditions.

Any realistic modelling of chloride diffusion must account for the effects of some key parameters influencing the kinetics and deleterious effects of chloride diffusion in concrete. Generally, it is believed that the free chlorides diffusing through the concrete pore solution cause corrosion (Hirao, et al., 2005). However, other studies indicate that bound chlorides

can also contribute to the corrosion process by being released or as bound compounds through electric influences (Glass & Buenfeld, 2000).

Hence, it is important to model this phenomenon. Different mathematical models are proposed to describe the relationship between bound and free chlorides. Freundlich and Langmuir non-linear binding isotherms are the most popular as expressed by equation A.1 and A.2, respectively (Glass, et al., 1997).

$$C_b = \alpha C_f^{\beta} \tag{A.1}$$

$$C_b = \frac{\alpha C_f}{1 + \beta C_f} \tag{A.2}$$

where, α and β are coefficients determined experimentally, C_b and C_f are the bound and free chloride concentration, respectively.

Tests have shown the dependency of binding capacity on temperature and chlorides concentration (Zibara, 2001). This is often modeled using Arrhenius law (Saetta et al., 1993)

$$D_2 = D_1 \, e^{\left(\frac{U}{R}\left(\frac{1}{T_0} - \frac{1}{T}\right)\right)} \tag{A.3}$$

where, D_1 and D_2 are the diffusion coefficients at reference temperature T_o and specified temperature T, respectively, U is the activation energy for chloride diffusion. R = 8.31 J/mol.K is the universal gas constant and e is the base of natural logarithm. The energy U is function of the water/cement (w/c) ratio (Saetta et al., 1993) as well as temperature, but

it varies between 29.6 to 45.8 kJ/mol. For a constant w/c, as indicated below, it can be expressed as function of temperature.

$$\frac{U}{R} = 4600 * \left[\frac{30}{(T - 263)} \right]^{0.39} \tag{A.4}$$

where T is the concrete temperature (^{o}K).

Chloride diffusion can only occur in the presence of water in the capillary pores. The dependency of the diffusion coefficient on pore relative humidity can be written as (Saetta et al., 1993)

$$D_2 = D_1 \left(1 + \frac{(1-h)^4}{(1-h_c)^4} \right)^{-1} \tag{A.5}$$

where, D_1 and D_2 are the diffusion coefficients at saturated condition and humidity level h, respectively. h is the pore relative humidity in concrete, and h_c is the humidity where the value of diffusion coefficient drops halfway between its maximum and minimum values. The value of h_c can be determined experimentally.

Maturity of concrete leads to change in the microstructure of concrete and it reduces the rate. This phenomenon can be modelled (Maage et al., 1996) using

$$D_2 = D_1 \left(\frac{t_{ref}}{t} \right)^m \tag{A.6}$$

where, D_1 and D_2 are the diffusion coefficients at reference time t_{ref} and considered time t, respectively. The t_{ref} refers to the time when the diffusion coefficient is measured, and m is

the age reduction factor. Quantity *m* can be calculated as shown below (Mangat & Molloy, 1994)

$$m = 2.5(w/c) - 0.6 \qquad \text{(A.7)}$$

In this study, the chloride surface concentration and temperature temporal variations are approximated in several ways to gauge the sensitivity of the chloride diffusion kinetics to them. Temperature profiles with constant 6-hours, daily, monthly, seasonally and yearly variations are used to approximate the actual temperature variation recorded for Toronto, Canada in a typical year. The surface chloride concentration is assumed either constant or allowed to vary monthly according to the reported values for Toronto. The dependency of the diffusion coefficient on temperature, w/c ratio and relative humidity will be modeled using equations A.3 to A.6. The main focus will be on the manner in which the concrete temperature and chloride temporal variation are approximated and the effect of the approximation on the chloride concentration profile through the concrete member thickness. The parametric analysis will first consider the effect of each parameter separately and then investigate their combined effect.

ANALYSIS METHOD

The equation governing both one dimensional chloride diffusion and heat conduction is (Zienkiewicz, 1977)

$$a\frac{\partial \phi}{\partial t} = \frac{\partial}{\partial x}\left(D\frac{\partial \phi}{\partial x}\right) \qquad \text{(A.8)}$$

where, for heat conduction, $a = \rho c$, ρ, c and $D = K_{xx}$ are the concrete density, specific heat capacity, and thermal conductivity, respectively. For chloride diffusion, $a = 1$ and $D = D_a$ is the apparent diffusion coefficient. The coefficient D_a can be written as (Martin-Perez et al., 2000).

$$D_a = \left(\frac{D_e}{1 + \frac{1}{w_e}\left(\frac{\partial C_b}{\partial C_f} \right)} \right) \tag{A.9}$$

where, w_e is the evaporable water content, D_e is the effective diffusion coefficient ignoring binding.

By introducing the effects of temperature, pore relative humidity, and maturity age on diffusion, equation A.9 can be modified as.

$$D_a^* = D_a \, \mathrm{e}^{\left(\frac{U}{R}\left(\frac{1}{T_0} - \frac{1}{T} \right) \right)} \left(1 + \frac{(1-h)^4}{(1-h_c)^4} \right)^{-1} \left(\frac{t_{ref}}{t} \right)^m \tag{A.10}$$

In this study, equation A.8 is solved by developing and validating a one-dimensional finite element program (Zienkiewicz, 1977).

One-way coupling is assumed between heat transfer and chloride diffusion process. In other words, temperature affects the diffusion rate but not vice versa. Hence, an incremental time-dependent analysis is performed where thermal analysis is conducted first and the temperature value at the end of the previous time step is used to compute the temperature

dependant value of moisture, chloride binding, and diffusion coefficient at the beginning of the new time step.

When binding is included, the problem becomes non-linear in which strictly speaking an iterative method needs to be applied to find the precise solution. However, diffusion in concrete is slow by nature, thus for small time increments the free chloride concentrations at the end of the previous time step can be used in conjunction with the selected isotherm to estimate $\frac{\partial C_b}{\partial C_f}$.

MODELED DIFFUSION SCENARIO

A finite element program is developed by the authors, using the MATLAB platform, to solve equation A.8, which governs time-dependent heat and mass transfer. The program is validated by comparing its results with available numerical and experimental data in the literature.

The modelled specimen is assumed to be part of a 200-mm thick concrete bridge deck slab having a one square meter surface area normal to the diffusion direction. In Canada, currently the minimum concrete cover for bridge deck slab is specified as 70 ± 20 mm ("CSA S6-14," 2014). However, for bridges built between 1970~1990, the minimum cover was specified as 50 mm. Thus, here the depths of interest for chloride concentration are 50 and 70 mm from the slab surface.

The typical annual temperature variation for Toronto, Canada is shown in Fig. A.1 (*Environment Canada*, 2017).

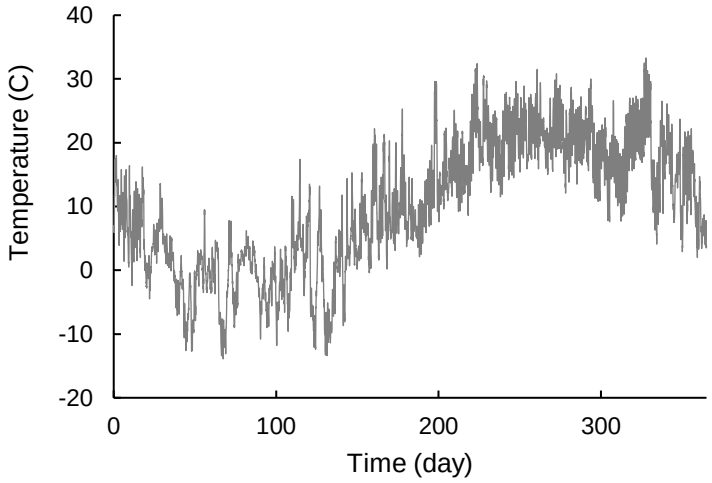

Fig. A.1. Hourly annual temperature for Toronto, Ontario, Canada

The typical monthly applied salt surface concentration, as reported by the City of Toronto, (*Salt Management Plan*, 2004) is illustrated in Fig. A.2. The figure also shows the equivalent computed average annual salt surface concentration that is used in the current analysis. For the purpose of this investigation, the authors have estimated the surface salt concentration from the actual amounts of rock salt usage. Note, however, the purpose of the current study is to investigate the effect of the numerical idealization of the actual salt and temperature temporal profiles on chloride diffusion in the concrete rather than the exact amount of salt used. If the diffusion coefficient is assumed to be independent of salt concentration, then the conclusions of the study will not be limited by the actual magnitude of the surface salt concentration.

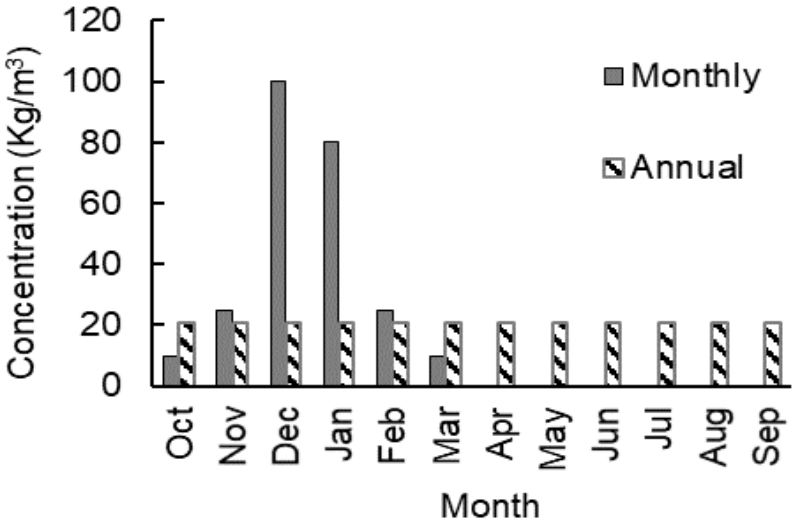

Fig. A.2. Annual salt concentration for Toronto, Ontario, Canada

The average annual relative humidity for the city of Toronto is reported as 75% (*Environment Canada*, 2017). BSB (Brunauer et al. 1969) adsorption isotherm is used to relate the pore relative humidity to the evaporable water content as follows

$$w_e = \frac{Ck_m V_m h}{(1-k_m h)\left[1+(C-1)k_m h\right]} \tag{A.11}$$

where, w_e is the evaporable water content expressed in terms of water per grams of cementitious material, V_m is the monolayer capacity, C and k_m are two parameters of the model. More information regarding the experimental parameters are provided by Xi et al. (1994).

The pore relative humidity h is assumed equal to the air relative humidity for the months where salt is not applied while during the salt application months, the pore relative humidity is assumed to be 100% due to the occurrence of rain and snow in these months.

For chloride binding, the Freundlich isotherm is used. A regression analysis by Dousti and Shekarchi (2015), considering different temperatures, concentrations, and cementitious materials, resulted in the following values of α and β for use in the Freundlich isotherm

$$\alpha = a_1 T^2 + b_1 T + c_1 \tag{A.12}$$

$$\beta = a_2 T^2 + b_2 T + c_2 \tag{A.13}$$

where, T is the temperature (°C), a_1, a_2, b_1, b_2, c_1, and c_2 are coefficients determined based on the concrete binder composition. For modeling binding, these equations were applied in the current study.

FINITE ELEMENT IDEALIZATION

The through thickness finite element discretization consists of linear one-dimensional elements. The mesh consists of uniform 7.5 mm long elements and the time step is taken as 6 hours throughout the analysis period. This discretization is applied to both the heat transfer and the diffusion analysis.

An additional node was added on the surface and was used to apply the chloride surface concentration. The concrete first node starts at 1 mm from the surface. This is needed when the varied surface concentration is applied because dropping the chloride concentration at the concrete first node will lead to diffusion from inside towards the free surface which does not occur in real-life.

The concrete used in the analysis is assumed to be made with Ordinary Portland Cement (OPC) and its properties are summarised in Table A.1.

Table A.1: Concrete properties adopted for OPC

Property	Value	Unit
Heat capacity	1.932×10^6	$J/m^3.°C$
Convective heat coefficient	0.07	$W/m^2.°C$
Thermal conductivity	1.4	W/m.°C
w/c (1)	0.3	--
Binder content	450	kg/m^3
First exposure time	120	Days
Effective Diffusion coefficient at 120 days	1×10^{-12}	m^2/s
Initial chloride concentration	0	kg/m^3 solution
α (2)	5.4 ~ 6.4*	--
β (3)	0.36 ~ 0.45*	--
w_e (4)	0.05 ~ 0.10*	m^3/ m^3 of concrete
h_c (5)	0.75	--

* values are function of temperature
(1) water to cement ratio
(2) binding parameter, calculated using equation 12
(3) binding parameter, calculated using equation 13
(4) evaporable water content, calculated using equation 11
(5) humidity level at which the value of diffusion coefficient drops halfway between its maximum and minimum values. Adopted from (Martin-Pérez, 1999)

All the properties in Table A.1, except the binding model, were adopted from (Martin-Pérez, 1999) The binding model used in the current investigation is given by equation A.12 and A.13 and is based on the work of (Dousti and Shekarchi, 2015).

With reference to Fig. A.3. in the analysis, the actual temperature variation is approximated by assuming constant average temperature over different lengths of time, viz. 6 hrs (quarter-diurnal), 12 hrs (semi-diurnal), 24 hrs (diurnal), monthly, seasonally, semi-annually, and annually. The air temperature is applied as convection boundary condition.

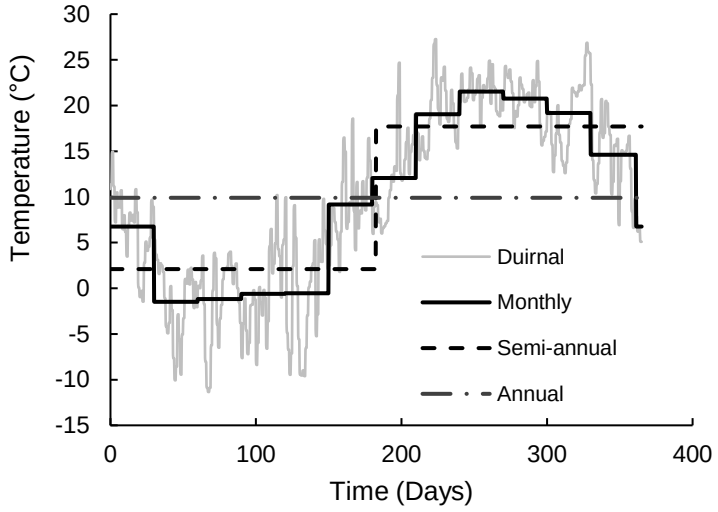

Fig. A.3. Temperature of concrete at 100 mm depth from the surface averaged over different durations

The salt surface concentration is assumed to either vary monthly, per the data provided by the City of Toronto, or assumed constant throughout the year as shown in Fig. A.2. The constant value is computed by averaging the actual annual amount of salt applied mainly in the winter over the entire year, which yields an average surface concentration of 20.8

kg/m^3. In practice, where actual annual variation is not known, it is not uncommon to use an average value as a first approximation.

FINITE ELEMENT VERIFICATION

Verification of the current finite element (FE) model was performed by comparing the results for a specific case analysed by (Martin-Pérez, 1999). The input data are given in Table A.2, which are the same as those used by Martin-Pérez. The binder is assumed to be 60% OPC and 40% slag and fly ash.

Table A.2: Concrete properties (Martin-Pérez, 1999) used for the current finite element model validation.

Property	Value	Unit
Heat capacity	1.932 x 10^6	J/m^3.°C
Convective heat coefficient	0.07	W/m^2.°C
Thermal conductivity	1.4	W/m.°C
w/c	0.3	--
Binder content	450	kg/m^3
First exposure time	120	Days
Effective Diffusion coefficient at 120 davs	1 x 10^{-12}	m^2/s
Surface chloride concentration	17.73	kg/m^3 solution
Initial chloride concentration	0	kg/m^3 solution
α	1.05**	--
β	0.36**	--
w_e	0.08**	m^3/ m^3 of concrete
h_c	0.75	--

** values are fixed and independent of temperature

The free chloride profiles obtained from the current analysis are shown in Fig. A.4 and are identical to the ones reported by Martin-Pérez in kg/m^3 of pore solution.

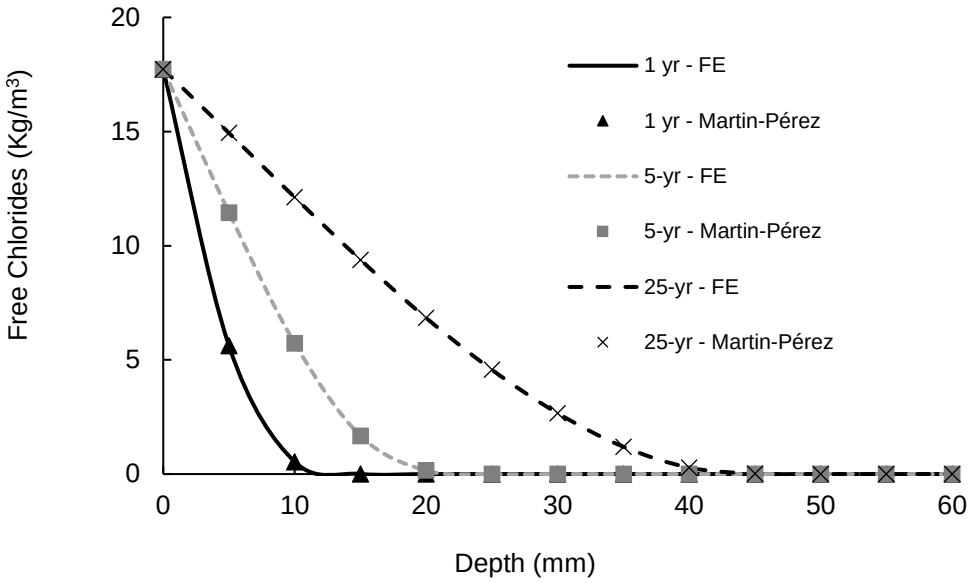

Fig. A.4. Free chloride's profile at different exposure durations using Martin-Pérez's parameters.

ANALYSIS RESULTS

Temperature Temporal Variation Effect

To investigate the effect of temperature temporal variation approximation on chloride profile, a fixed surface chloride concentration of 20.8 kg/m^3 is assumed, and the temperature is assumed to vary as approximated in Fig. A.3. The resulting slab chloride profile after fifty years is shown in Fig. A.5.

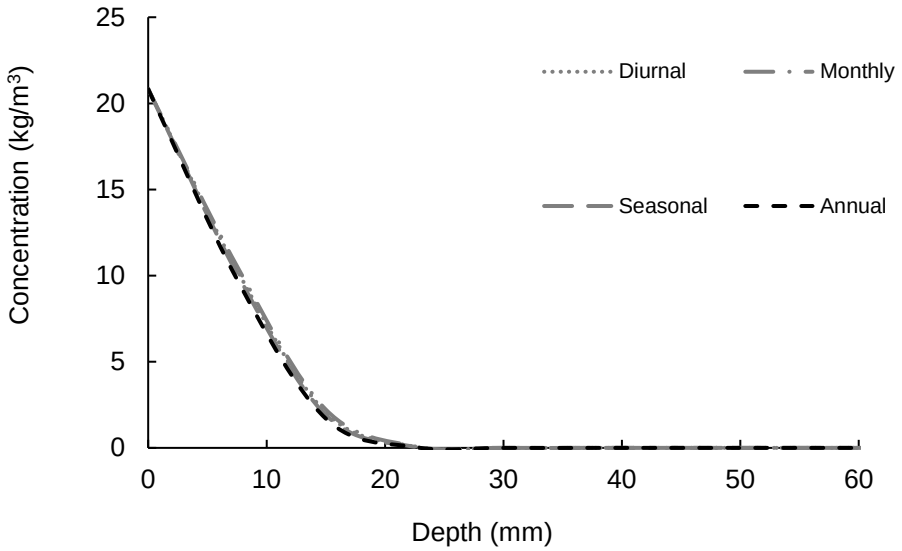

Fig. A.5. Free chloride's profile at 50-year using fixed surface concentration of 20.8 kg/m^3

It is clear from Fig. A.5 that the temperature temporal variation approximation has negligible effect on the chloride concentration profile through the slab.

It is worth mentioning that assuming heat transfer by conduction and convection may not be adequate in every situation because transfer by radiation may play an important role.

Chloride Surface Concentration Effect

Assuming constant annual temperature of 9.9 ^{o}C and either a fixed (F) chloride surface concentration throughout the analysis period or monthly variable (V) concentration as shown in Fig. A.2, the diffusion analysis was performed for twenty-five, fifty, and hundred years. Fig. A.6 shows the computed free chloride concentration profiles through the slab thickness.

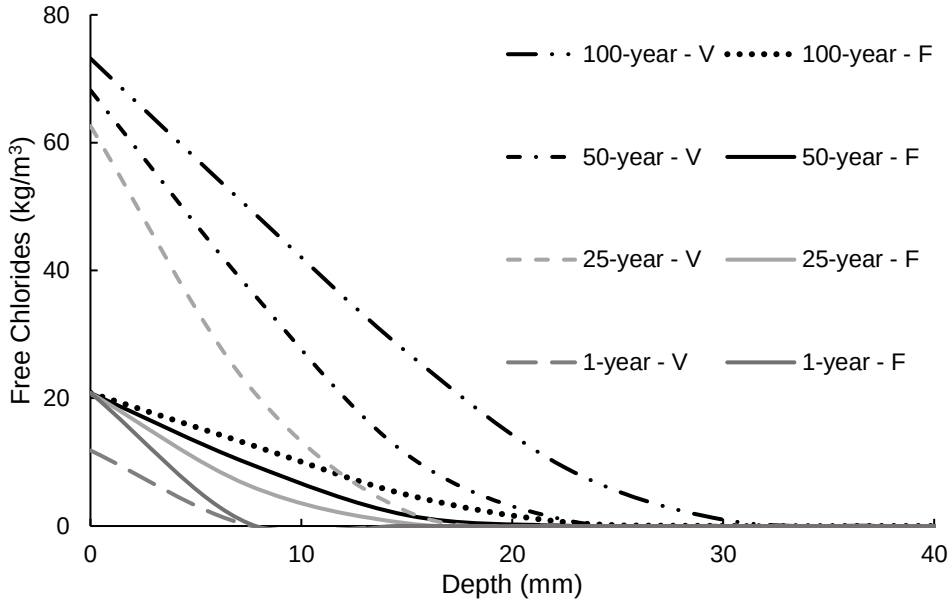

Fig. A.6. Free chloride profile after exposure to fixed (F) or variable (V) surface chloride concentration at constant temperature of 9.9°C

It can be concluded from the latter figure that up to 5 years a fixed surface chloride profile leads to approximately the same penetration depth as given by the variable surface chloride, thereafter, the fixed surface chloride profile underestimates the depth of penetration. The difference between the results of the two approximations becomes particularly obvious after ten years of exposure.

The above difference between the results of the two approximations is further highlighted by the free chloride concentration variation with time of exposure at depths of 7.5 mm and 15 mm. It is evident that the assumption of a fixed surface concentration dramatically

underestimates the chloride concentration, relative to the values predicted assuming variable surface concentration. Note, the point of this analysis is comparison of the relative values of the concentration rather than their absolute values.

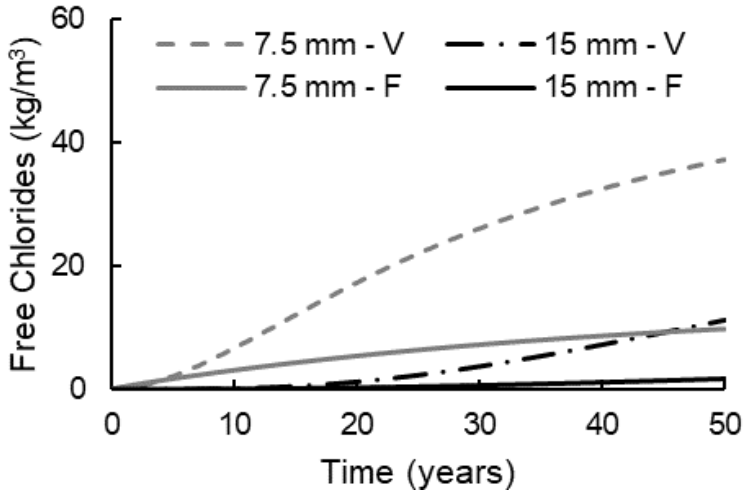

Fig. A.7. Comparison of free chloride concentration at 7.5 mm and 15 mm from the slab surface based on

assumed fixed versus variable surface chloride concentration and constant temperature of 9.9°C.

Assuming either variable or fixed surface chloride concentration, Fig. A.8 shows the total and bound chloride concentration profiles through the thickness of the slab after 50 years. Once again, the two approximations lead to dramatically different results, and the

assumption of a fixed concentration underestimates the expected chloride concentration within the slab.

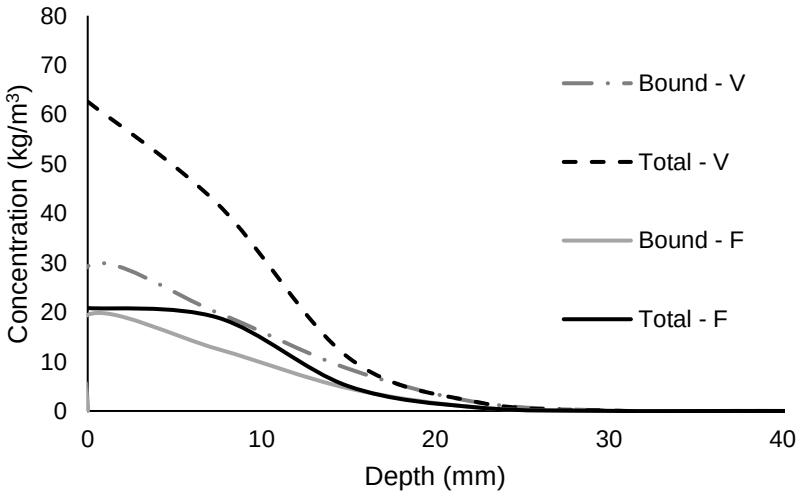

Fig. A.8. Bound and total chloride concentration profiles at 50-year for assumed fixed and variable surface chloride concentrations under constant temperature of 9.9°C.

It can be inferred from Fig. A.8 that at shallow depths, the concrete can bind almost all the chloride in the case of fixed annual surface concentration. On the other hand, for variable concentration, a much lower percentage of chloride is bound, consequently, the free chloride concentration remains high.

Combined Effects of Surface Concentration and Temperature Variations

Analyses were performed assuming 6-hourly constant or annually constant concrete surface temperature variation, but monthly variable chloride surface concentration. The results of the analyses are depicted in Fig. A.9, which shows the temporal variation of chloride concentration at 7.5 mm and 15 mm from the concrete surface.

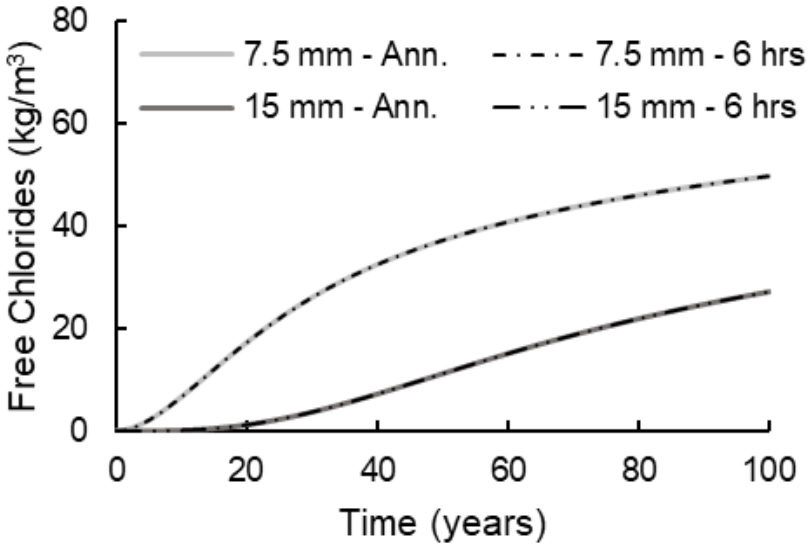

Fig. A.9. Free chloride concentration at two concrete depths for temporally variable surface chloride concentration under 6-hourly constant or annually constant temperature exposure

As found earlier, the temperature approximation method has practically no effect on the chloride concentration at these depths. As the depths are arbitrarily chosen, the overall conclusion of the analysis is that the assumption of a constant average annual temperature is adequate for computing the chloride concentration profile within a concrete member.

CONCLUSIONS

The effects of the approximation method used to represent the actual temporal variation of concrete surface temperature and chloride concentration on chloride concentration profile in a 200 mm thick concrete slab were investigated. The temperature was assumed constant 6-hourly, daily, monthly, seasonally or annually while the chloride surface concentration was assumed constant annually or monthly. The actual annual temperature and surface salt concentrations variations used in the analysis were obtained from data provided by the Canadian environment ministry, and the City of Toronto, respectively. Considering the concrete properties, temperature and humidity conditions, the surface salt concentration profile and the method of analysis used in this study, the following conclusions are reached:

(1) Despite the actual variable temperature that a concrete member may be exposed to during the year, when modelling chloride diffusion, the assumption of a constant annual average temperature seems adequate for determining the chloride concentration profile through the member thickness.

(2) To obtain a relatively accurate estimate of the chlorides concentration profile through the member thickness, the surface chlorides temporal variation must be accurately represented in the diffusion analysis. Use of an average annual surface concentration may grossly underestimate the chloride concentration within the member.

In the current study, the chlorides surface concentration was assumed to be constant either monthly or annually, but further analysis is needed to determine how other temporal

variations, e.g. weekly variation, of this parameter will affect the chloride diffusion kinetics.

ACKNOWLEDGEMENT

The authors would like to thank the Natural Sciences and Engineering Research Council (NSERC) of Canada for its financial support of this research. The first author would like to thank McMaster University for its graduate scholarship and for the McMaster Dean's Excellence Engineering Doctoral Award.

REFERENCES

Brunauer, S., Skalny, J., & Bodor, E. E. (1969). Adsorption on Nonporous Solids. Journal of Colloid and Interface Science, 30(4), 546-552.

CSA S6-14. (2014). Canadian Highway Bridge Design Code: CSA Group, Mississaugua, Ontario, Canada.

Dousti, A., & Shekarchi, M. (2015). Effect of Exposure Temperature on Chloride-Binding Capacity of Cementing Materials. Magazine of Concrete Research, 67(15),821-832.

Environment Canada. (2017). (https://weather.gc.ca/)

Glass, G. K., & Buenfeld, N. R. (2000). The Influence of Chloride Binding on The Chloride Induced Corrosion Risk in Reinforced Concrete. Corrosion Science, 42(2), 329-344.

Glass, G. K., Hassanein, N. M., & Buenfeld, N. R. (1997). Neural Network Modelling if Chloride Binding. Magazine of Concrete Research, 49(181), 323-335.

Hirao, H., Yamada, K., Takahashi, H., & Zibara, H.. (2005). Chloride Binding if Cement Estimated by Binding Isotherms if Hydrates. Journal of Advanced Concrete Technology, 3(1), 77-84.

Maage, M., Helland, S., Poulsen, E., Vennesland, O., & Carlsen, J. E. (1996). Service Life Prediction of Existing Concrete Structures Exposed to Marine Environment. ACI Materials Journal, 93(6), 602-608.

Mangat, P. S., & Molloy, B. T. (1994). Prediction of Long-term Chloride Concentration in Concrete. Materials and Structures, 27(170), 338-346.

Martin-Perez, B., Zibara, H., Hooton, R. D., & Thomas, M. D. A. (2000). A Study of The Effect of Chloride Binding on Service Life Predictions. Cement and Concrete Research, 30(8), 1215-1223.

Martin-Pérez, B.. (1999). Service Life Modelling of R.C. Highway Structures Exposed to Chlorides. (Doctor of Philosophy), University of Toronto, Toronto.

MATLAB and Simulink Release 2017b, The MathWorks, Inc., Natick, Massachusetts, United States.

Saetta, A. V., Scotta, R. V., & Vitaliani, R. V. (1993). Analysis of Chloride Diffusion into Partially Saturated Concrete. ACI Materials Journal, 90(5), 441-451.

Salt Management Plan. (2004). City of Toronto. (https://www1.toronto.ca/city_of_toronto/transportation_services/snow_management/files/pdf/02smp.pdf)

Xi, Y. P., Bazant, Z. P., & Jennings, H. M. (1994). Moisture Diffusion in Cementitious Materials - Adsorption-Isotherms. Advanced Cement Based Materials, 1(6), 248-257.

Zibara, H.. (2001). Binding of External Chlorides by Cement Pastes. Doctor of Philosophy Dissertation, University of Toronto, Toronto.

Zienkiewicz, O. C. (1977). The Finite Element Method, 3d expanded and rev. edition, McGraw-Hill, New York.

APPENDIX - B

WALKTHROUGH THE CORE COMPUTER PROGRAM USED IN THE RESEARCH

DESCRIPTION OF THE PROGRAM

This program is written in MATLAB Platform language (The MathWorks Inc. 2018). The objective of this program is to solve the reactive transport problem in porous media. It can be applied to solve the problems of chloride diffusion and carbonation process in concrete material. The latest version of this program addresses the problem of chloride diffusion in pre-carbonated concrete material. It uses a composition of Finite Element Method and other numerical schemes (i.e. Gauss Elimination and Newton Raphson method) to solve the governing differential and ordinary equations. It is consisted of two main modules: Transport and Chemical modules.

The Transport module solves Nernst-Planck-Poisson's system of equations. It also includes Richard equation to model the movement of water in unsaturated media. This module deals with the movement of species and applies the mass conservation of species and moisture in the studied medium.

The chemical module on the other hand deals with chemical mass balance of the species in the medium and the homogenous and heterogeneous (i.e. dissolution/precipitation) chemical reactions taking place. It uses the output of the transport module and its output is fed to the transport module for the next time step.

The flowchart in Figure B-1 demonstrates the implementation of the NPP reactive transport model in the current study.

PROGRAM INPUT

The input of the program are physical and chemical properties of concrete and its pore solution. It includes concrete density; porosity; tortuosity; cement content; water content; temperature; initial pore solution concentration; solids concentrations; boundary conditions; depth of analyzed sample; time step; and analysis duration. In case of combined chloride and carbonation case, the properties are needed for both virgin and carbonated concrete.

PROGRAM OUTPUT

The output of the program consists of the profiles of pore solution species, water content, potential difference (voltage), solid phases, porosity, and diffusion coefficients.

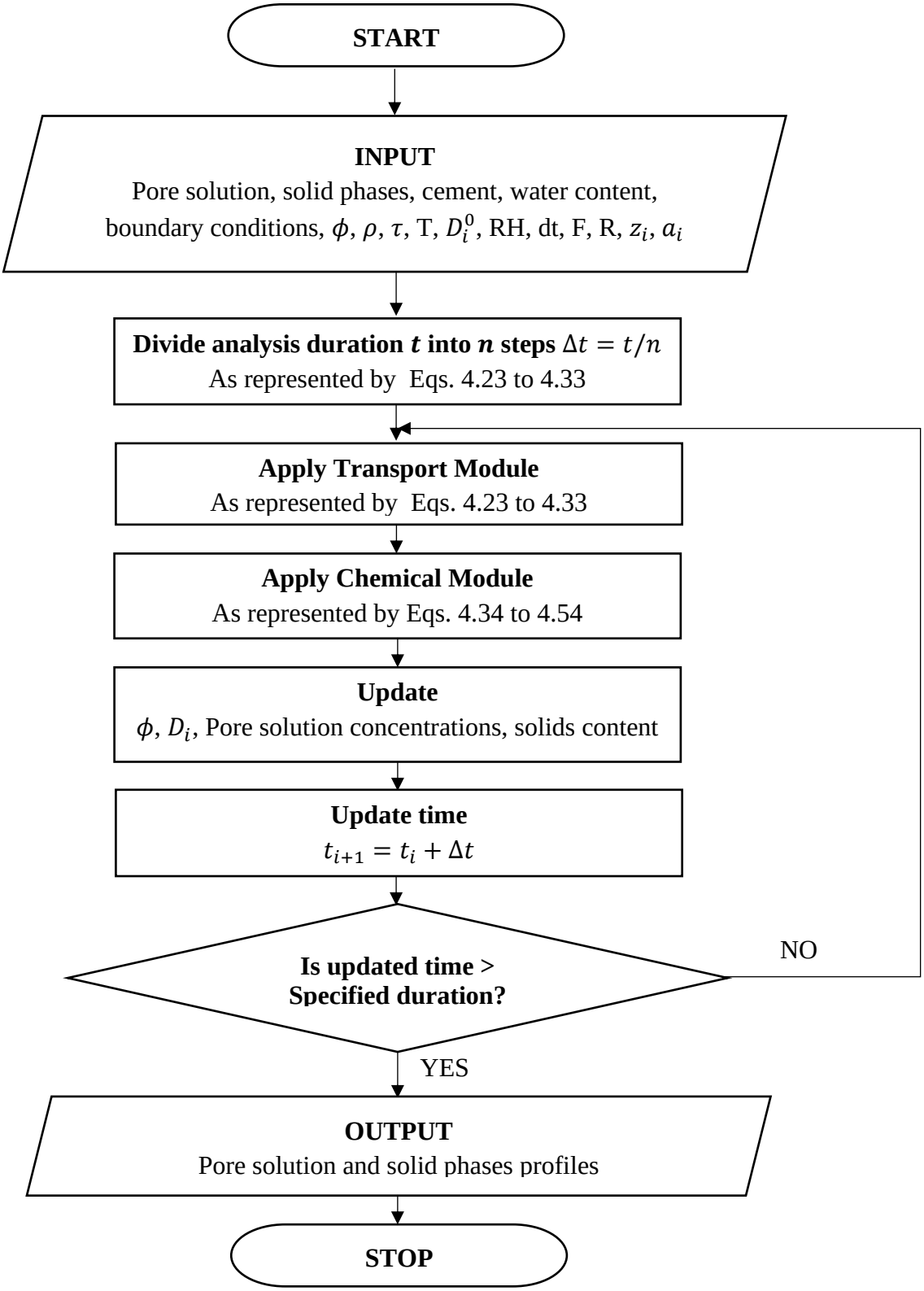

Fig. B.1. Flowchart for the finite element implementation of the model

FINITE ELEMENT MESH

The finite element mesh used for modelling diffusion through 50 mm concrete sample comprised a non-uniform mesh of 100 elements. The element length was chosen as 0.1 mm for the first 5 mm from the exposed surface, 0.5 mm for the region located from 5 to 10 mm from the exposed surface, and 1 mm for the remining depth. The number of elements will increase if bigger depth is considered. The time step is selected as 1800 sec for chloride diffusion case and 900 sec for carbonation based on sensitivity analysis conducted by the authors.

SAMPLE PROGRAM INPUT (CHLORIDE DIFFUSION CASE)

The input of the program is summarized in Table B-1:

Table B.1: Concrete properties and pore solution composition

Property	**Value**	**Property**	**Value**
Cement type	CSA, T10	Porosity	13.4 %
w/c	0.65	Tortuosity	0.0368
Mixture proportions	**(kg/m^3)**	**Diffusion Coefficients**	**(x10^{-11} m^2/s)**
Cement	280	OH^-	19.4
Water	182	Na^+	4.9
Coarse aggregates	1065	K^+	7.2
Fine aggregates	833	SO_4^{2-}	3.9
Density	2360	Ca^{2+}	2.9
		$Al(OH)_4^-$	2.0
Cement composition	**(% mass)**	Cl^-	7.5
CaO	62.10		
SiO_2	20.40	**Initial pore solution**	**(mmol/L)**
Al_2O_3	4.30	OH^-	273.5
SO_3	3.20	Na^+	133.5

		K^+	140.1
Initial solids phases	**(g/kg)**	SO_4^{2-}	1.7
Portlandite (CH)	35.1	Ca^{2+}	1.7
C-S-H	73.5	$Al(OH)_4^-$	0.1
Ettringite (AFt)	2.9	Cl^-	0
Monosulfate (AFm)	25.2		

The sample is subjected to 0.5 M sodium chloride solution which is maintained constant throughout two months. The sample is kept saturated and thus moisture diffusion is neglected.

SAMPLE PROGRAM OUTPUT (CHLORIDE DIFFUSION CASE)

The chloride diffusion output associated with the input data above is demonstrated in Figures B.2 to B.11.

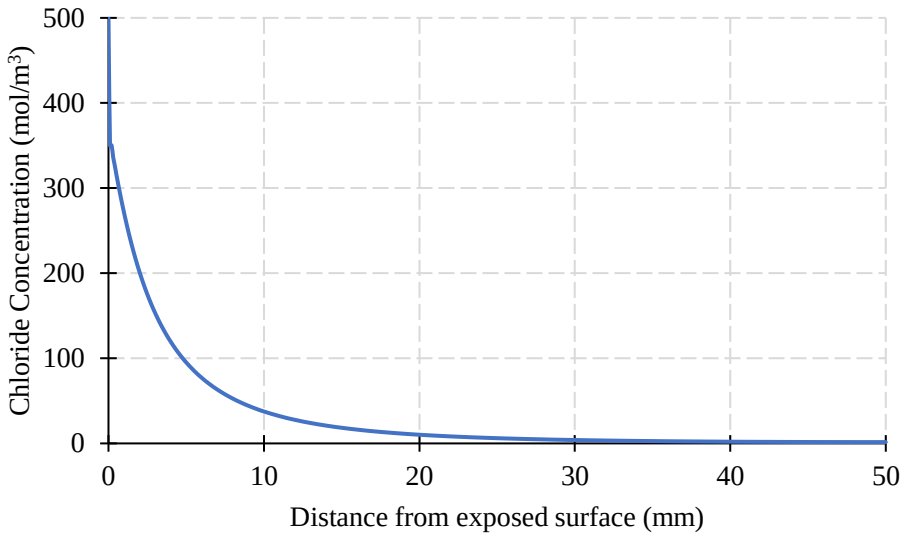

Fig. B.2. Chloride ion profile at two months of salt exposure

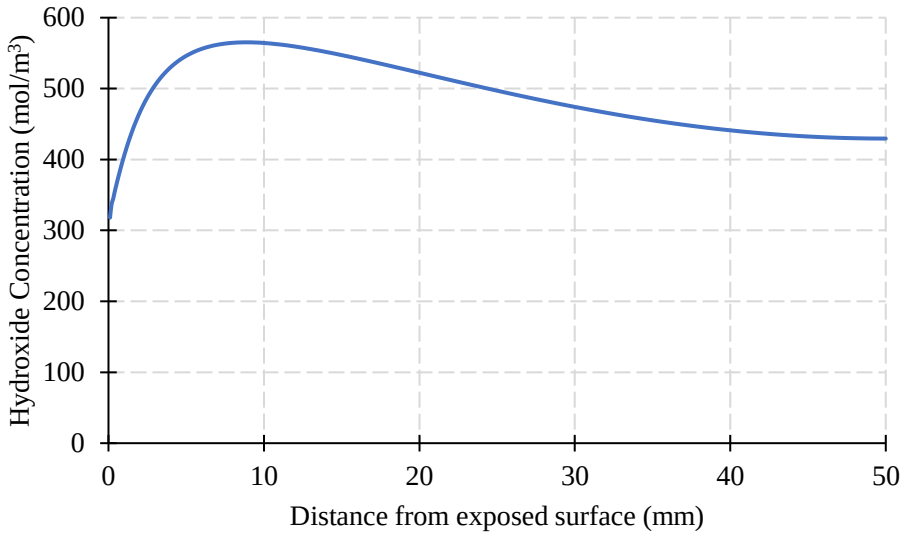

Fig. B.3. Hydroxide ion profile at two months of salt exposure

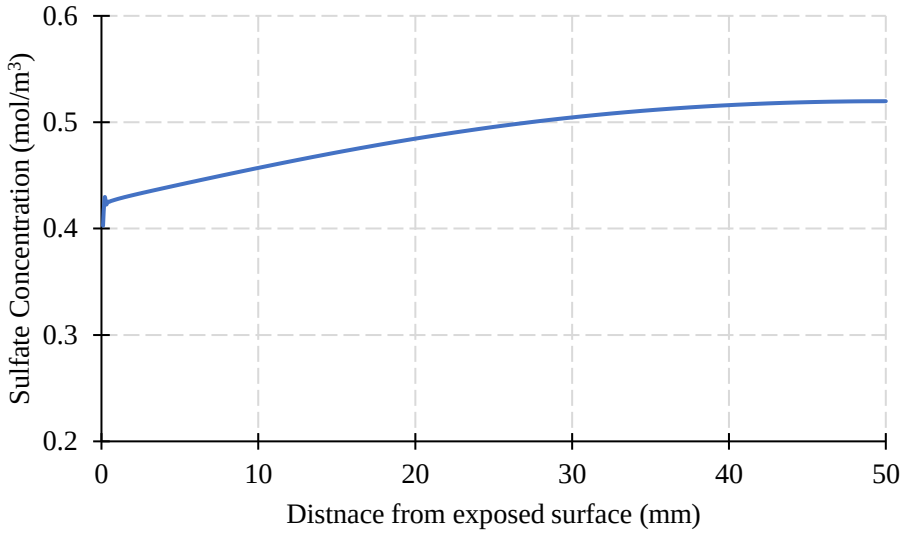

Fig. B.4. Sulfate ion profile at two months of salt exposure

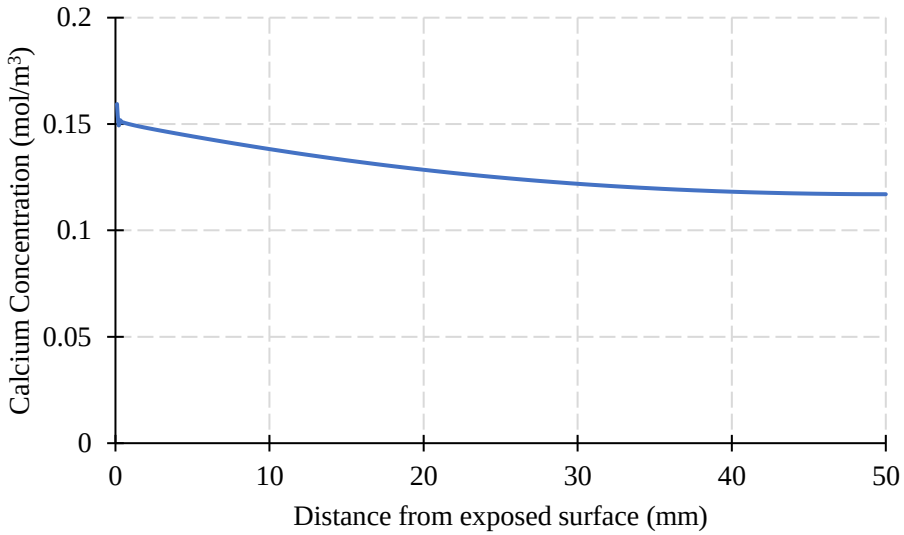

Fig. B.5. Calcium ion profile at two months of salt exposure

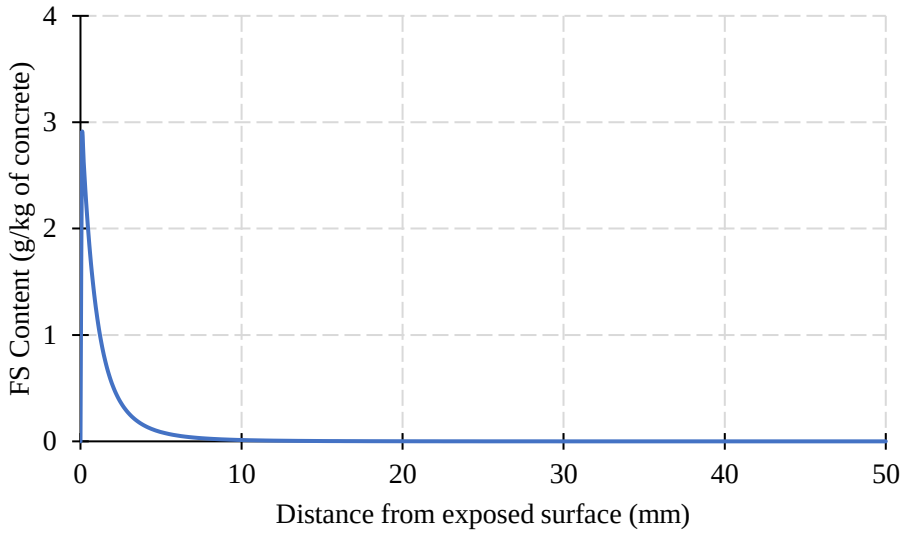

Fig. B.6. Friedel's salt profile at two months of salt exposure

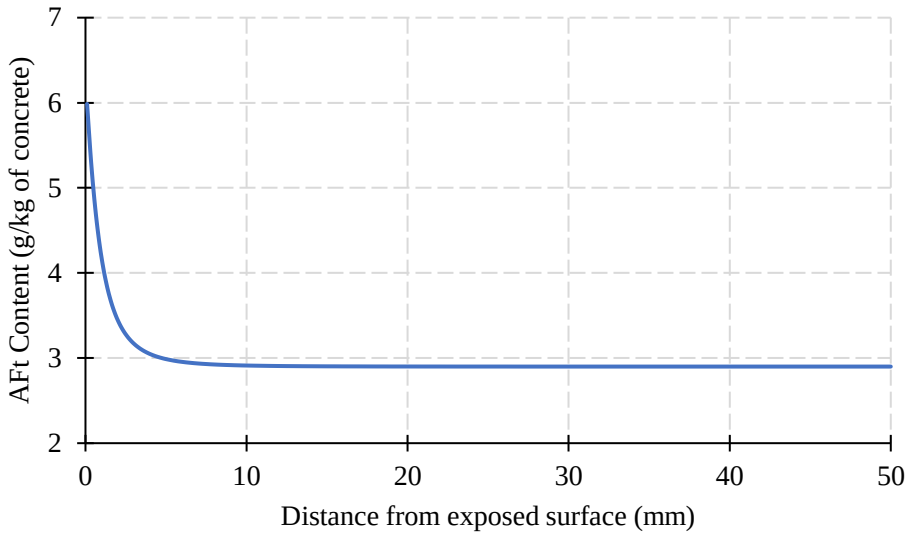

Fig. B.7. Ettringite profile at two months of salt exposure

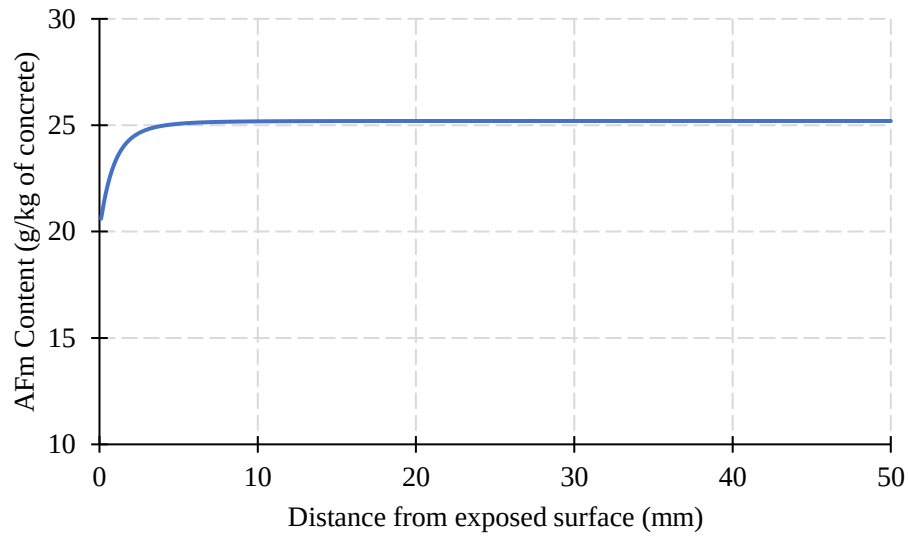

Fig. B.8. Monosulfate profile at two months of salt exposure

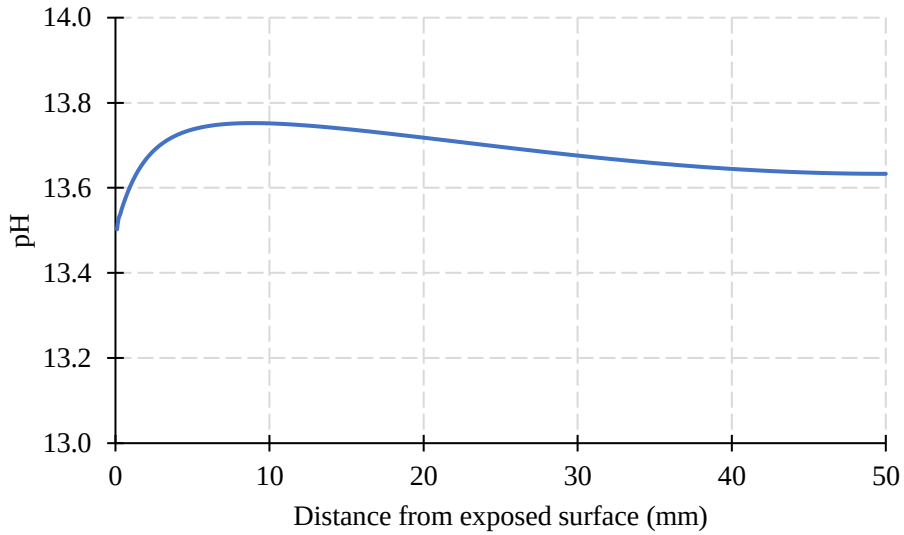

Fig. B.9. pH profile at two months of salt exposure

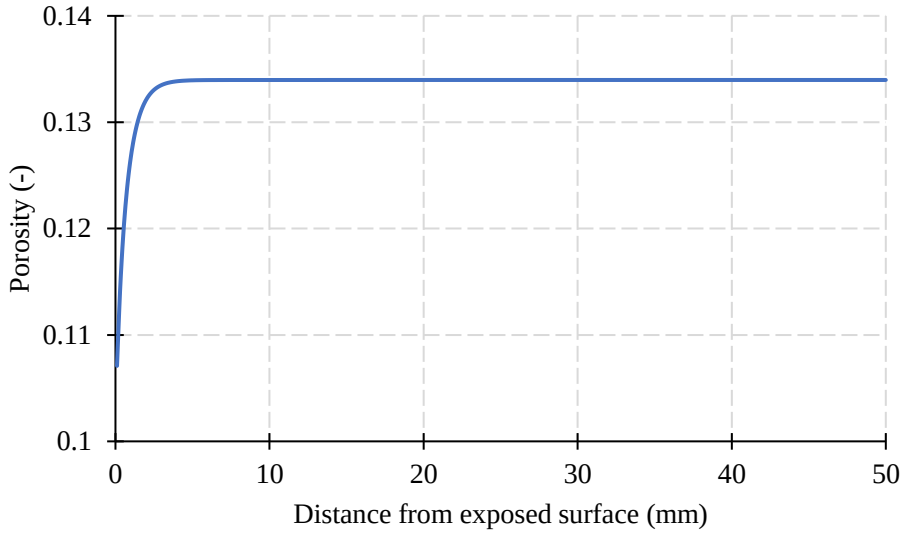

Fig. B.10. Porosity profile at two months of salt exposure

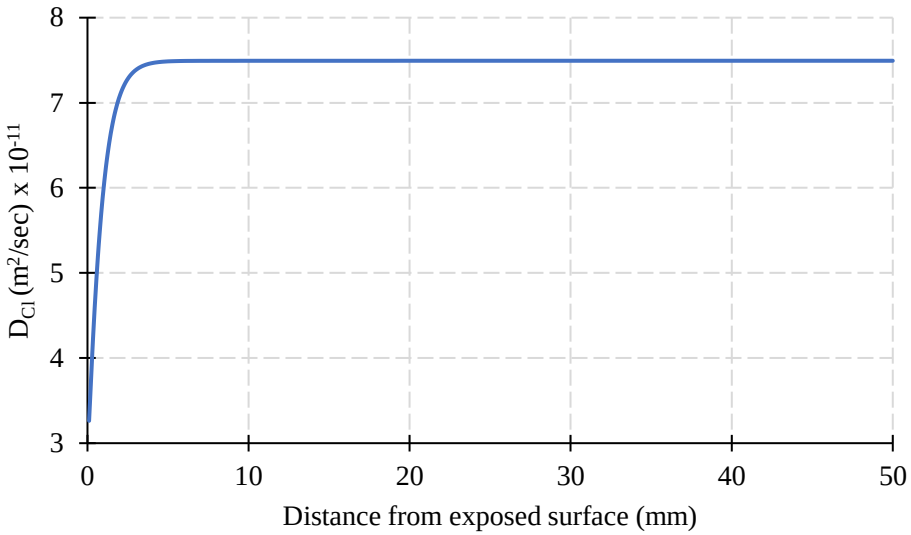

Fig. B.11. Chloride Diffusion coefficient profile at two months of salt exposure

REFERENCES

The MathWorks Inc. 2018. “MATLAB.” https://www.mathworks.com/.`